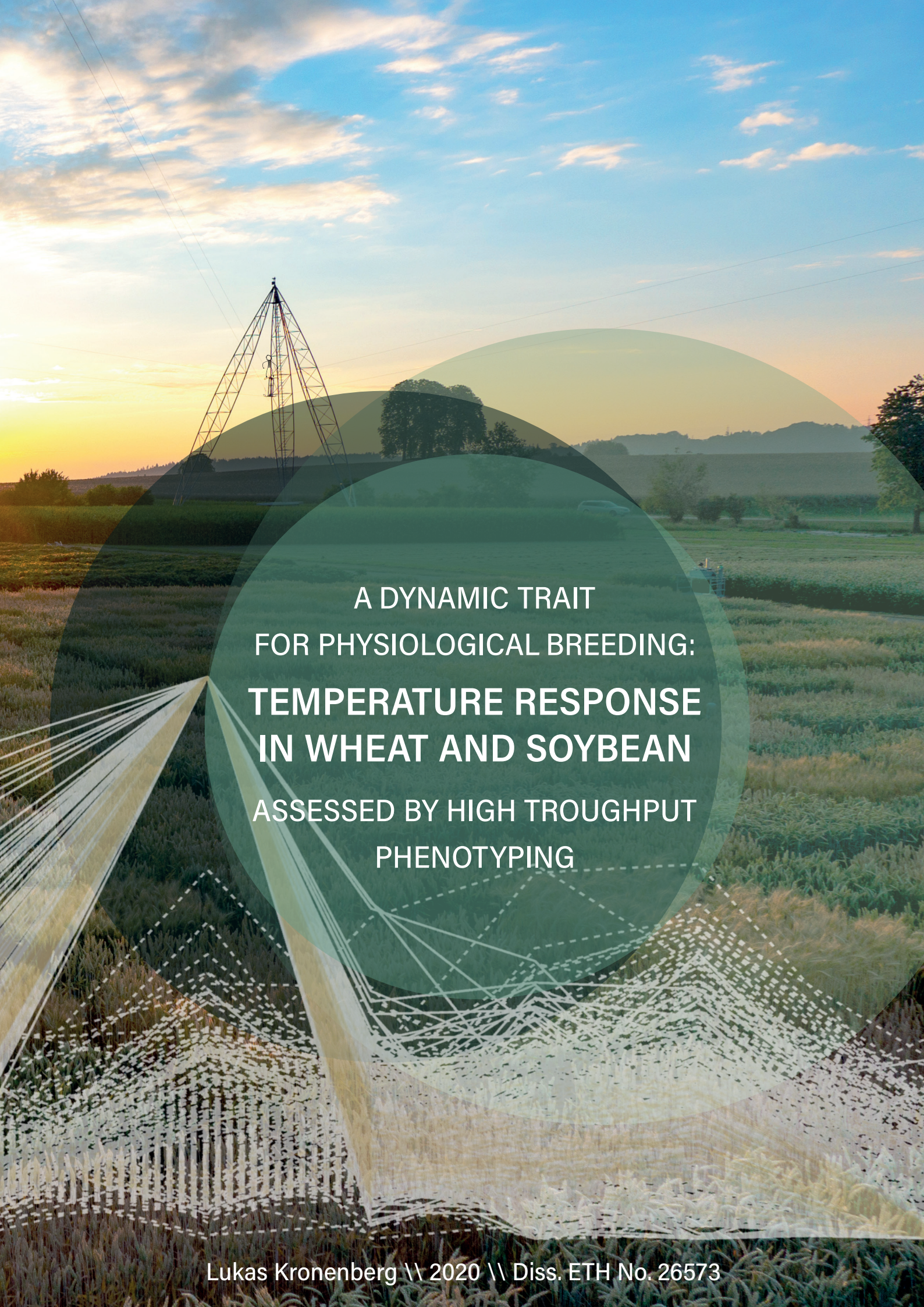

A DYNAMIC TRAIT FOR PHYSIOLOGICAL BREEDING: TEMPERATURE RESPONSE IN WHEAT AND SOYBEAN ASSESSED BY HIGH TROUGHPUT PHENOTYPING

Lukas Kronenberg \\ 2020 \\ Diss. ETH No. 26573

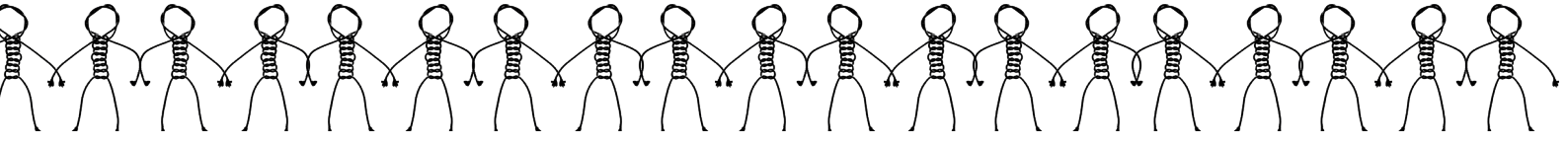

DISS. ETH NO. 26573

A dynamic trait for physiological breeding: Temperature response in wheat and soybean assessed by high throughput phenotyping

A thesis submitted to attain the degree of

DOCTOR OF SCIENCES of ETH ZURICH

(Dr. sc. ETH Zurich)

presented by

Lukas Kronenberg

MSc. ETH in Agricultural Sciences

born on 20.12.1989

citizen of Dagmersellen

accepted on the recommendation of

Prof. Dr. Achim Walter (examiner)

PD Dr. Andreas Hund (co-examiner)

Prof. Dr. Simon Griffiths (co-examiner)

2020

Table of Contents

Summary ..... **iii**

Zusammenfassung ..... **vii**

1 General introduction **1**

1.1 Temperature effects on plant growth and development 1
1.2 Phenotyping 2
1.3 Linking lab and field 4
1.4 Temperature sensing in plants 5
1.5 Advances in genomics 5
1.6 Aims and structure of the thesis 6

2 Monitoring the dynamics of wheat stem elongation: Genotypes differ at critical stages **9**

Abstract 9
2.1 Introduction 10
2.2 Material and methods 12
2.3 Results 16
2.4 Discussion 21
2.5 Conclusion and outlook 24

3 Temperature response of wheat affects final height and the timing of key developmental stages under field conditions **27**

Abstract 27
3.1 Introduction 28
3.2 Material and methods 29
3.3 Results 33
3.4 Discussion 44
3.5 Conclusion 47

4 Understanding wheat physiological and phenological phases linked with environmental interactions **49**

Abstract 49
4.1 Introduction 50
4.2 Materials and methods 52
4.3 Results 57
4.4 Discussion 61
4.5 Conclusion 63

5 Diel temperature regime markedly affects gene expression, carbohydrate metabolism and diel leaf growth in soybean **65**

Abstract 65

5.1 Introduction 66
5.2 Results 67
5.3 Discussion 75
5.4 Material and methods 77

6 General discussion 83

6.1 High throughput phenotyping techniques deliver access to the investigation of dynamic traits 83
6.2 Temperature response is a heritable trait affecting many aspects of plant development 84
6.3 Temperature response across developmental stages, indoors and outdoors 89
6.4 Complex traits can be investigated under controlled conditions, if the settings are right 92
6.5 Could temperature response be a beneficial trait for plant breeding? 93

7 References 97

Supplementary material chapter 2 121

Figures 121

Supplementary material chapter 3 123

Figures 123
Tables 128

Supplementary material chapter 5 130

Figures 130
Tables 135

Acknowledgements 137

Curriculum vitae 139

Summary

Crops form the basis of human nutrition, be it for direct consumption or as animal feed. In an ever-changing environment, plant breeders face the challenge of constantly adapting and improving crops to maintain yield stability and to increase yield. Temperature is the most important environmental factor influencing plant adaptation and yield. The current increase in global temperature is threatening crop productivity and yields. In several important crops, yields have stagnated in many regions of the world during the last decades, possibly because breeding process has not kept pace with the changes in climate and agricultural management. The severity of this problem may increase in the future. For instance in wheat, a recent study predicted a global yield decline of 6 % per °C increase in global temperature. Averting this negative development requires improved breeding tools and strategies. It has been proposed that improved local adaptation through physiological breeding may be an avenue to mitigate the negative effects of climate change. Yields could be improved by selection for secondary traits that are related to higher yield or improved performance under unfavourable conditions. However, such approaches require a deeper understanding of the physiological aspects of yield formation in crops and the genotype by environment interaction of traits related to crop development and yield.

To date, our understanding of ambient temperature response in plants is still scarce. It is known that all plants respond to temperature throughout their entire life cycle and that warm temperatures generally increase the rate of development up until a certain optimum temperature. However, it is unclear, how this response is genetically controlled and whether there is exploitable genetic variability in this response. If there is such variability for temperature in crops, this might be used to tailor crop development to specific environments in an optimal way for yield relevant traits. Alternatively, adaptation to unfavourable temperature conditions could be improved by modifying the sensitivity to temperature. Most physiological knowledge about temperature response today comes from research in the model species *Arabidopsis thaliana,* which is generally conducted under controlled laboratory conditions. Therefore, it is unclear how well these findings translate to crop species grown in natural field conditions.

The overall aim of this thesis was to investigate dynamic response of growth to temperature in the field in single leaves and whole crop stands. Furthermore, the aim was to compare temperature response in the field to the response under controlled conditions as well as the temperature response across developmental stages. The general hypothesis was that temperature has a direct effect on short-term growth dynamics in plants, which is measurable under natural field conditions and that this temperature response is genetically controlled. Growth is a good indicator for plant adaptation and fitness and is very sensitive to external stimuli. Therefore, we considered growth as optimal trait to investigate ambient temperature response in the field. As model crops we used wheat and soybean. Wheat is the most widely grown staple food crop in the world. Soybean is among the most important dicot summer crop species and is a valuable feed and food crop.

In recent years, we witnessed great progress in phenotyping technology. Making use of digital imaging technologies such as RGB-, multispectral- and thermal imaging cameras or LiDAR sensors, different platforms were developed that allow for precise measurement of plant growth and development in high temporal resolution on several levels. The ETH field phenotyping platform FIP is such a system that allows the monitoring of hundreds of plots growing in a standard crop rotation in the field. Other methods developed in the ETH Crop Science Group allow for the precise measurement of single leaf growth in the field as well as in controlled conditions.

In a first step, we used the FIP to investigate wheat growth dynamics during stem elongation (SE), which is the critical phase for yield formation in wheat. We measured canopy height in 330 genotypes every three to four days during SE in three growing seasons. We found that wheat displays genotype specific growth dynamics during SE and that the timing of SE and final height extracted from the data are highly heritable. Furthermore, we found that there is an interdependency between final height and the timing of SE.

Based on these results, we investigated temperature response during SE by regressing daily stem elongation rates against temperature. The investigated wheat varieties displayed a large variation in temperature response, which was highly heritable ($H^2 = 0.81$ across three years). Temperature response was correlated to the timing of stem elongation and final height, thus reflecting the interdependencies found in the previous experiment. The results suggested that genotypes with a low temperature response display an early start of stem elongation, reduced final height and a longer stem elongation phase. Thanks to recent advancements in genomics, there is now a fully annotated reference genome available for wheat. We conducted a genome wide association study (GWAS) with the temperature response data and mapped the associated loci to the reference genome. We found that the circadian clock gene *EARLY FLOWERING 3 (ELF3)* as well as *FRIGIDA* putatively mediate temperature response in wheat. *ELF3* was previously associated with earliness in cereals and a very recent study in wheat also showed that it is involved in wheat temperature response.

In a next experiment, we investigated temperature response of wheat leaf elongation in the field and in the greenhouse. The temperature response measured in the greenhouse showed a strong correlation with temperature response during SE in the field. However, the genotype ranking of temperature response of leaves measured in the field did not correlate with the response in the greenhouse or the response during SE. We hypothesised that this may be due to the large difference in temperature range between the single experiments. To further investigate the correlation between the start of SE and temperature response in SE, we determined the timing of floral transition in genotypes contrasting for temperature response in SE. The timing of floral transition confirmed the correlation found in the previous experiment.

In soybean, we focussed on the effect of diel (24 h) temperature patterns on leaf growth dynamics. Based on findings from the literature, soybean leaves are expected to display pronounced growth in the night and to be hardly affected by external stimuli. When we measured soybean leaf growth in the field, we found that the opposite was the case: leaf growth showed a diel pattern that closely followed temperature, with maximum growth in the early afternoon. Therefore, we set up an experiment under controlled conditions with two treatments differing in their diel temperature settings. The first treatment had a binary temperature regime, commonly used in plant research under controlled conditions, with constant day and constant night temperatures. The second treatment had a gradually fluctuating temperature regime mimicking the temperature conditions observed in the field. The results showed that diel growth dynamics of soybean leaves are highly responsive to the diel temperature pattern. Whereas plants in the first treatment exhibited the reported growth pattern with growth at night, leaf growth in the second treatment closely followed temperature replicating the pattern observed in the field. Furthermore, switching from one temperature regime to the other resulted in an immediate adjustment to the respective diel growth pattern. The respective temperature treatments not only altered the diel growth pattern but also caused significant differences in in diel starch and sucrose concentration pattern between the two the treatments. Furthermore, the different temperature regimes caused differential expression of 5'042 genes between the treatments. The binary temperature regime induced a daytime synchronization of genes controlling cell division and plants in the field-like temperature regime displayed an upregulation of genes of the circadian clock morning and evening complex.

The results of this thesis show that dynamic traits like growth response to temperature become accessible on a genotypic level through modern phenotyping techniques. This is of high relevance for plant breeding. In order to mitigate the adverse effects of climate change on crops, a better understanding of genotype by environment interactions is of paramount importance. Furthermore, we are, to the best of our knowledge, the first to report a highly heritable temperature response during wheat stem elongation in a large set of genotypes. As temperature response was correlated to floral transition as well as stem elongation duration, this result implies that temperature response might be exploitable as a breeding trait for local adaptation and yield improvement. The fact that the candidate genes identified by GWAS are known genes of the *Arabidopsis* flowering pathway and that *ELF3* was reported to be involved in the control of earliness in wheat gives additional support to these findings.

Our results from soybean highlight the importance of environmental settings in controlled condition studies. The change in the diel temperature pattern did not only produce a different phenotypic behaviour but also significantly altered carbohydrate metabolism and gene expression. In contrast, using a more realistic temperature regime allowed for closely replicating the growth pattern found in the field. Therefore, more realistic environmental settings could lead to better transferability of results obtained under controlled conditions to the field.

Together, the findings deepen our understanding of temperature response in crop plants and offer new opportunities for plant breeding and modelling. Furthermore, they provide a good example of opportunities and threats concerning the transferability of results from controlled conditions to the field.

Zusammenfassung

Kulturpflanzen bilden die Grundlage unserer Ernährung; wir verzehren sie entweder direkt oder nutzen sie als Futtermittel für Nutztiere. In einer sich ständig verändernden Umwelt stehen die Pflanzenzüchter vor der Herausforderung, die Pflanzen an die neuen Bedingungen anzupassen und sie nach Möglichkeit zu verbessern. Dadurch soll die Ertragsstabilität erhalten und die Erträge gesteigert werden. Die Temperatur ist in diesem Zusammenhang eine der wichtigsten Umweltvariablen. Der derzeitige, globale Anstieg der Temperaturen ist eine ernstzunehmende Bedrohung für den Pflanzenertrag. Bei einigen wichtigen Nutzpflanzen stagnierten die Erträge in den letzten Jahrzehnten, und das in allen Regionen der Welt. Ein möglicher Grund für diese Stagnation besteht darin, dass der Züchtungsprozess nicht mit dem Klimawandel und der landwirtschaftlichen Praxis Schritt zu halten vermochte.

Dieses Problem wird in Zukunft wohl noch dringlicher. So prognostizierte etwa eine aktuelle Studie einen weltweiten Rückgang der Weizenerträge von 6 % im Falle eines Anstiegs der globalen Temperatur um 1°C. Um dieser negativen Entwicklung gegenzusteuern, bedarf es verbesserter Züchtungsverfahren und -strategien. Eine vielversprechende Strategie besteht darin, die lokale Anpassung der Pflanzen durch physiologische Züchtung zu verbessern. Die Erträge lassen sich steigern, so die Hoffnung, indem man sich auf sekundäre Merkmale konzentriert, die mit einem höheren Ernteertrag oder einer verbesserten Leistung unter ungünstigen Bedingungen korrelieren. Dafür brauchen wir jedoch sowohl ein besseres Verständnis der physiologischen Aspekte der Ertragsbildung, als auch ein besseres Verständnis über die Wechselwirkung zwischen Genotyp und Umwelt für jene Merkmale, die mit der Pflanzenentwicklung und dem Ertrag zusammenhängen.

Unser Verständnis der Art und Weise, wie Pflanzen auf ihre Umgebungstemperatur reagieren, ist bisher relativ begrenzt. Wir wissen, dass Pflanzen über ihren gesamten Lebenszyklus hinweg auf die Temperatur reagieren, und dass warme Temperaturen ihre Entwicklungsrate in der Regel bis zu einer bestimmten optimalen Temperatur erhöhen. Es ist jedoch unklar, wie diese Reaktion genetisch gesteuert wird und ob es eine genetische Variabilität in dieser Reaktion gibt. Gäbe es eine solche Variabilität in der Temperaturabhängigkeit von Wachstum und Entwicklung, könnte diese genutzt werden, um die Pflanzenentwicklung mit Blick auf ertragsrelevante Merkmale optimal auf die jeweilige Umgebung abzustimmen. Die Anpassung an ungünstige Temperaturbedingungen könnte man dann über die Anpassung der Temperaturempfindlichkeit erreichen. Die meisten physiologischen Erkenntnisse über die pflanzliche Temperaturreaktion basieren auf Untersuchungen an der Modellart *Arabidopsis thaliana*. Meistens wurden diese Erkenntnisse unter kontrollierten Laborbedingungen gewonnen. Es ist eine offene Frage, inwiefern diese Erkenntnisse auch für Kulturpflanzenarten gelten, die unter natürlichen Feldbedingungen angebaut werden.

Das übergeordnete Ziel dieser Arbeit war die Untersuchung der dynamischen Wachstumsreaktion auf die Temperatur im Feld; sowohl in einzelnen Blättern als auch in ganzen Pflanzenbeständen. Weiter sollte die Temperaturabhängigkeit im Feld mit der Temperaturabhängigkeit unter kontrollierten Bedingungen, sowie der Temperaturabhängigkeit über verschiedene Entwicklungsstufen hinweg verglichen werden. Die zentrale Hypothese lautete: Die Temperatur hat einen direkten, unter natürlichen Feldbedingungen messbaren, Einfluss auf die kurzfristige Wachstumsdynamik bei Pflanzen. Überdies wurde angenommen, dass diese Temperaturabhängigkeit genetisch kontrolliert wird. Das Pflanzenwachstum reagiert empfindlich gegenüber äusseren Reizen und eignet sich demnach als Indikator für Anpassung und Fitness. Daher betrachteten wir Wachstum als optimale Eigenschaft, um die Temperaturabhängigkeit im Feld zu untersuchen. Als Modellpflanzen verwendeten wir Weizen und Soja. Weizen ist die am weitesten verbreitete Grundnahrungsmittelpflanze der Welt. Soja gehört zu den wichtigsten zweikeimblättrigen Sommerpflanzenarten und ist eine wertvolle Kulturpflanze.

In den letzten Jahren wurden wir Zeugen von beachtlichen Fortschritten im Bereich der Phänotypisierung von Pflanzen im Feld. Unter Einsatz digitaler Bildgebungstechnologien wie RGB-, Multispektral- und Wärmebildkameras oder LiDAR-Sensoren wurden Plattformen entwickelt, anhand derer die Entwicklung und das Wachstum der Pflanzen in hoher zeitlicher Auflösung auf unterschiedlichen Organisationsstufen gemessen werden kann. Ein solches System ist die ETH-Feldphänotypisierungsplattform FIP. Über diese Plattform lassen sich Hunderte von Parzellen, die in einer Standard-Fruchtfolge auf dem Feld wachsen, überwachen. Andere in der ETH Gruppe für Kulturpflanzenwissenschaften entwickelte Methoden erlauben die präzise Messung des Einzelblattwachstums sowohl im Feld als auch unter kontrollierten Bedingungen.

In einem ersten Schritt haben wir mit der FIP die Wachstumsdynamik von Weizen während des Schossens untersucht, welches eine kritische Phase für die Ertragsbildung bei Weizen ist. In 330 Genotypen haben wir über drei Vegetationsperioden hinweg alle drei bis vier Tage die Bestandeshöhe gemessen. Es zeigte sich, dass Weizen während dem Höhenwachstum über eine Genotyp-spezifische Wachstumsdynamik verfügt und dass die aus den Daten ermittelten Zeitpunkte von Beginn und Ende des Schossens sowie die Endhöhe selbst stark vererbbar sind. Darüber hinaus haben wir festgestellt, dass zwischen der endgültigen Höhe und dem Beginn des Schossens eine Abhängigkeit besteht.

Auf der Grundlage dieser Ergebnisse untersuchten wir die Temperaturabhängigkeit während des Schossens, indem wir den Zusammenhang zwischen täglichen Höhenwuchsraten und der jeweils herrschenden Temperatur mittels linearer Regression beschrieben. Die untersuchten Weizensorten zeigten eine große Variation ihrer Temperaturabhängigkeit und eine hohe Erblichkeit ($H^2 = 0{,}81$ über drei Jahre) für dieses Merkmal. Die Temperaturabhängigkeit korrelierte mit dem Zeitpunkt des Schossens und der Endhöhe, was die im dem vorangegangenen Versuch festgestellten Abhängigkeiten bestätigt. Die erhaltenen Resultate deuten darauf hin, dass Genotypen mit einer wenig ausgeprägten Temperaturabhängigkeit früher mit dem Schossen beginnen, eine reduzierte

Endhöhe erreichen und eine längere Höhenwachstumsphase aufweisen. Dank den jüngsten Fortschritten in der Genomik steht nun ein vollständig annotiertes Referenzgenom für Weizen zur Verfügung. Wir führten eine genomweite Assoziationsstudie (GWAS) mit den Temperaturabhängigkeitsdaten durch und kartierten die assoziierten genetischen Loci auf dem Referenzgenom. Die Ergebnisse deuten darauf hin, dass das zur zirkadianen Uhr gehörige Gen *EARLY FLOWERING 3 (ELF3)* sowie *FRIGIDA* die Temperaturabhängigkeit im Weizen steuern könnten. *ELF3* war zuvor mit intrinsischer Frühreife im Getreide assoziiert worden. Eine kürzlich erschienene Studie fand ausserdem, dass dieses Gen an der Temperaturreaktion des Weizens beteiligt ist.

In einem nächsten Experiment im Weizen untersuchten wir die Temperaturabhängigkeit des Blattwachstums im Feld und im Gewächshaus. Die im Gewächshaus gemessene Temperaturabhängigkeit korrelierte stark mit der Temperaturabhängigkeit während dem Höhenwachstum im Feld. Allerdings stimmte die Rangordnung der Genotypen in Bezug auf die Temperaturabhängigkeit der im Feld gemessenen Blätter nicht mit der Reaktion im Gewächshaus oder der Reaktion während dem Höhenwachstum überein. Dies ist, so unsere Annahme, auf den großen Temperaturunterschied zwischen den einzelnen Experimenten zurückzuführen. Um die Korrelation zwischen dem Beginn des Schossens und der Temperaturabhängigkeit im Höhenwachstum weiter zu untersuchen, haben wir den Zeitpunkt der Blüteninduktion durch Sezieren des Apikalmeristems in kontrastierenden Genotypen bestimmt. Diese wurden anhand ihrer Temperaturabhängigkeit des Höhenwachstums ausgesucht. Der Zeitpunkt der Blüteninduktion bestätigte die im vorherigen Experiment gefundene Korrelation zwischen dem Schossen und der Temperaturabhängigkeit im Höhenwachstum.

Im Fokus unserer Soja-Versuche stand der Einfluss von diurnalen (24 h) Temperatur-Mustern auf die Wachstumsdynamik der Blätter. In der Literatur wird erklärt, dass Sojabohnenblätter nachts stark wachsen und dabei kaum von äusseren Reizen beeinflusst werden. Als wir das Wachstum der Sojabohnenblätter auf dem Feld gemessen haben, stellten wir fest, dass das Gegenteil der Fall war: Das diurnale Blattwachstum folgte klar der Temperatur, mit einem Wachstumsmaximum am frühen Nachmittag. Aus diesem Grund haben wir ein Experiment unter kontrollierten Bedingungen mit zwei Versuchsvarianten durchgeführt, die sich in ihren diurnalen Temperaturverläufen unterschieden. Die erste Variante hatte ein binäres Temperaturregime mit konstanten Tages- und Nachttemperaturen, welches in der Pflanzenforschung unter kontrollierten Bedingungen üblich ist. Die zweite Variante hatte ein sich graduell änderndes Temperaturregime, welches mit den im Feld beobachteten Temperaturbedingungen vergleichbar ist. Die Ergebnisse zeigten, dass die Wachstumsdynamik der Sojabohnenblätter stark vom Tagestemperaturmuster abhängt. Während Pflanzen in der ersten Variante das erwartete Wachstumsmuster mit starkem Wachstum in der Nacht zeigten, folgte das Blattwachstum in der zweiten Variante eng der Temperatur und replizierte das im Feld beobachtete Muster. Darüber hinaus führte der Wechsel von einem Temperaturvariante zur anderen zu einer sofortigen Anpassung an das jeweilige tägliche

Wachstumsmuster. Die unterschiedlich verlaufenden Temperaturen veränderten nicht nur das diurnale Wachstumsmuster, sondern bewirkten auch signifikante Unterschiede in Bezug auf die diurnalen Stärke- und die Saccharose Konzentration. Darüber hinaus wurden infolge der verschiedenen Temperaturvarianten 5'042 Genen unterschiedlich exprimiert. Die binäre Temperaturvariante bewirkte eine zeitliche Synchronisation der an der Steuerung der Zellteilung beteiligten Gene. Die Pflanzen, welche unter feldähnlichen Temperaturen gezogen wurden, zeigten eine Hochregulierung von Genen des zirkadianen Morgen- und Abendkomplexes.

Diese Arbeit zeigt, dass sich dynamische Merkmale wie die Temperaturabhängigkeit des Wachstums dank moderner Phänotypisierungstechniken auf genotypischer ebene identifizieren lassen. Dies ist für die Pflanzenzüchtung hoch relevant. Um die negativen Auswirkungen des Klimawandels auf den Kulturpflanzenertrag zu mildern, ist ein besseres Verständnis der Genotyp-Umwelt-Interaktion von grösster Bedeutung. Darüber hinaus gelang es erstmals, die hoch erblich Temperaturabhänigkeit während des Schossens bei einer Vielzahl von Weizen-Genotypen zu etablieren. Die Temperaturabhänigkeit korreliert, wie wir zeigten, mit der Blüteninduktion und dem Beginn des Streckungswachstums. Daraus folgt, dass sich die Temperaturabhänigkeit als Züchtungsmerkmal für die lokale Anpassung und Ertragsverbesserung nutzen lässt. Die Tatsache, dass es sich bei den durch GWAS identifizierten Kandidatengenen um bekannte Gene des Netzwerkes zur Regulation der Blüteninduktion in *Arabidopsis* handelt und dass *ELF3* mit der Kontrolle der Frühreife im Weizen assoziiert ist, unterstützt diese Ergebnisse zusätzlich.

Unsere Ergebnisse aus der Sojabohne unterstreichen die Bedeutung der Umweltbedingungen in kontrollierten Experimenten. Eine Veränderung im diurnalen Temperaturverlauf führte nicht nur zu einem veränderten phänotypischen Verhalten, sondern auch zu einer signifikanten Veränderung des Kohlenhydratstoffwechsels und der Genexpression. Im Gegensatz dazu konnte durch die Verwendung eines realistischeren Temperaturverlaufs ein Wachstumsmuster erzeugt werden, wie es im Feld beobachtet werden kann. Realistischere Umgebungsbedingungen unter kontrollierter Anzucht können die Übertragbarkeit der erzielten Ergebnisse auf das Feld demnach entscheidend verbessern.

Zusammengefasst verbessern die Untersuchungsergebnisse unser Verständnis des Temperaturverhaltens von Kulturpflanzen und bieten neue Strategien für die Pflanzenzüchtung und -modellierung. Darüber hinaus bieten sie Ansätze zur besseren Übertragbarkeit von Ergebnissen aus kontrollierten Bedingungen auf das Feld.

1 General introduction

1.1 Temperature effects on plant growth and development

Temperature is a major abiotic factor determining plant growth and development throughout a plant's life cycle (Baxter, 2013; Zanten *et al*., 2013). Limiting cold and extreme warm temperatures are among the most important abiotic stress factors. In alpine regions, temperature is the most important factor limiting the occurrence of species and setting the limit of the treeline (Körner & Paulsen, 2004; Körner, 2008; Paulsen & Körner, 2014). In temperate regions, winter crops that grow to a considerable size in cold conditions after autumn sowing and that can endure freezing temperatures in winter are very successful. While cold temperatures conditions limit growth and development in winter and early spring, supra-optimal temperatures and heatwaves in summer can drastically hamper crop performance (Zanten *et al*., 2013). A plant's susceptibility to adverse environmental conditions strongly depends on the phenological stage at the occurrence of such stresses. Flowering is such a critical stage, in which critically high or low temperatures can have a drastic impact on yield. Thus, one strategy to escape the negative effects of stressful environmental conditions is to adjust the phenology, so the most sensitive stages are likely to occur in favourable environmental conditions.

In temperate cereals such as wheat (*Triticum aestivum*), vegetative to reproductive transition and flowering are mainly controlled by photoperiod response, vernalisation response and earliness per se genes (Slafer *et al*., 2015). Photoperiod sensitivity has often been proposed as an approach to optimize the timing of critical phases in wheat under the assumption that different insensitivity alleles would affect different stages (*i.e.* vegetative, early and late reproductive phase) differently (Slafer *et al*., 1996, 2001; González *et al*., 2002; Pérez-Gianmarco *et al*., 2018). The insensitivity alleles *Ppd-D1a*, *Ppd-A1a* and *Ppd-B1a* have been found to reduce time to anthesis by decreasing amount in the given order (Worland, 1996; Pérez-Gianmarco *et al*., 2018). However, as a detailed, recent study shows, none of them seems to affect any of the developmental phases exclusively (Pérez-Gianmarco *et al*., 2018). The roles of vernalisation and photoperiod in the flowering pathway of wheat and barley have been well investigated on the genomic level (Trevaskis *et al*., 2007a; Kippes *et al*., 2015; Trevaskis, 2015).

Ambient temperature apart from vernalisation or critically high or low temperatures also has a profound impact on growth and development. It is well established, that plants respond to temperature in all developmental phases and that warm ambient temperatures generally fasten growth and development (Slafer & Rawson, 1994, 1995a,d; Atkinson & Porter, 1996; Fischer, 2011; Slafer *et al.*, 2015). Under non-stressful conditions, the rate of development increases from a crop specific base temperature to an optimum temperature, at which developmental rate is fastest (Slafer *et al.*, 2015). Hence, the most widely used model to describe the timing of plant development is thermal time, also known via the concept of 'growing degree-days' (Monteith, 1984; Slafer *et al.*, 2015; Parent *et al.*, 2018). There, the rate of development is assumed to increase linearly with temperature-corrected

calendar time (°Cd) between species-specific cardinal (base and optimum) temperatures (Slafer *et al.*, 2015). Species with tropical origin generally have higher cardinal temperatures than species of temperate origin (Slafer *et al.*, 2015). Also, variation in cardinal temperatures has been reported within species and depending on the developmental stage (Porter *et al.*, 1987; Grimm *et al.*, 1993; Slafer & Rawson, 1995c; Porter & Gawith, 1999; Cober *et al.*, 2001; Fischer, 2011; Slafer *et al.*, 2015). The observed variation in cardinal temperatures and variation in developmental sensitivity towards temperatures in the cardinal range lead to the concept of environment specific temperature response ideotypes (Atkinson & Porter, 1996). Thus, yields could be improved by selecting for environment and growth stage specific temperature responses (Atkinson & Porter, 1996), similar to the above mentioned specific photoperiod requirements. Yet, many open questions remain concerning ambient temperature sensing and response in plants. Studies investigating crop temperature response often use temperature means across whole developmental phases and a limited number of genotypes (*reviewed in:* Atkinson & Porter, 1996; Porter & Gawith, 1999; Fischer, 2011; Luo, 2011). Few studies investigated temperature response dynamically by measuring growth in high temporal resolution (Poiré *et al.*, 2010; Parent & Tardieu, 2012; Grieder *et al.*, 2015; Nagelmüller *et al.*, 2016, 2018). These studies used a limited number of genotypes and only few studies (Grieder *et al.*, 2015; Nagelmüller *et al.*, 2016, 2018) were performed under field conditions. Investigating dynamic temperature response in a large set of genotypes under field conditions requires precise measurement of growth in high temporal resolution, a task requiring most modern phenotyping technology.

1.2 Phenotyping

Today the term 'plant phenotyping' often refers to image-based techniques that aim at a quantification of compounds, photosynthesis, development, architecture, volume or biomass of single plants or plant stands (Furbank & Tester, 2011; Fiorani & Schurr, 2013; Junker *et al.*, 2015; Walter *et al.*, 2015). Phenotyping procedures are conducted to investigate physiological principles involved in the control of basic plant functions as well as for selecting superior genotypes in plant breeding programs. Typically, these procedures analyse static traits that are quantified at one specific point in time, such as plant size, ear number, canopy cover (CC, percentage of the ground covered by plant canopy) or disease intensity. Images acquired with usual RGB-cameras, multi-, hyperspectral, chlorophyll fluorescence or thermography sensors form the typical suite of methods applied in contemporary phenotyping. Some of the imaging procedures have originally been designed for detecting total leaf area of small rosette model plants such as *Arabidopsis thaliana* in controlled conditions (Granier *et al.*, 2006; Jansen *et al.*, 2009) Other procedures have been developed in the field in the context of remote sensing or precision agriculture (Mistele & Schmidhalter, 2008; Araus & Cairns, 2014).

Quantitative imaging in the field is challenging due to a number of non-trivial nuisance factors. Variable illumination, the dependence of the spectral composition of reflected sunlight on weather conditions as well as plant movements due to wind or rain cause

difficulties in the acquisition of high quality images. In order to retrieve quantitative information, many images are consecutively acquired throughout the season. These have to be segmented (*e.g.* dissected in 'plant' and 'soil' pixels), spatially assigned and standardized for illumination to be comparable. Moreover, in order to provide meaningful information about the performance of plants in a certain environmental context, a set of environmental parameters needs to be recorded throughout a relevant time period to analyse genotype x environment interactions.

Hence, automated phenotyping approaches have first been successful under controlled conditions, especially in the case of research on cereal species such as rice (Yang *et al.*, 2014), wheat (Rajendran *et al.*, 2009) and barley (Hartmann *et al.*, 2011). In these approaches, single plants have been analysed in a static context, meaning that side-by-side comparisons of a range of plant genotypes were performed in a given set of environmental conditions. The dynamic response of plants has only been analysed in few approaches (Walter *et al.*, 2007; Jansen *et al.*, 2009; Chen *et al.*, 2014; Parent *et al.*, 2015; Yates *et al.*, 2019). In these approaches, the reaction of growth towards an onset of drought stress, towards dynamical changes of light or temperature has been followed, requiring analysis of plant size or of another trait at several consecutive points in time.

In traditional breeding approaches crop performance is evaluated by the 'breeder's eye', meaning that plants are classified according to their vigour or according to defined traits in small plots in the field (van Ginkel *et al.*, 2008). This represents a serious bottleneck for the dissection of complex traits, for which several thousand plots have to be observed in the same environment, which exceeds the capabilities of classical phenotyping (White *et al.*, 2012). Improvements of these methods are typically sought for in the domain of automation. However, this is done mostly with respect to the acquisition of images and not with respect to the quantification of other traits. Thus, a number of recent research projects have been dealing with the establishment of mobile field phenotyping platforms often termed "phenomobiles" (Deery *et al.*, 2014). Examples of such phenomobiles comprise lightweight, bicycle-like systems pushed through the field (White & Conley, 2013), trailers pulled by tractors (Busemeyer *et al.*, 2013) or devices attached to conventional tractors (Svensgaard *et al.*, 2014). Moreover, unmanned aerial vehicles (UAV) and other remote or proximal sensing platforms have been explored for their capabilities to contribute to plant breeding by assessing genetic variability of plants in a field; for a review of such approaches see (Sankaran *et al.*, 2015).

The investigation of dynamic traits such as plant growth in response to environmental covariables requires precise phenotypic data in sufficient temporal resolution. Novel phenotyping platforms hold the promise of supplying such data. Previous work has shown that LiDAR systems are able to quantify growth dynamics in field-grown crops (Friedli *et al.*, 2016a). From 2014 onwards, a novel field phenotyping platform was established at the research field site of ETH crop science at Eschikon (Kirchgessner *et al.*, 2016). In chapter two of this thesis, the goal was to implement the measurement strategy proposed by Friedli et al. (2016) in the FIP.

1.3 Linking lab and field

When plants are grown in pots and in climate chambers, they are exposed to a different setting of environmental parameters compared to plants grown in the field (Passioura, 2006; Poorter *et al.*, 2012), which makes it difficult to deduct field responses from 'laboratory' experiments. Yet, it would increase the throughput and power of breeding experiments enormously, if breeding experiments could be performed under controlled conditions, with the reliability that the genetic variability observed in the greenhouse would be comparable to the one in the field, as has been partly achieved for growth response to water stress in barley (Chen *et al.*, 2014) and wheat (Parent *et al.*, 2015).

Obviously, it is difficult to control the light regime with respect to homogeneity, intensity and spectral composition in the growth chamber in a highly repetitive way (Massonnet *et al.*, 2010) and this also holds true for factors other than light (Porter *et al.*, 2015). An abiotic factor that can be precisely controlled in growth chambers is temperature. Therefore, progress in connecting lab to field phenotyping can be expected to proceed most rapidly for the topic of temperature response. Even though temperature is among the most determining environmental factors affecting growth and development, it has not yet received its due regard (Körner, 2003, 2006).

Most of our mechanistic knowledge about temperature sensing comes from experiments performed in climate chambers. In these studies however, exposure to cold temperatures has often been performed in an unrealistic setting (*as pointed out by* Winfield *et al.*, 2010) by transferring plants from one constant temperature regime to a much colder, but also constant temperature regime. Transcriptome analysis of wheat showed that when transitions are done in a way that is better simulating field conditions (Winfield *et al.*, 2009, 2010), a more meaningful picture emerges: It was shown that many genes are differentially expressed, which orchestrate many seemingly disparate physiological and biochemical processes. Some genes code for effector molecules directly involved in stress alleviation, whereas others code for proteins involved in signal transduction or for transcription factors controlling the expression of further groups of genes.

In wheat, there is a broad genetic variability in terms of cold acclimation and winter hardiness (Monroy *et al.*, 2007). This was an important factor for the breeding success of wheat. Among soybean genotypes, the genetic variability in adaptation to low temperatures is smaller and the genetic basis of this variability is unclear. What is known is (Kidokoro *et al.*, 2015) that the cis-acting element DRE (dehydration-responsive element)/CRT plays an important role in activating gene expression in response to cold stress. The *Arabidopsis* DREB1/CBF genes that encode DRE-binding proteins function as transcriptional activators in the cold stress responsive gene expression. Also, it is known that soybean gene expression fluctuates throughout 24 h and that e.g. genes related to drought are more responsive during the day compared to the night (Rodrigues *et al.*, 2015). From *Arabidopsis* it is known that gene expression is affected by time of day, revealing an interaction between cold and diurnal regulation that drives transcriptome changes (Bieniawska *et al.*, 2008).

The response of growth to temperature is generally thought to be linear within the physiological growth limits of the plant. Yet, when temperature is close to the upper or lower limit of a species, growth response is not well investigated – also because of a lack of analysis methods. More detailed analyses have shown that growth and plant development respond sigmoidally to temperatures (Parent & Tardieu, 2012), but the exact function is unclear. In wheat, for example, there is a controversy whether the relationship between leaf elongation rate and temperature is linear (Gallagher, 1979), exponential (Peacock, 1975) or partly exponential with a saturation towards high temperatures (Voorend *et al.*, 2014). Also, it is unclear to which extent temperature responses differ among genotypes (Slafer & Rawson, 1995c; Grieder *et al.*, 2015; Nagelmüller *et al.*, 2016) and whether the response during different points in time of the diel (24h) cycle is different. Throughout plant ontogeny, growth response to temperature is not constant (Slafer & Rawson, 1995c). This has been found in cereal crops but it is unclear, whether this also holds true in non-cereal, dicotyledonous species. On account of different organization of leaf growth zones, diel growth patterns of mono- and dicot plants differ pronouncedly (Walter *et al.*, 2009). Further insight in the dynamic effects of temperature on growth and development in different developmental phases will offer new opportunities in crop adaptation to different environments and yield improvement. Given sufficient water and nutrients, temperature is presumed to be the main driver for developmental rate in plants (Slafer & Rawson, 1994). The fine tuning of developmental rates in critical physiological stages has been proposed as a means to increase crop adaptation and yield (Miralles & Slafer, 2007). A better understanding of the physiological basis underlying the growth and developmental response to temperature could provide the necessary target sites for such endeavours.

1.4 Temperature sensing in plants

To date, most of our knowledge about temperature sensing and response comes from the model species *Arabidopsis thaliana*. Temperature sensing in plants depends on a large network of signalling factors (Penfield, 2008) that is connected to the sensing of other stimuli such as e.g. light (Franklin, 2009). The flowering locus and transcription factors such as the C-repeat binding factor (CBF) are involved in plant temperature sensing (Thomashow, 2010), but there are a lot of unresolved questions with respect to cold perception, signalling and regulation of low-temperature response (Knight & Knight, 2012). CBF is not only involved in temperature sensing but it also confers cold tolerance and mediates growth retardation (Zhou *et al.*, 2014). This means that there is a direct correlation between the retardation of growth and the resistivity to chilling temperatures.

1.5 Advances in genomics

Methods from the field of molecular genetics, such as quantitative trait locus (QTL) mapping and genome wide association studies (GWAS) allow the linking of phenotypic observation to the putatively causative genomic regions using genetic markers such as single sequence repeats (SSR) or the now more commonly used single nucleotide

polymorphisms (SNP). The identification of the causative genomic region however requires the localization of the associated markers on the genome. In the absence of a reference genome sequence, this is done with genetic maps constructed based on linkage between markers. This approach is comparably coarse and requires additional fine mapping in order to narrow down the causative regions.

The rapid advances in sequencing technology during the last decade led to a dramatic decrease in sequencing costs and increased availability of sequence data and genomic information. Well annotated, high quality reference genome sequences have recently been published for various crop species, such as rice (Kawahara *et al.*, 2013), barley (The International Barley Genome Sequencing Consortium, 2012), maize (Schnable *et al.*, 2009), common bean (Schmutz *et al.*, 2014), pigeon pea (Varshney *et al.*, 2012), chickpea (Varshney *et al.*, 2013), soybean (Schmutz *et al.*, 2010) and wheat (Consortium IWGSC *et al.*, 2018). These resources enable the link of phenotypic data to the underlying genetic architecture and causative regions more directly and with higher precision of localization. Methods like gene expression analysis through RNA sequencing (*i.e.* transcriptomics) allow for the direct identification of genes or gene groups at a certain point in time.

1.6 Aims and structure of the thesis

Temperature response is a trait of high importance with respect to crop yields in the context of global warming. For example, wheat yields are predicted to decrease by 6 % for every °C of temperature increase globally (Asseng *et al.*, 2015). Thus, a deeper understanding of temperature response in field crops is needed to improve local adaptation of crops and mitigate adverse effects of climate change. As described above, our knowledge of temperature response is scarce, especially for field grown crop plants. Specifically, it is unclear, how well findings from controlled conditions are transferable to the field and how well temperature response measured in specific organs, *i.e.* leaves, can be transferred to whole plants or how temperature response varies across developmental stages. To date, most of our knowledge on physiology and underlying genetics is based on the model species *Arabidopsis thaliana*. However, direct transfer of knowledge from *Arabidopsis* to crop plants is difficult, not the least due to the complexity and missing co-linearity of crop genomes (Spannagl *et al.*, 2011). Thanks to the availability of genomic data as well as high throughput phenotyping technologies as discussed above, complex traits have now become examinable in situ. Therefore, we set out to investigate temperature response directly in agronomically important crop species.

The general hypothesis for this thesis was that temperature has a direct effect on short-term growth dynamics in plants, which is measurable under natural field conditions and that this temperature response is genetically controlled. Therefore, the overall aim of this thesis was to investigate dynamic response of growth to temperature in the field using a dicot and a monocot crop species as model plants. Further, we compared temperature response between single leaves and whole crop stands as well as temperature response in the field and under controlled conditions.

As monocot model species, we used wheat (*Triticum aestivum*). Wheat is together with rice and maize among the three most important crops with a current global seed yield of ca. 772 Mt/a (FAO 2017). After rice, it is the world's most important source of calories. As an annual winter crop, wheat requires cold, vernalizing temperatures in order to gain flowering competence. Wheat is resilient towards cold temperatures and is therefore very successful in temperate climates. However, wheat is susceptible to heat, especially around anthesis. Due to its effects on phenology and yield, temperature is a very important covariate during the reproductive phase of wheat, which was the main focus of chapter two and three of this thesis.

Chapter 2: Measuring growth dynamics during wheat stem elongation

In order to investigate growth dynamics and their response to temperature during the reproductive phase of wheat, accurate canopy height measurements in the field in high temporal resolution are necessary. Friedli *et al*. (2016a) demonstrated that terrestrial 3D laser scanning has this potential in terms of accuracy and possible temporal resolution. However, they were not able to detect genotypic differences in growth pattern due to a lack of genotypic variation and limited measurement points (Friedli *et al.*, 2016a).

In chapter two, we used a terrestrial laser scanner mounted on the field phenotyping platform FIP to measure growth dynamics in a large, diverse set of genotypes in a bi-weekly measurement routine during stem elongation. We tested the system's capability of accurate canopy height measurements in appropriate temporal resolution to determine genotype specific growth dynamics during wheat stem elongation. We further tested the hypothesis that there is considerable genetic diversity at critical stages of this dynamics and determined interactions between different stages and their relation to final plant height.

Chapter 3: Temperature response during wheat stem elongation

In chapter three, we analysed three seasons of short-term growth dynamics during stem elongation in their response to temperature. The hypothesis is tested, whether final height can be dissected into temperature-independent elongation, temperature dependent elongation and the duration of the stem elongation phase. The relationship between temperature response, timing of the stem elongation phase, temperature-independent growth and final height are analysed on the phenotypic level as well as on the genomic level through genome wide association studies (GWAS).

Chapter 4: Wheat leaf growth in the greenhouse and in the field

Based on the results of chapters two and three, the focus of chapter four is on wheat leaf growth in response to temperature. Wheat temperature response in the vegetative phase will be compared to temperature response in the reproductive phase and the replicability between field measurements and greenhouse measurements will be investigated. Further, the connection between temperature response and floral transition as indicated by the results of chapter three will be investigated.

Chapter 5: Temperature dependence of diel leaf growth pattern in soybean

As a dicot model species, we used soybean (*Glycine max*). Soybean is among the most important dicot summer crop species, with a current global yield of ca. 353 Mt/a (FAO 2017). Due to its protein and oil profile, soybean is a valuable feed and food crop. As a legume with the ability to fix nitrogen via the symbiosis with rhizobia, it is also an important element of balanced crop rotations. Soybean is not well cold-acclimated. Higher performance in cold conditions would allow growing soybean even in more temperate climates. Soybean could then replace maize in crop rotations and thereby improve nutrient balances of regular agricultural crop rotations. For soybean, a more rapid development under cool field conditions in the juvenile stage and an earlier onset of flowering would be highly desirable. Flowering time also is regulated by a complex network of factors (Jung & Müller, 2009a). Earlier flowering can confer enormous stress resistance by avoiding potentially stressful situations in summer drought or heat. Therefore, an improved understanding of the velocity to arrive at flowering and of the onset of flowering is crucial for crop improvement. Leaf growth of dicot plants has been reported to be mainly controlled by endogenous regulators and to be less affected by external stimuli (Walter *et al.*, 2009; Ruts *et al.*, 2012). Recent, hitherto unpublished results indicate a temperature dependence in dicot leaf growth depending on the temperature range. The focus of chapter five will therefore be to analyse temperature effects on leaf growth dynamics in soybean under controlled conditions and under field conditions and to elucidate regulatory mechanisms on the level of metabolism and transcription.

2 Monitoring the dynamics of wheat stem elongation: Genotypes differ at critical stages

Lukas Kronenberg[A,B], Kang Yu[A], Achim Walter[A] and Andreas Hund[A]

[A]Institute of Agricultural Sciences, Group of Crop Sciences, ETH Zürich, Universitätstrasse 2, LFW C54.1, 8092 Zürich, Switzerland

[B]Corresponding author Email: lukas.kronenberg@usys.ethz.ch

*This chapter is a reprint of the paper published in Euphytica **213**: 157, doi: 10.1007/s10681-017-1940-2, under the same title.*

Abstract

Stem elongation is a critical phase for yield formation in wheat (*Triticum aestivum)*. This study proposes the use of terrestrial laser scanning (TLS) for phenotyping of growth dynamics during wheat stem elongation in high temporal resolution and high throughput in the field. TLS was implemented on a novel field phenotyping platform carrying a cable suspended sensor head moveable in 3D over a 1 ha field. Canopy height was recorded on 335 winter wheat genotypes across two consecutive years. Scans were done in 3-d intervals during the stem elongation phase. Per day, 714 plots (two replications plus checks) were scanned within 3.5 hours. The results showed that canopy height increased linearly with thermal time. Based on this linearity, 15% and 95% of final height were used as proxy measures for the onset and termination of stem elongation, respectively. We observed high heritability between 0.76 and 0.91 for the onset, termination and duration of stem elongation. The onset of stem elongation showed a positive covariance with the termination of stem elongation and final height indicating some regulatory dependencies. Yet there was no apparent relationship between onset and duration of stem elongation. Due to its precision, the TLS method allows to measure the dynamics of stem elongation in large sets of genotypes. This in turn offers opportunities to investigate the genetic control of the transitions between early vegetative growth, stem elongation and flowering. Understanding the genetic control of these transitions is an important milestone towards knowledge-based crop improvement.

Keywords: wheat, stem elongation, growth, phenotyping, development

2.1 Introduction

Stem elongation (SE) is a critical phase for yield formation in wheat (*Triticum aestivum*) and has been proposed as a target site to improve yield and environmental adaptation of wheat (Miralles *et al.*, 2000; González *et al.*, 2003a).

Physiological Background

Although SE itself is a growth trait, it has been shown to be strongly related to developmental progress in the field (Slafer *et al.*, 1995). Under field conditions, SE starts after the formation of the terminal spikelet and ends with anthesis (Slafer *et al.*, 2009). Between these two events, active spike growth takes place (Slafer *et al.*, 2009). Due to this co-occurrence, the SE phase is considered to be critical for potential yield in wheat. This has been proposed quite early (Hudson, 1934; Fischer, 1985; Slafer *et al.*, 2001) and was widely confirmed in later years (Kirby, 1988; Slafer *et al.*, 1996, 2001). Spike dry weight at anthesis is largely related to grain number per spike (Fischer, 1985; Slafer *et al.*, 2001), which in turn has been found to be more yield determining than individual grain weight (Slafer *et al.*, 2001 *and references cited therein*), especially in connection with environmental variation of yield (Fischer, 1985; Calviño & Monzon, 2009).

The number of fertile florets and the related spike dry weight depend on the duration of the SE and concurrent spike growth period (Slafer *et al.*, 1996, 2001; González *et al.*, 2003a). It has been proposed that a prolonged SE phase would allow for more dry matter accumulation by the spike due to its longer growth phase, which would ultimately increase yield (Slafer *et al.*, 1996; Miralles & Slafer, 2007; Whitechurch *et al.*, 2007).

Numerous studies focus on photoperiod effects on SE duration (Slafer *et al.*, 2001; Whitechurch & Slafer, 2002; González *et al.*, 2003a; Miralles *et al.*, 2003; Fischer, 2011). It was shown under controlled (Miralles *et al.*, 2000) as well as under field conditions (Whitechurch & Slafer, 2002; González *et al.*, 2003b), that manipulation of photoperiod affects SE duration. The genetics of photoperiod response in wheat have been studied and associated alleles have been found (Mohler *et al.*, 2004; Slafer *et al.*, 2009). Yet, many uncertainties remain in understanding the genetic control of SE duration (Fischer, 2011).

The investigation of growth dynamics during stem elongation is a promising approach to gain further insight in the physiological and genetic mechanisms that control stem elongation duration and its effect on yield. However, studies on wheat growth and development during stem elongation are usually based on a relatively small number of genotypes (Porter & Gawith, 1999). A precise characterisation of the growth dynamics during stem elongation along with the identification of potential key stages during this period in a large set of genotypes could therefore provide helpful information.

Growth dynamics during stem elongation have been studied with focus on single internodes or leaves (Kirby, 1988). Internode elongation has been described as a sigmoidal curve with a prominent middle phase of constant growth in wheat (Kirby, 1988) as well as in maize (Fournier & Andrieu, 2000). On canopy level over the whole SE period, height growth can

therefore be interpreted as multiple stacked sigmoidal curves. We assume that this may be well explained by a linear function.

Growth phenotyping

The quantification of SE growth dynamics and their response to environmental variables requires accurate plant height measurements in high temporal resolution. Especially if the aim is to perform genetic studies, these measurements have to be done on a large number of genotypes at the same time. Traditional methods (*i.e.* measurement by yardstick) lack the necessary throughput and accuracy to perform this task.

In recent years, many novel measurement techniques have become available from the field of plant phenotyping, using a wide range of optical sensors (see Walter *et al.*, 2015 for a review). 3D-Laserscanning has been established as a tool to capture plant architecture under lab- or greenhouse conditions (e.g. Dornbusch *et al.*, 2012; Paulus *et al.*, 2014; Kjaer & Ottosen, 2015). Recently, field phenotyping for height development has been achieved in several platforms (Virlet *et al.*, 2016). 3D terrestrial laser scanning (TLS) has successfully been used for wheat, maize and soybean canopy height measurements in the field (Friedli *et al.*, 2016a). The method developed by Friedli *et al.* (2016a) involves a laser scanner mounted on a tripod. Multiple scans at different positions in the observed field, registered by the means of stationary reference targets, resulted in accurate canopy height measurements under high temporal resolution (Friedli *et al.*, 2016a). The scanner has a technical accuracy of 0.2 cm in 10 m distance. The accuracy of the system measured as average position deviations of the stationary reference targets over time was 0.84 cm with a standard deviation of 0.39 cm. Linear regression between hand measured canopy height and TLS canopy height yielded an R^2 of 0.99 (Friedli *et al.*, 2016a).

Very recently, a unique multi-sensor field phenotyping platform (FIP) allowing for non-invasive measurements on an area of 1 ha by means of a cable-suspended sensor head was developed and built at ETH Zürich (Kirchgessner *et al.*, 2016). The TLS canopy height measurement approach developed by Friedli *et al.* (2016a) was integrated in the system and successfully tested for soybean height measurements (Kirchgessner *et al.*, 2016).

In the present study, TLS plant height measurement under field conditions with the FIP is applied in a set of 335 European wheat genotypes. The set comprises genotypes from the GABI Wheat association panel which consists of European elite cultivars (Kollers *et al.*, 2013) complemented with Swiss wheat varieties. The aims of this study are to:

(A) Test the capability of the measurement system for accurate wheat canopy height measurements in high temporal resolution.
(B) Determine growth dynamics of European wheat during stem elongation.
(C) Evaluate the hypothesis that there is considerable genetic diversity at critical stages of this dynamics.
(D) Determine interactions between the different stages and their relationship to final plant height.

2.2 Material and methods

Plant material and experimental design

During the wheat seasons 2015 and 2016 a field experiment was conducted at the research station of the institute of agricultural science of ETH in Eschikon 33, 8315 Lindau, Switzerland (47.449°N, 8.682°E, 520 m a.s.l.; soil type: eutric cambisol). In 2015, a total of 339 European winter wheat cultivars comprising 300 varieties from the GABI Wheat panel (Kollers *et al.*, 2013) complemented with important Swiss cultivars were sown in an augmented design consisting of two lots. Each was divided into 17 rows and 21 columns resulting in 357 micro-plots with a size of 1.5 m by 1.5 m. One variety was repeated 19 times per lot in order to account for field heterogeneity (see Fig. 1b). Border effects were minimized by surrounding the lots with buffer plots. Sowing was done on October 20, 2014 with a drill sowing machine at a blade distance of 0.17 m resulting in 370 plants m^{-2}. Fertilization and plant protection was performed according to recommended agricultural practice. In 2016, the experiment was repeated with slight alterations to the design. 335 genotypes were sown in two lots with 18 rows and 20 columns each. Four old Swiss varieties present in the 2015 field experiment were excluded due to their lodging susceptibility. The sowing date for the 2016 season was October 13, 2015.

Canopy height measurements

Canopy height was measured every 3-4 days from April 16 until July 10, 2015 and from April 11 until July 4 2016 by using a FARO® Laser Scanner Focus3D S 120 (Faro Technologies Inc., Lake Mary USA) mounted on the FIP (Fig.1a, for a detailed description of the system see Kirchgessner *et al.*, 2016). The laser scanner produces a three dimensional point cloud representing the scanned area relative to the scanner. In each lot, 16 scans were taken at defined positions on every measurement date. The 16 resulting scan point clouds were then stationed and merged together into one single scan point cloud using the software Scene 5.4.4.41689 (Faro Technologies Inc., Lake Mary USA). The stationing of the scans was facilitated by the use of eight spherical reference targets with a diameter of 20 cm (Laserscanning Europe GmbH., Magdeburg Germany), positioned on fixed locations in the field. For a detailed description of the scanner and the applied settings, see Friedli *et al.* (2016a).

Average canopy height of each plot was extracted from the scan point cloud using the custom MATLAB (version 2013b, The MathWorks Inc., Natick, MA, 2000) application CAHST. The software including a manual and example data is available for download from SourceForge (http://sourceforge.net/projects/cahst4tls). In a first step, the z-coordinates (*i.e.* the height) of all scan points were corrected by the soil level by subtracting the respective z-coordinates of a height map of the soil. The soil map was retrieved from a scan of the soil performed six weeks after sowing when soil was still largely visible. This resulted in a height map for the complete scan point cloud for every measurement date (Fig. 1d). In a second step, the point height was extracted for the centre (0.5 m by 0.5 m) of each plot by applying a grid. Third, the normalized cumulated point height frequency was

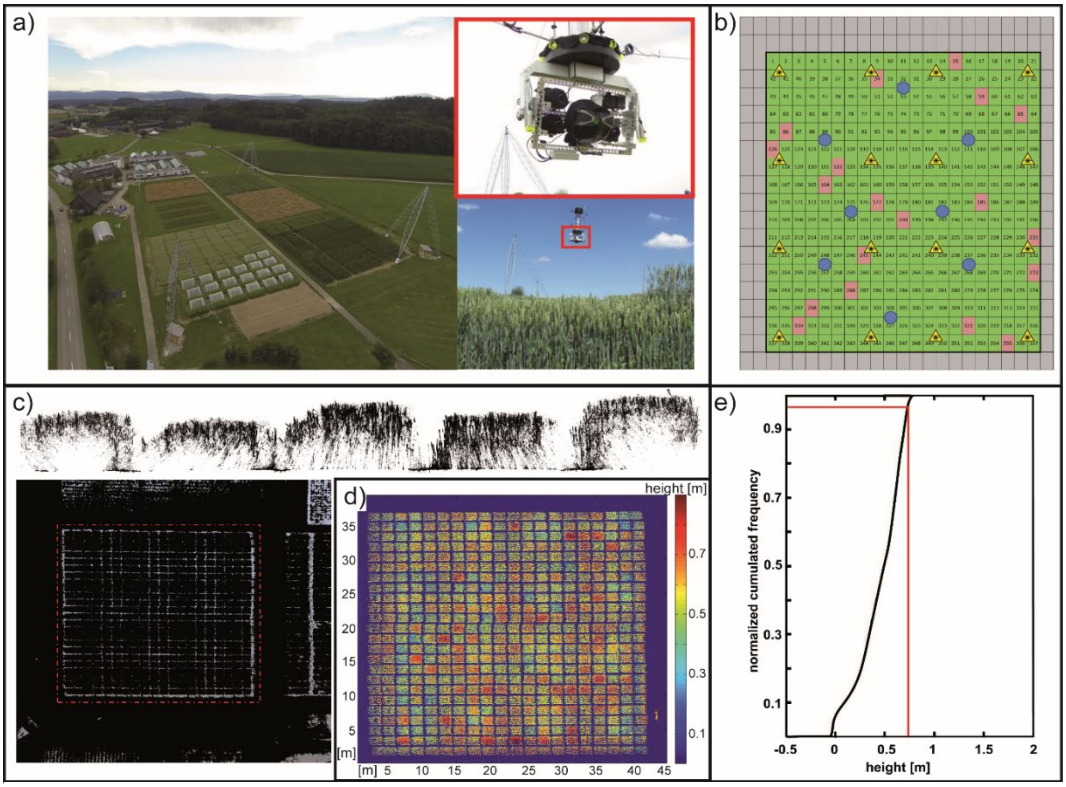

Fig. 1: Overview of the Field Phenotypig Platform (FIP) and the 3D terrestrial laser scanning (TLS) system to measure plant height: **a)** FIP overview with poles sustaining the rigging system (picture supplied by D. Constantin, M. Rehak and Y. Akhtman, EPFL ENAC TOPO) and sensor head; **b)** positions of the TLS (triangles), reference sphere (dots) and "check" varieties (red squares); **c)** scan point cloud with highlighted area of the experimental field and a cross section through the scan point cloud region of 5 adjacent plots; **d)** height map of soil corrected point cloud a scan of one lot; **e)** normalized cumulated frequency of the height distribution of scan points for one plot; the red line shows the 97th percentile

calculated. Of this, the 97th percentile was taken as canopy height of the plot in question (Fig. 1e). Friedli *et al.* (2016a) tested several filtering approaches to extract canopy height from scan point clouds. They found the 99th percentile of all points to be the best measure for canopy height in wheat due to the exclusion of outliers and therefore reduced risk of overestimation. In our data however, percentiles above the 97th percentile didn't exclude critical outliers. All further data analysis was performed using the software RStudio (RStudio Team, 2015) with the environment R (R Core Team, 2015).

In a subset of 48 plots per lot, plant height was measured manually with a commercial yardstick in 2015. On every measurement day the average height of 10 randomly chosen plants in the centre of each plot was regarded as plot canopy height. For the 96 plots in which reference measurements were conducted, TLS plant height was correlated with manual plant height. To test the accuracy of the TLS measurement, a linear model fit was applied over all measurement dates.

Meteorological data

Temperature data was retrieved from a weather station of the federal Swiss meteorological network Agrometeo (www.agrometeo.ch) based in Lindau at ca. 250 m distance to the field trial. Hourly maximum and minimum temperature was recorded 5 cm above soil. Based on this data, growing degree-days (GDD, McMaster & Wilhelm, 1997) were calculated for both seasons following:

$$Tmean_d = \frac{\sum \frac{max\ T_{d,h} + min\ T_{d,h}}{2} - base\ T}{24} \qquad \text{Eq. 1}$$

$$GDD = \sum_{d=1}^{n} Tmean_d \qquad \text{Eq. 2}$$

where $Tmean_d$ is the mean temperature for day d after sowing, $max\ T_{d,h}$ and $min\ T_{d,h}$ are hourly maximum and minimum temperatures for that day and $base\ T$ is the base temperature set at 0°C. In cases of $(max\ T_{d,h} + min\ T_{d,h}) < 0$, the term was set to zero. GDD are the summed up daily temperature sums from 1 to n days after sowing.

There were data gaps of four and five hours on 2015-03-27 and 2016-06-20 respectively. These were filled with temperature data measured at 10 cm above soil by the weather station located at the research station.

Growth dynamics

Linear regression of canopy height against GDD until final canopy height (FH) was performed for each plot separately following:

$$CH = a + b \cdot GDD + \varepsilon \qquad \text{Eq. 3}$$

where CH and GDD are the canopy height and the growing degree days since sowing, respectively, on the different measurement dates and ε is the residual. The estimated parameter a and b represent the intercept and slope. Calculation was done using R lmList() (Bates *et al.*, 2015).

Final height was defined as the inflection point of the canopy height vs time curve for each plot (Fig. 2). This was done with an algorithm combining the maximum canopy height value, the mean value of the last five measurement points and the point of maximum difference between measurement points and a straight line drawn between first and last measured point. This method created false values e.g. in the case of lodging incidents. Therefore, for each plot FH was visually checked on plotted canopy height vs time including date and final height calculated by the algorithm and manually corrected in case of error. In addition, GDD was calculated from sowing until 15% FH (GDD_{15}) and 95% FH GDD_{95} were reached. This was done by linear interpolation of normalized plant height between consecutive measurement dates. Some genotypes already exceeded 15% FH at the first measurement date. In those cases, GDD_{15} was obtained by linear extrapolation of normalized plant height to days prior to the first measurement date, based on the linear regression slope of measured plant height until FH versus time (Fig. 2). SE duration (GDD_{SE}) was calculated as the difference between GDD_{95} and GDD_{15}. The five parameters FH, intercept of canopy height versus GDD, GDD_{15}, GDD_{95} and GDD_{SE} were used to quantify genotype specific growth habits.

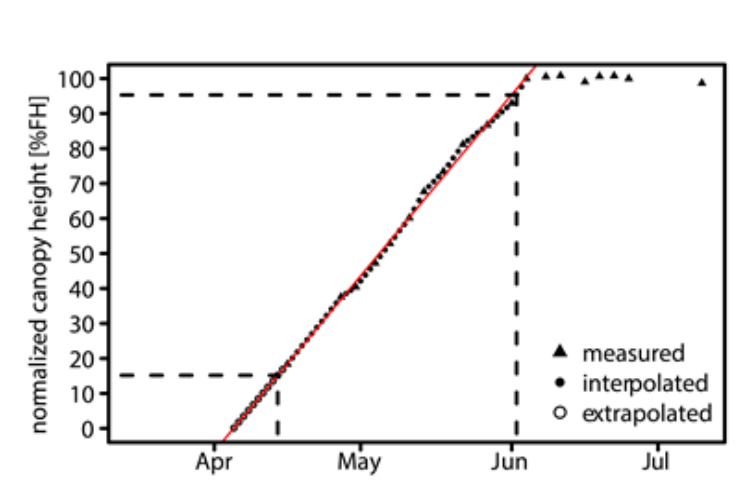

Fig. 2: Normalized canopy height versus time of a single wheat plot. Black dots show the interpolated canopy height between measurement points (black triangles). The solid red line shows the linear regression line of canopy height until final height versus time. Based on the linear regression, canopy height was extrapolated to determine the date of 15% final height (black circles). Dotted black lines show the date of 15% (l.) and 95% (r.) final height respectively.

Genotypic predictors across both years were calculated in a two-step approach using the R-package *asreml* (Butler, 2009). In a first step, a linear mixed model was applied for each individual year:

$$Y_{ijkl} = \mu + g_i + L_j + LR_{jk} + LC_{jl} + \varepsilon_{ijkl} \qquad \text{Eq. 4}$$

where $Y_{i,j}$ is either GDD_{15}, GDD_{95}, GDD_{SE}, FH or the slope of canopy height versus time, μ is the respective intercept, g_i is the effect of the ith genotype (i= 1, …, 335), L is the jth replicate (j = 1, 2 for replicate in each different lot of the FIP) and $\varepsilon_{i,j}$ is the residual error. To control spatial variability additional incomplete blocks were defined where LR is the effect of the kth row in the jth lot and LC is the effect of the lth range in the jth lot. A first order autocorrelation (AR1) model was applied for each lot to account for range- and row wise autocorrelation among plots.

In a second step, a linear model was applied on the genotypic best linear unbiased estimates (BLUEs) from both individual years to obtain genotypic best linear unbiased predictors (BLUPs) across both years:

$$Y_{ij} = \mu + g_i + y_j + \varepsilon_{i,j} \qquad \text{Eq. 5}$$

where Y_{ij} is either GDD_{15}, GDD_{95}, GDD_{SE}, FH or the slope of canopy height versus time, μ is the intercepty_j the fixed effect of the jth year (j = 2014 and 2015), g_i is the random effect i^{th} genotype; and ε_{ij} the residual error including the genotype-by-year interaction.

For all traits, heritability was calculated from genotypic mean values following (Eq. 9):

$$h^2 = \frac{\sigma_G^2}{\sigma_G^2 + \frac{\sigma_\varepsilon^2}{R}} \qquad \text{Eq. 6}$$

where σ_G^2 and σ_ε^2 are the genetic and the error variance, respectively and R = 2 is the number of replicates (years) per genotype (Falconer & Mackay, 1996).

The experiment is being repeated in the wheat season 2017. In order to validate findings related to the beginning of stem elongation (see results; Fig. 7), destructive samples were taken on April 07 (before stem elongation stared) and May 12, 2017 (during early stem elongation), in a subset of 14 genotypes. These comprised the seven earliest (RUNAL, QUATUOR, CARIBOU, CH COMBIN, RICHEPAIN GARCIA, CH CLARO) and seven latest genotypes (SEMPER, NUTKA, RYWALKA, OSTKA STRZELECKA, TONACJA, ZENITH, ZYTA) for GDD_{15} based on best linear unbiased predictors of all 335 genotypes across both years 2015 and 2016. On both sampling dates, three plants per plot in the two replications per genotype were destructively sampled. For each genotype, the average plant size (length from stem base to leaf tip), the height of the ear relative to the stem base and the number of nodes (according to Lancashire *et al.*, 1991) was recorded. Analysis of variance was performed on the individual sampling dates to test for differences between the early and the late group for each trait, by applying a linear mixed model with group and replicate as fixed- and genotype as random variable.

2.3 Results

Verification of TLS plant height measurements

Linear regression between TLS and manual plant height over all measurement dates showed a very strong linear relationship, with R^2 = 0.99, slope = 1.02 and intercept = -0.096 (Fig.3). Pearson correlation coefficients for individual measurement dates varied between 0.80 and 0.98. Plant height measurements were consistent over time.

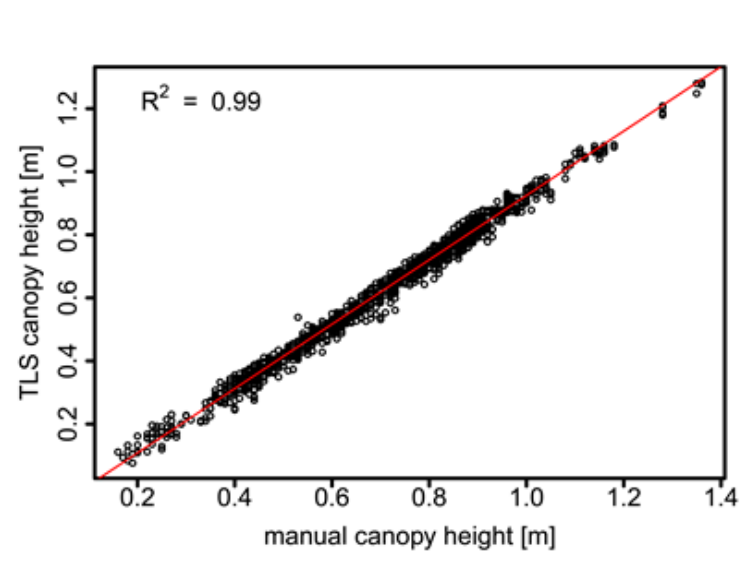

Fig. 3: Linear regression between canopy height measured with terrestrial laser scanning and manually measured canopy height. Data is based on a subset of 96 plots measured on 18 consecutive measurement dates.

Growth dynamics

The average canopy height of all 335 genotypes observed in this study showed similar development in both growing seasons 2015 and 2016 (Fig. 4). Canopy height development clearly followed a linear trend across the whole SE period. The two years differed mainly in the intercept of canopy height versus time with only marginal differences in slopes. Temperature sums across winter and spring (meteorological seasons) were similar in both years, with 1080 GDD in 2015 and 1074 GDD in 2016. However, there were considerable differences when single seasons were compared: The winter season 2014/2015 was colder compared to the winter 2015/2016, with 145 GDD versus 234 GDD from December 1 until February 28/29. Spring (March 1 until May 31) on the other hand was warmer in 2015, with 935 GDD compared to 840 GDD in 2016 (Fig. 5). Average canopy height was considerably higher in 2016 compared to 2015. Across both years, the date when average final height was reached differed only by two days.

Linear regression of canopy height against time and GDD for individual plots showed a strong linear relationship. Correlation between canopy height and time yielded an average R^2 of 0.99 in both years, ranging from 0.92 to 0.99 in 2015 and from 0.81 to 0.99 in 2016. Canopy height versus GDD had an average R^2 of 0.98 ranging from 0.92 to 0.99 in 2015 and an average R^2 of 0.99 ranging from 0.78 to 0.99 in 2016 (Fig. S1).

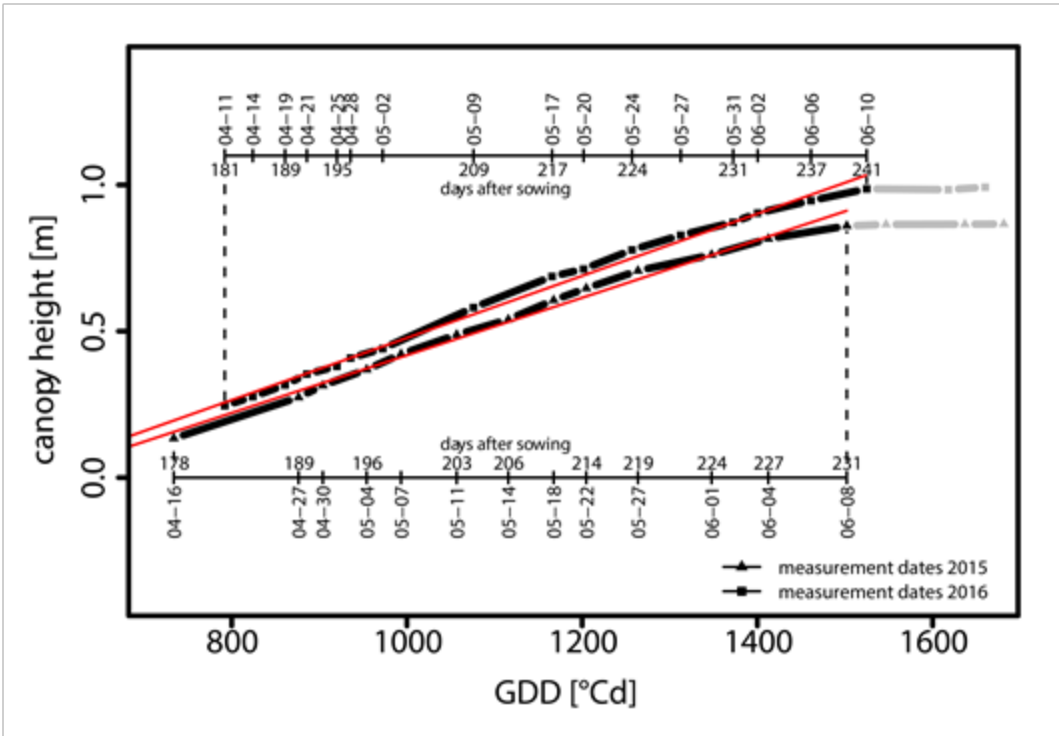

Fig. 4: average canopy height of all 335 genotypes plotted versus growing degree days since sowing (GDD) for each measurement date in 2015 (triangles) and 2016 (squares). The solid red lines show the linear regression line of average plant height versus GDD.

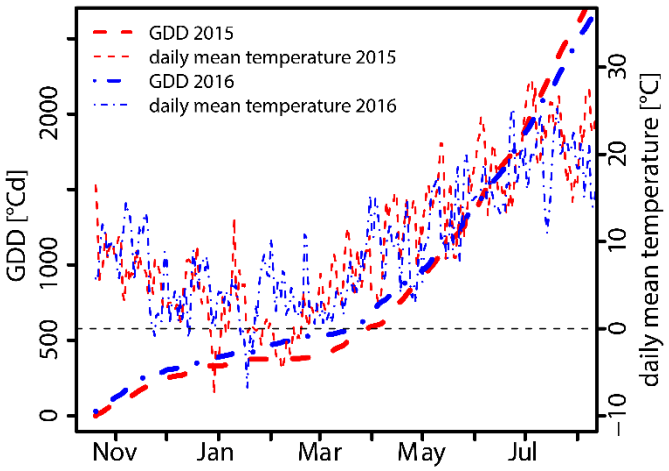

Fig. 5: Climate conditions for the two wheat growth seasons (red dashed: Oct 2014 – Jul 2015; blue dot-dash: Oct 2015 – Jul 2016. Thick lines show growing degree days since sowing, thin lines show daily mean air temperature.

Analysis of variance revealed significant genotypic differences in linear height development (slopes of the linear model; Eq. 3) as well as for GDD_{15}, GDD_{95} GDD_{SE} and FH over two years ($p<0.001$). All these traits had high heritabilities across two years, ranging from 0.74 to 0.93 (Table 1). Best linear unbiased predictors (BLUPs) for the genotype effects showed high variability, with a maximum difference of 159 GDD for GDD_{15}, 298 GDD for GDD_{95}, 224 GDD for GDD_{SE} and 0.59 m for FH (Fig.S2). The distributions of BLUPs showed negative skewness for GDD_{15} and GDD_{95} and positive skewness for GDD_{SE} and FH, indicating a slight tendency for short, late genotypes with short stem elongation periods in the population.

Correlation analysis among the traits used to characterize genotypic growth habit showed strong to very strong positive correlations among FH, GDD_{15}, GDD_{95} (Fig.6). There was a high correlation between GDD_{15} and GDD_{95} and between GDD_{95} and GDD_{SE}. In contrast, GDD_{15} versus GDD_{SE} showed a very weak negative correlation ($r = -0.09$). The slope of the linear regression correlated strongly with FH and GDD_{15} and weakly with GDD_{95}.

Correlations among GDD_{15}, GDD_{95} and GDD_{SE} duration suggested that these growth stages are partially inter-dependent. There were moderate correlations among GDD_{15}, GDD_{95} and final plant height. Stem elongation duration was strongly linked with GDD_{95} but not to any other observed trait. The interdependencies among traits suggest that they are not independently selectable within the evaluated set of genotypes. The response of GDD_{95} and FH to a selection for GDD_{15} is illustrated in Fig.7. The presented values for the 5th and 95th percentile are based on the average of all genotypes with GDD_{15} outside the 5th percentile ($n = 13$) and outside the 95th percentile ($n = 11$), respectively. The values for the 25th and

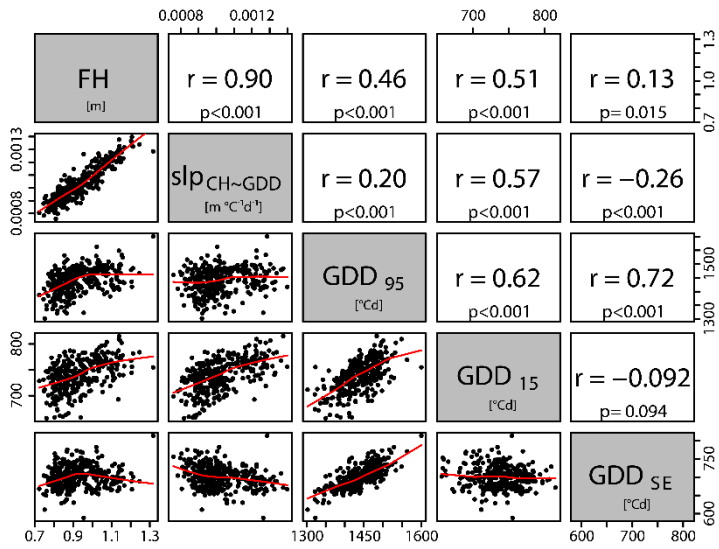

Fig. 6: Correlations among the traits final canopy height (FH), linear model slope of canopy height versus growing degree days (GDD; $slp_{CH\sim GDD}$), GDD until 15% final height (GDD_{15}), GDD until 95% final height (GDD_{95}), and duration of stem elongation phase (GDD_{SE}). The upper panel shows Pearson correlation coefficients based on best linear unbiased predictors of all 335 genotypes and corresponding p-values. The lower panel shows scatterplots and lowess curves of the value pairs between the respective traits.

75th percentile are based on the average of all genotypes with values within the 5% range around the respective percentiles (n = 14 for the 25th, and n = 17 for the 75th percentile) and the values for the 50th percentile are based on the population average. Genotypes with a successively later start of stem elongation (GDD_{15}) reach their final height successively later and become taller. Selecting genotypes with values around the 25th and 75th percentile of GDD_{15} results in variability in GDD_{95} and FH inside the range of variation explained by their covariation with GDD_{15} (Fig. 7, yellow rectangle). Selection in the population extremes (< 5% and > 95%; Fig. 7) however exceed that range. The selection of the latest

Table 1: Heritabilities across both years for final height (FH), intercept ($Intercept_{CH\sim GDD}$) and slope ($Sope_{CH\sim GDD}$) of linear regression between canopy height and growing degree days (GDD), GDD until 15% (GDD_{15}) and 95% (GDD_{95}) final canopy height and duration of stem elongation (GDD_{SE}).

Trait	Heritability
FH	0.96
$Intercept_{CH\sim GDD}$	0.88
$Sope_{CH\sim GDD}$	0.93
GDD_{95}	0.91
GDD_{15}	0.85
GDD_{SE}	0.76

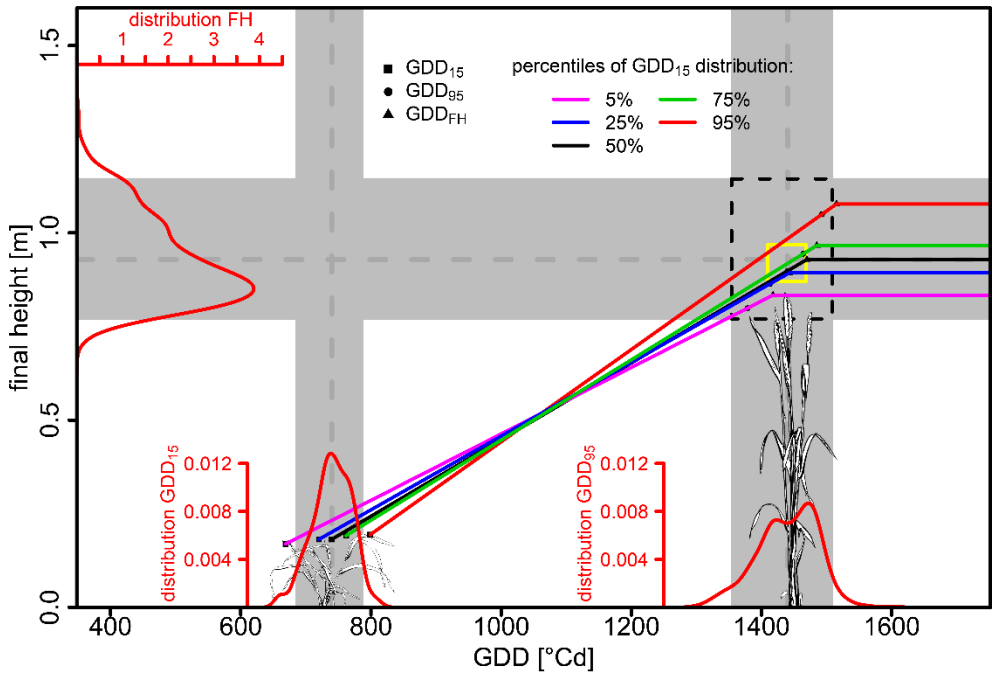

Fig. 7: The interdependency among GDD_{15}, GDD_{95} and FH from the perspective of a selection based on GDD_{15}. The grey shaded areas show the range of the 95% interval of the genotypic variation (BLUPs) for GDD_{15}, GDD_{95} and FH. The width and height of the yellow rectangle shows the variance in this range of GDD_{95} and FH respectively, which is explained by GDD_{15} based on the R2 of the correlation analysis (Fig. 6). Coloured lines indicated the co-selection of GDD_{95} and FH in case of a selection of genotypes of the 5th, 25th, 50th, 75th and 95th percentile (see text for details) of the genotypic variation in GDD_{15}, respectively.

5% (> 95%) among the varieties for GDD_{15}, led to the co-selection of a late final height and a tall canopy. In tendency, shorter genotypes are also earlier (positive correlation between GDD_{15} and FH, $R^2 \sim 0.25$).

The seven earliest and latest genotypes for GDD_{15} were evaluated for morphological differences in 2017. On the first sampling date, the apical meristem was still not more than 1 cm above the shoot base for both groups. However, the early genotypes had on average already a 5.7 cm greater plant size ($p < 0.01$) and a slight tendency towards a greater ear height (n.s.; Fig. 8). On the second sampling date, the early genotypes had a 4.5 cm greater plant size ($p < 0.001$), a 2.8 cm greater ear height ($p < 0.1$) and on average 0.5 more nodes nodes ($p < 0.05$) (Fig. 8).

2.4 Discussion

TLS enables high throughput phenotyping of canopy height with high spatial and temporal resolution

TLS measurements with the scanner mounted on the FIP resulted in highly precise canopy height measurements. The obtained R^2 from linear regression against reference measurements are analogous to those obtained by Friedli *et al.* (2016a). The intercept of the regression indicates an underestimation of plant height measured by TLS relative to the hand measurements by roughly 10%. The explanation for this is that choosing the 97th height percentile of the scan point cloud might be too restrictive. Taking the 100th percentile as plot height reduces the intercept to close to zero but also reduces R^2 drastically (data not shown). The 97% threshold was adopted to remove numerous outliers in the point

cloud of the scan, due to objects above the canopy, such as parts of the sensor head, flying insects etc. Since the discrepancy between hand and TLS measurement is constant, it can easily be corrected and does not affect the ranking between genotypes.

One aim of the present study was to test, whether the employed TLS approach with the field phenotyping platform is suitable in terms of accuracy and throughput. The obtained results show that the applied TLS approach is suitable to measure growth during SE precisely enough to detect genotypic differences in SE at a high temporal resolution. Concerning throughput, the system with the applied settings allowed measuring plant height in total of 714 plots within 3.5 h, including the time for setting up the device and spherical targets. This is fast enough to screen a genetic mapping population (Grieder *et al.*, 2015), as has been confirmed in this study. With the current setting, the needed time would even allow screening twice a day or during the night and thus further increase temporal resolution.

In the present study, we measured wheat canopy height in a time resolution of three days on a large set of genotypes which well represents European elite wheat germplasm. Previous studies investigating wheat growth during SE had a measurement frequency similar to the present study (Siddique *et al.*, 1989; Flink *et al.*, 1995) or even higher in the case of (Kirby, 1988) who measurement daily. The number of observed genotypes in those studies was however significantly lower compared to the present study. Kirby (1988) and Flink *et al.* (1995) used one variety each, the former in a greenhouse experiment, the latter in a field trial. Siddique *et al.* (1989) used a total of 26 varieties in three field experiments. In these studies, plant height or length of single stem organs was measured by hand. This allows for high accuracy and time resolution given a small enough number of experimental units. It would however be impossible on a scale as proposed here.

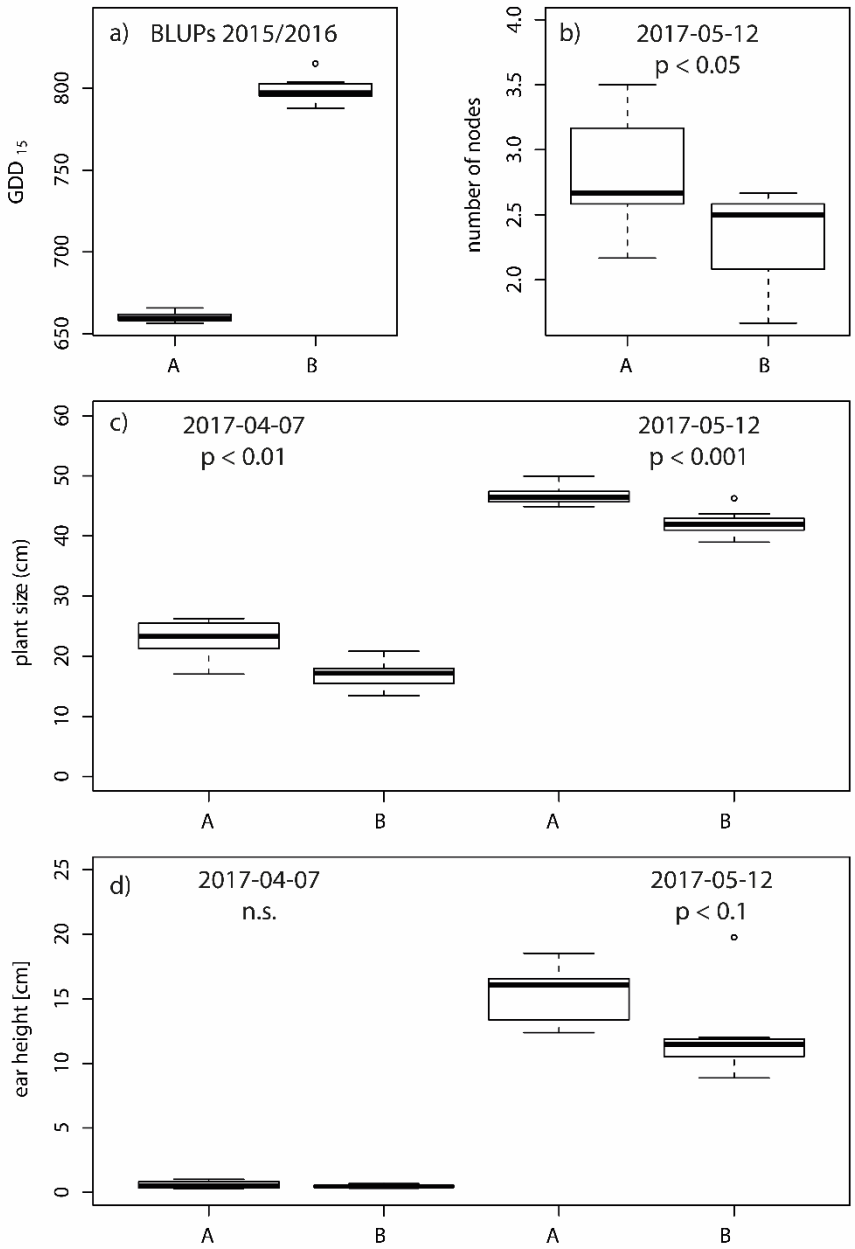

Fig. 8: Boxplots of best linear unbiased predictors (BLUPs across season 2015 and 2016) of the earliest (A) and latest (B) seven genotypes with regard to the growing degree days at which 15% of final plant height (GDD_{15}) was reached (a). Boxplots of the performance of the selected groups in 2017 with regard to the number of nodes at the elongating stem (**b**), the plant size (length from stem base to leaf tip, (**c**) and ear height above the stem base (**d**) either before (April 7) or after the start of stem elongation (May 12). Each boxplots is based on the mean of the seven genotypes per group.

The wheat canopy showed an almost linear increase in height during the stem elongation phase

We observed a more or less linear height development for almost all genotypes between the start of stem elongation until the final height was reached. It has been reported previously, that single internode elongation in wheat (Kirby, 1988) and maize (Fournier & Andrieu, 2000) follows a sigmoidal trend. Based on the present study, we assume that the sum effect of the elongation dynamics of all elongating internodes can be described as linear. The results show that wheat growth during the stem elongation follows a clear linear trend. However, if growth rates between consecutive measurement dates are considered (data not shown, for an illustration see Fig. 2), consistent deviation over time from this linear trend can be observed. One explanation for this could be that the sum of sigmoidal single internode elongations does not result in a linear function. On the other hand, the linear relationship found in this study is highly significant with high R^2 across all genotypes. Applying a non-linear regression did not result in a better model fit (data not shown). Therefore, SE could indeed be linear and the deviations could offer opportunities to investigate responses to short term fluctuations of environmental parameters.

TSL enabled a precise measurement of three highly heritable traits: the beginning and end of stem elongation, as well as final height

By means of TLS we could quantify three potentially independent traits: i) the onset of stem elongation, ii) the end of stem elongation and iii) the final height. Due to the linearity of stem elongation, the measuring times might be reduced in future experiments by focussing on the critical phases of the beginning and end of stem elongation. The high heritability of these traits across the two years indicates sufficient response to selection. Yet their co-variance indicates pleiotropic effects or epistatic interactions of the underlying genes. Such effects should be taken into account when aiming for trait-based selection. We did not take into account population structure as possible reason for these dependencies. However, the population used shows little population structure (Kollers *et al.*, 2013) and it seems unlikely that it would be the primary cause of the observed relationship. The duration of stem elongation was primarily influenced by the variation in GDD_{95} while the variation in GDD_{15} had little influence. This independence between SE duration and the duration of prior phases has been reported before (Whitechurch *et al.*, 2007). Our results suggest that variation in GDD_{15} has an indirect effect on GDD_{95} but does not affect SE duration.

We propose TSL measurements for determining the difficult-to-measure onset of stem elongation

The beginning of stem elongation is a stage which is usually difficult to measure non-destructively and with high throughput. Termination of SE can be regarded as a proxy measure for flowering time, which is an important breeding trait that has been much exploited (Jung & Müller, 2009b; Borràs-Gelonch *et al.*, 2012). Also final height may be efficiently determined by hand measurements or, by one single TLS scan at the end of flowering. However, the variability of GDD_{15} (*i.e.* the onset of SE) could be a beneficial

new proxy measure to evaluate the beginning of stem elongation. It is one of five critical stages of wheat which is frequently used in crop models (Holzkämper *et al.*, 2015). Yet, it is the only stage among the five that is difficult to assess on a large set of genotypes. Whereas crop emergence, the 3-leaf stage, anthesis and physiological maturity can be evaluated non-destructively in a fairly rapid manner, the beginning of stem elongation must be determined destructively. Plants need to be dissected to determine the time at which the first node, which is hidden within the leaf sheaths, is approximately 1 cm above the tillering node (Pask *et al.*, 2012). Accordingly, a reliable proxy measure for this critical stage will greatly enhance our understanding about its genetic control and importance for crop improvement.

Based on the two years data, we selected early and late types with regard to GDD_{15} and evaluated following season. The selected genotypes clearly differed for plant size before the onset of stem elongation. Accordingly, the selection was not only affecting timing but also growth type. As stems were not elongated at the early sampling date, the greater plant size must be related to longer leaves. This indicates, that also the baseline, *i.e.* the plant height before stem elongation is an important parameter, when selecting for earliness using the height dynamics. Nevertheless, the advanced earliness of the early group compared to the late group is supported by its advanced development at the second damping date indicated by more nodes and taller plants. To what degree the two traits, taller plants with longer leaves and earlier start of stem elongation be genetically linked needs to be subject of further evaluations. Remarkably, three of the seven earliest genotypes (CH CLARO, RUNAL and CH COMBIN) are elite varieties derived from the Swiss breeding program at Agroscope and widely grown in Switzerland.

2.5 Conclusion and outlook

We observed a high heritability for the onset of stem elongation. By selecting earliest and latest genotypes, we could show that the early plants were not only elongating earlier but plants were already taller. Accordingly, the initial height before stem elongation should be determined in future experiments. Large field phenotyping platforms such as the FIP are suitable for determining the genetic basis of complex traits which are difficult to assess in normal field settings. The systems stationarity confines its application to a single environment, which limits its application for breeding related studies, where multiple environments are desired. Yet the high heritabilities of the observed traits across years indicate that it might be sufficient to evaluate them in a limited number of years or environments. Furthermore, drone technology is advancing rapidly. Canopy height measurement with drones is currently possible from digital images as well as drone carried light weight laser scanners, although it might lack the accuracy as proposed in our study. However, the accuracy of UAV plant height measurement can be expected to increase in the near future. This would allow for the application of the approach proposed in this study in multiple environments. Thus, the timing of the onset and end of stem elongation could be integrated in large scale breeding programs at low labour cost. A genome wide

association study (GWAS) is in progress to identify the genomic regions controlling the evaluated traits.

Acknowledgements

We thank Norbert Kirchgessner for his constant support for operating the FIP and for his support during the analysis of scan point data using his software package CAHST. We also sincerely thank Hansueli Zellweger for managing and nursing our field experiment. Special thanks are dedicated to Caterina Schürch for drawing the wheat plants shown in figure 9 and to the ETH Crop Phenotying class 2017 for the support during sampling and evaluation of the contrasting groups. Finally, we thank the anonymous reviewers for their helpful comments and suggestions as well as the Swiss Federal Office for Agriculture FOAG which supported this project.

3 Temperature response of wheat affects final height and the timing of key developmental stages under field conditions

Lukas Kronenberg[a], Steven Yates[b], Martin P. Boer[c], Norbert Kirchgessner[a], Achim Walter[a], Andreas Hund[a]

[a] Crop Science, Institute of Agricultural Sciences, ETH Zürich, 8092 Zurich, Switzerland
[b] Molecular Plant Breeding, Institute of Agricultural Sciences, ETH Zürich, 8092 Zurich, Switzerland
[c] Biometris, Wageningen University & Research, 6708 PB Wageningen, The Netherlands

This chapter is a reprint of the manuscript with the same title submitted to Journal of Experimental Botany on 2019-09-03, currently under review and available as preprint on bioRxiv (https://doi.org/10.1101/756700).

Abstract

In wheat, the timing and dynamics of stem elongation are tightly linked to temperature. It is yet unclear if and how these processes are genetically controlled. We aimed to identify quantitative trait loci (QTL) controlling temperature-response during stem elongation and to evaluate their relationship to phenology and height. Canopy height of the GABI wheat panel was measured between 2015 and 2017 in bi-weekly intervals in the field phenotyping platform (FIP) using a LIDAR. Temperature-response was modelled using a linear regression between stem elongation and the mean interval temperature.

The temperature-response was highly heritable ($H^2 = 0.81$) and positively related to a later start and end of stem elongation as well as an increased final height (FH). Genome-wide association mapping revealed three temperature-responsive and four temperature-irresponsive QTL. Furthermore, putative candidate genes for temperature-response QTL were frequently related to the flowering pathway in *A. thaliana* while temperature–irresponsive QTLs corresponded with growth and reduced height genes. These loci, together with the loci for start and end of stem elongation accounted for 49% of the variability in height.

This demonstrates how high throughput field phenotyping in combination with environmental covariates can contribute to a smarter selection of climate-resilient crops.

Key Words: field phenotyping, wheat, physiology, temperature-response, development, plant height

3.1 Introduction

Temperature is a major abiotic factor affecting plant growth and development. As a consequence of Global warming, wheat production could decrease by 6% per °C global temperature increase (Asseng *et al.*, 2015). While heat stress during critical stages can drastically reduce yield (Gibson & Paulsen, 1999; Farooq *et al.*, 2011), warm temperatures can decrease yield by accelerating development and thereby shortening critical periods for yield formation (Fischer, 1985; Slafer & Rawson, 1994). However little is known about how temperature affects development and growth, and how this is genetically controlled.

The critical phase for yield formation in wheat is stem elongation (SE); happening between the phenological stages of terminal spikelet initiation and anthesis (Slafer *et al.*, 2015). The start of SE coincides with the transition from vegetative to reproductive development, when the apex meristem differentiates from producing leaf primordia to producing spikelet primordia (Trevaskis *et al.*, 2007a; Kamran *et al.*, 2014). During SE, florets are initiated at the spikelets until booting (Kirby, 1988; Slafer *et al.*, 2015). An increased duration of stem elongation increases the number of fertile florets due to longer spike growth and higher dry matter partitioning to the spike (González *et al.*, 2003b). This in turn increases the number of grains per spike and therefore yield (Fischer, 1985). Modifying the timing of the critical phenological stages (transition to early reproductive phase and flowering) and SE duration has been proposed as way to increase wheat yield or at least mitigate adverse climate change effects on yield (Slafer *et al.*, 1996; Miralles & Slafer, 2007; Whitechurch *et al.*, 2007). The recent warming trend causes a faster advancement in phenology. For example over the past decade flowering time occurred earlier in Germany, which is attributable to both, increased temperature and selection for early flowering (Rezaei *et al.*, 2018).

Final height is also an important yield determinant. During the "green revolution" wheat yields increased by the introduction of reduced height genes (*Rht*). The resulting dwarf and semi dwarf varieties benefit from improved resource allocation from the stem to the spike and reduced lodging, allowing more intensive nitrogen application (Hedden, 2003). Gibberellin insensitive *Rht* genes (*Rht-A1*, *Rht-B1*, and *Rht-D1*) were shown limit cell wall extensibility which decreases growth rates (Keyes *et al.*, 1989) without affecting development (Youssefian *et al.*, 1992a). Whilst the allele *Rht-B1c* (Wu *et al.*, 2011) and the GA sensitive *Rht12* dwarfing gene (Chen *et al.*, 2013) delay heading.

The main abiotic factors affecting the timing of floral initiation and flowering are temperature and photoperiod; with temperature affecting both vernalisation and general rate of development (Slafer *et al.*, 2015). These developmental transitions are controlled by major genes involved in the flowering pathway, namely; vernalisation (*Vrn*), photoperiod (*Ppd*) and earliness per se (*Eps*) genes (Slafer *et al.*, 2015). The *Ppd* and *Vrn* genes define photoperiod and vernalisation requirements which jointly enable the transition to generative development and define time to flowering. Whereas *Eps* genes fine tune the timing of floral transition and flowering, after vernalisation and photoperiod requirements are fulfilled (Zikhali & Griffiths, 2015). While vernalisation and photoperiod response are

well known, the role of temperature *per se* remains less clear. Temperature affects all developmental phases and warmer ambient temperatures generally accelerate growth and development in crops (Slafer & Rawson, 1994, 1995a,d; Atkinson & Porter, 1996; Fischer, 2011; Slafer *et al.*, 2015). But it is unclear, if temperature-response governs growth rate and development independently. If so, the question remains whether there is enough genetic variability in temperature-response to be used in a breeding context (Parent & Tardieu, 2012).

Genotypic variation for growth response to temperature was reported for wheat leaf elongation rate (Nagelmüller *et al.*, 2016), as well as for canopy cover growth (Grieder *et al.*, 2015). Kiss *et al*. (2017) reported significant genotype by temperature interactions in the timing of stem elongation as well as temperature dependent differences in the expression of *Vrn* and *Ppd* genes under controlled conditions. Under field conditions, the response of stem elongation to temperature has not yet been investigated in high temporal resolution.

In recent years, new high throughput phenotyping technologies have enabled monitoring plant height with high accuracy and frequency in the field (Bendig *et al.*, 2013; Friedli *et al.*, 2016b; Holman *et al.*, 2016; Aasen & Bareth, 2018; Hund *et al.*, 2019). We have previously demonstrated that the ETH field phenotyping platform (FIP; Kirchgessner *et al.*, 2016) can be used to accurately track the development of canopy height in a large set of wheat genotypes using terrestrial laser scanning (Kronenberg *et al.*, 2017). Considerable genotypic variation was detected for the start and end of SE which correlated positively with final canopy height (Kronenberg *et al.*, 2017).

While many temperature-independent factors affecting plant height are known, the influences of temperature-dependent elongation and timing of the elongation phase is less clear. To address this, we aimed to dissect final height into the following components: i) temperature-independent elongation, ii) temperature-dependent elongation and iii) the duration of the elongation phase determining by the start and end of the process. To achieve this we present a method to assess and measure these three processes under field conditions by means of high-frequency, high-throughput phenotyping of canopy height development. The resulting data were combined with genetic markers to identify quantitative trait loci controlling the aforementioned processes.

3.2 Material and methods

Experimental setup, phenotyping procedures and extracted traits

Field experiments were conducted in the field phenotyping platform FIP at the ETH research station in Lindau-Eschikon, Switzerland (47.449°N, 8.682°E, 520 m a.s.l.; soil type: eutric cambisol). We used a set of approximately 330 winter wheat genotypes (335 – 352 depending on the experiment) comprising current European elite cultivars (GABI Wheat; Kollers *et al.*, 2013), supplemented with thirty Swiss varieties. These were monitored over three growing seasons in 2015, 2016 and 2017. Details about the

experimental setup for the growing seasons 2015 and 2016 are described in Kronenberg *et al*. (2017). Briefly, the field experiments were conducted in an augmented design with two replications per genotype using micro plots with a size of 1.4 by 1.1 m. In the growing season 2017, the experiment was repeated again, with minor changes in genotypic composition. This resulted in 328 genotypes present across all three experiments.

Canopy height was measured twice weekly from the beginning of shooting (BBCH 31) until final height using a light detection and ranging (LIDAR) scanner (FARO R Focus3D S 120; Faro Technologies Inc., Lake Mary USA) mounted on the FIP (Kirchgessner *et al.*, 2016). Canopy height data was extracted from the LIDAR data as described in Kronenberg et al. (2017). Spatial heterogeneity at each measuring date was corrected by applying two-dimensional P-splines to the raw canopy height data within each year using the R-package SpATS (Rodríguez-Álvarez *et al.*, 2018). The start, end, and duration of stem elongation with final canopy height (FH) were extracted from the height data as described by Kronenberg *et al*. (2017): Normalized canopy height was calculated as percent of final height at each day of measurement for every plot and then linearly interpolated between measurement points. Growing degree-days until 15% final height (GDD_{15}) and 95% final height (GDD_{95}) were used as proxy traits for start and end of stem elongation, respectively. SE duration was recorded in thermal time (GDD_{SE}) as well as in calendar days ($time_{SE}$), as the difference between GDD_{95} and GDD_{15} (Kronenberg *et al.*, 2017).

In order to investigate short-term growth response to temperature, average daily stem elongation rates (SER) were calculated for each plot as the difference (Δ) in canopy height (CH) between consecultive timepoints (t):

$$SER = \frac{\Delta CH}{\Delta t} \qquad \text{Eq. 1}$$

Extracting growth response to temperature

Temperature response was modelled by regressing average daily stem elongation rates (SER) against average temperature of the respective interval for each plot within the respective year following

$$SER = (a \times T) + b_{T_{crit}} + \varepsilon \qquad \text{Eq. 2}$$

where T is the ambient temperature, a is the coefficient of the linear regression (*i.e.* growth response to ambient temperature; $slp_{SER\sim T}$) and ε denotes the residual error. b_{Tcrit} is the model intercept at the temperature, at which the correlation between intercept ($int_{SER\sim T}$) and slope is zero (*see below*). Per definition, the intercept of a linear model would be calculated at T = 0 °C, *i.e.* far outside the range of observed temperatures. In the observed data, the intercept at T = 0 °C correlated strongly negative with the slope (Fig. 1A) and thus, did not add much additional information concerning the performance of the evaluated genotypes. Likewise, an intercept at 20 °C, at the upper range of the observed data correlated strongly positive with the slope (Fig. 1 A). Grieder *et al*. (2015) performed a similar analysis for the canopy cover development during winter and found a similar, strongly negative correlation

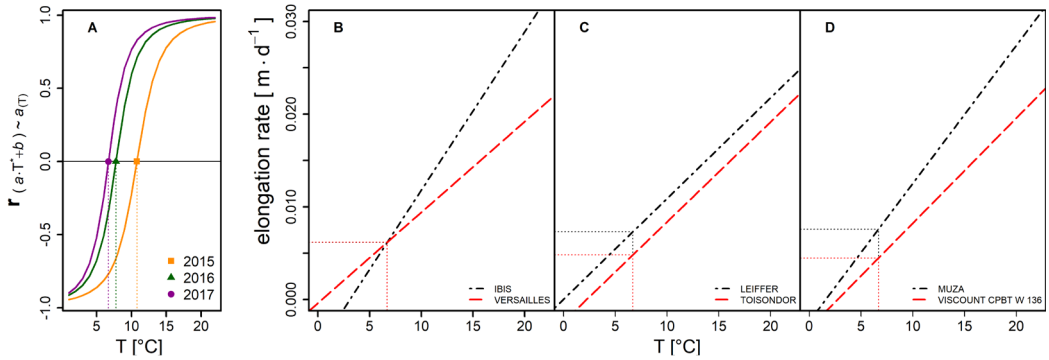

Fig. 1: Illustration and interpretation for the parameters of the applied temperature response model (eq. 2). A: Distribution of Pearson correlation coefficients between intercept and slope of the linear model for individual years, depending on the temperature, at which the intercept is calculated. Dotted vertical lines indicate the critical temperature (T_{crit}) for individual years used to calculate the intercept. **B-D:** Illustration of the relation between intercept and slope on contrasting genotypes (dashed and dash-dotted lines). **B:** same vigour but different in temperature-response. **C** both have the same T-response but differ in vigour. **D** Genotypes differ in vigour as well as in T-response. Horizontal and vertical dotted lines indicate vigour and T_{crit} respectively. The two contrasting genotypes per example **(B-D)** were selected from the 2017 data based on their vales for slope and intercept.

between temperature-response (slope) and growth at 0 °C (intercept). We sequentially calculated the intercept at temperatures from 1 °C to 22 °C for all plots within a year and then calculated the Pearson correlation coefficient between slope and intercept at each temperature (Fig. 1 A). Thus, we empirically determined the critical temperature value (T_{crit}) at which the correlation between slope and intercept was zero (Fig. 1A). Hence, T_{crit} is the point where intercept and slope are independent. Due to this independence, the value of the intercept at T_{crit} can be interpreted as intrinsic growth component independent of temperature response herein referred to as "vigour". Following this, two genotypes can show the same vigour but differ markedly in temperature-response (Fig. 1B), have the same temperature-response but differ in vigour (Fig. 1C), or differ for both, temperature response and vigour (Fig. 1D).

Statistical Analysis

All statistical analysis were performed in the R environment (R Core Team, 2015). Best linear unbiased estimations (BLUEs), predictors (BLUPs) and broad sense heritabilities (H^2) were determined for all traits using the R-package *asreml* (Butler, 2009). In a first step, BLUEs were calculated within each year using:

$$Y = \mu + g + \varepsilon \qquad \text{Eq. 3}$$

Where Y is the respective trait (FH, GDD_{15}, GDD_{95}, GDD_{SE}, $int_{SER\sim T}$ or $slp_{SER\sim T}$), μ is the overall mean, g the fixed genotype effect and ε is the residual error.

In a second step, 3-year BLUPs were calculated using

$$Y = \mu + g + y + \varepsilon \qquad \text{Eq. 4}$$

where Y are the single-year BLUEs for the respective traits derived from eq. 3, μ is the overall mean, g is the genotype effect, y is the year effect and ε is the residual error. Broad sense heritabilities were calculated following Falconer and Mackay (1996) as

$$H^2 = \frac{\sigma_G^2}{\sigma_G^2 + \frac{\sigma_\varepsilon^2}{3}} \qquad \text{Eq. 5}$$

where σ_G^2 and σ_ε^2 are genotypic and residual variance, respectively, from eq. 4 .

The three year BLUPs of GDD_{15}, GDD_{95}, GDD_{SE}, FH, $int_{SER\sim T}$, and $slp_{SER\sim T}$ were used for correlations and genome wide association study (GWAS).

Association study

The genetic basis of temperature-response was investigated by GWAS. GWAS was performed on the different traits to compare the phenotypic correlations with the underlying genetic architecture of the traits. As a positive control final height data made in Germany and France by Zanke *et al*., (2014b) was also compared and analysed.

Genotyping data was made previously by the GABI wheat consortium represented by the Leibniz Institute of Plant Genetics and Crop Plant Research (IPK; Zanke *et al.*, 2014a) using the 90K illumina SNP-chip (Cavanagh *et al.*, 2013; Wang *et al.*, 2014). Monomorphic SNPs were discarded. The remaining markers were mapped to the IWGSC reference genome (Consortium (IWGSC) *et al.*, 2018) by BLASTN search using an E-value threshold < $1e^{-30}$. The genome position with the lowest E-value was assigned as the respective marker location. Markers that could not be unequivocally positioned were dropped. After filtering SNPs with a minor allele frequency and missing genotype rate < 0.05, a total of 13,450 SNP markers and 315 genotypes remained in the set. The reference genome position of *Rht*, *Ppd*, *Vrn* and putative *Eps* genes was determined with BLASTN search as described above using published GenBank sequences (Table S1).

To mitigate against multiple testing, relatedness and population structure; three different methods were used to calculate marker trait associations (MTA) between phenotypic BLUPs and SNP markers:

i) We used a mixed linear model (MLM) including principal components among marker alleles as fixed effects and kinship as random effect to account for population structure (Zhang *et al.*, 2010). This approach was chosen to stringently prevent type I errors. The MLM GWAS was performed using the R Package GAPIT (v.2, Tang *et al.*, 2016). Kinship was estimated according to VanRaden (2008).

ii) In a generalised linear model (GLM) framework implemented in PLINK (Purcell *et al.*, 2007), association analysis was performed using SNP haplotype blocks consisting of adjacent SNP triplets. Using haplotype blocks takes the surrounding

region of a given SNP into account, thus increasing the power to detect rare variants (Purcell *et al.*, 2007).

iii) Finally, the FarmCPU method (Liu *et al.*, 2016) was used, which is also implemented in GAPIT. FarmCPU tests individual markers with multiple associated markers as covariates in a fixed effect model. Associated markers are iteratively used in a random effect model to estimate kinship. Confounding between testing markers and kinship is thus removed while controlling type I error, leading to increased power (Liu *et al.*, 2016).

For all methods, a Bonferroni correction was applied to the pointwise significance threshold of $\alpha = 0.05$, to avoid false-positives. Hence, only markers above $-\log_{10}(P\text{-value}) >= 5.43$ considered significant.

Linkage disequilibrium (LD) among markers was estimated using the squared correlation coefficient (r^2) calculated with the R package SNPrelate (Zheng *et al.*, 2012). A threshold of $r^2 = 0.2$ (Gaut & Long, 2003) was applied to calculate the chromosome specific distance threshold of LD decay. Putative candidate genes were identified by searching the IWGSC annotation of the reference genome (Consortium (IWGSC) *et al.*, 2018) for genes associated with growth and development within the LD distance threshold around the respective MTA.

3.3 Results

Phenotypic results

We measured the canopy height of 710 – 756 plots per year, containing 335 – 352 wheat genotypes, for three consecutive years. In each season measurements were made between 17 and 22 times during stem elongation. Thus resulting in an average of 122 canopy height measurement points per genotype. From these data we extracted growth rates and the timing of critical stages. Plot based growth rates within single years indicate a clear relation between growth and temperature for the period of stem elongation, as depicted in Fig. 2. Towards the end of the measurement period in June, there was a larger deviation, which was also reflected in the quality of plot based linear model fits of SER versus temperature (*see* Eq. 2), summarized in Fig. S1. For the 2015 and especially the 2016 experiment, R^2 values were low and except for the 2017 experiment, the parameter estimates were not statistically significant (Fig. S1A). Inspection of the best and worst model fits however shows, that failure of fitting the model for single plots was levelled out by the replications within genotypes (Fig. S1B), therefore allowing for confident estimates of genotypic means of the model parameters (see below). Analysis of variance revealed significant ($P < 0.001$) genotypic effects for both $slp_{SER\sim T}$ and $int_{SER\sim T}$ within single years as well as across three years. Both traits showed high heritabilities across years ($H^2 = 0.81$ for $slp_{SER\sim T}$ and $H^2 = 0.77$ for $int_{SER\sim T}$) and very high heritabilities within single years (Table 1). Using the BLUPs of $slp_{SER\sim T}$, $int_{SER\sim T}$ and temperature sum for stem elongation (GDD_{SE}), final height could be predicted with high accuracy across different years ($0.82 <= R^2 <= 0.85$) by

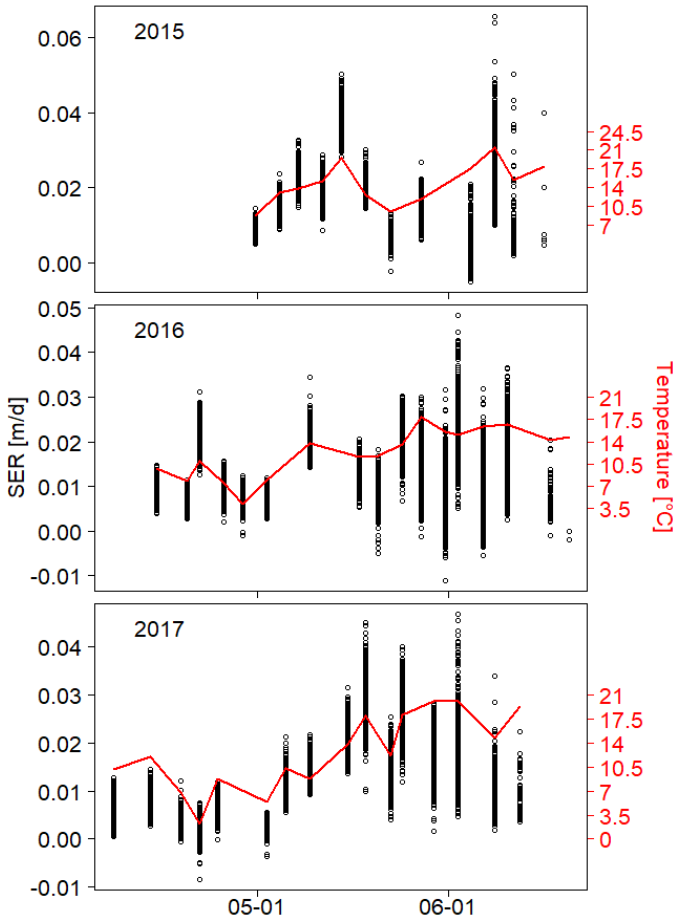

Fig. 2: Relationship between stem elongation rate (SER) and temperature. Plot based SER raw data (n > 700/a) of > 330 genotypes (black dots) as well as temperature (solid red line) is plotted against calendar time for the years 2015-2017.

training a linear model on the BLUPs of one year and predicting it on the BLUPs of another independent year. Training the model on the 3-year BLUPs resulted in a prediction accuracy of single years between $R^2 = 0.93$ and $R^2 = 0.95$ (Fig. 3). High heritabilities within years ($0.75 <= H^2 <= 0.99$) as well as across three years ($0.54 <= H^2 <= 0.98$; Table 1), were also found for other traits; final height, start of SE, end of SE and SE duration.

Phenology, temperature-response and final height were positively correlated

To evaluate the relationships between the traits measured, Pearson correlation coefficients were calculated for each trait pair. If not indicated otherwise, the reported correlations were highly significant ($P < 0.001$).

Positive correlations were found among GDD_{15}, GDD_{95} and FH ($0.36 <= r <= 0.64$, Fig. 4), indicating that taller varieties were generally later. Temperature response ($slp_{SER\sim T}$) and vigour ($int_{SER\sim T}$) also showed a strong, positive relationship with final height ($r = 0.85$ and

Table 1: Heritabilities of the investigated traits in single years and across all three years.

	heritability			
trait	**BLUPS 2015**	**BLUPS 2016**	**BLUPS 2017**	**3Y-BLUPS**
$int_{GR\sim T}$	0.93	0.95	0.84	0.77
$slp_{GR\sim T}$	0.96	0.91	0.94	0.81
FH	0.99	0.99	0.98	0.98
GDD_{15}	0.93	0.94	0.9	0.82
GDD_{95}	0.75	0.91	0.91	0.84
$time_{SE}$	0.85	0.84	0.85	0.59
GDD_{SE}	0.76	0.83	0.85	0.54

r = 0.65, respectively). However, only temperature-response correlated with GDD_{15} and GDD_{95} (r = 0.63 and r = 59, respectively), whereas vigour did not (r < 0.26, Fig. S2).

As expected, stem elongation duration in thermal time (GDD_{SE}) was negatively correlated with GDD_{15} (r = -0.44) and positively correlated with GDD_{95} (r = 0.4). But, GDD_{SE} did not correlate with final height (r = -0.01, P = 0.878) or temperature-response (r = 0.006, P = 0.289). Although GDD_{SE} negatively correlated with vigour (r = -0.32). In contrast, SE duration in calendar days ($time_{SE}$) was negatively correlated with temperature-response (r = -0.35) and GDD_{15} (r = -0.82), indicating a longer SE phase for earlier genotypes. Other weak correlations (r < 0.3), that are not discussed, are shown in Fig. S2.

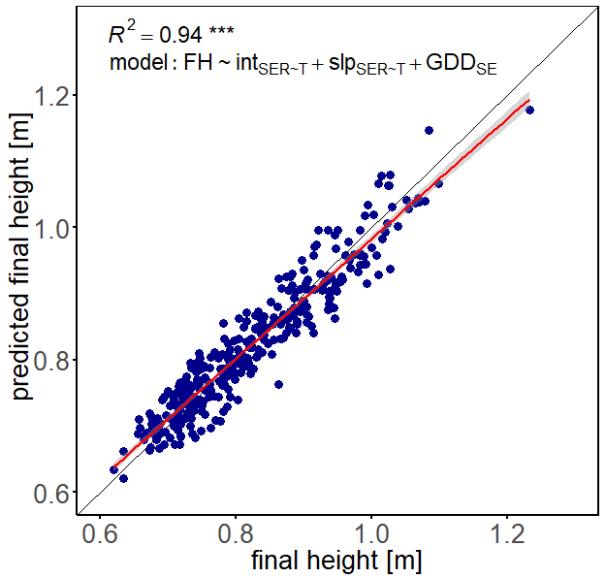

Fig. 3: Prediction of final height using BLUPs for slope and intercept of temperature response and the temperature sum in stem elongation. The linear model $FH \sim int_{SER\sim T} + slp_{SER\sim T} + GDD_{SE}$ was trained on BLUPs across 3 years and tested on the BLUPs of the year 2017.

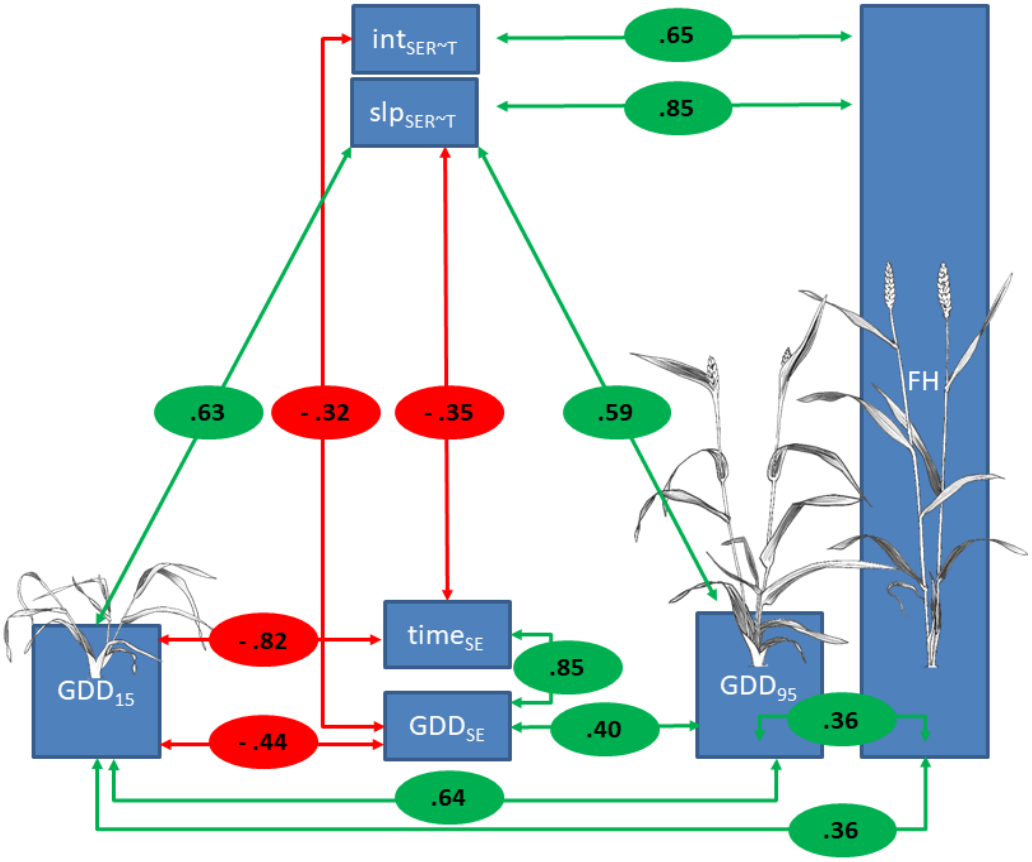

Fig. 4: Key correlations among investigated traits. Pearson correlation coefficients between respective traits are given in red and green circles, where red denotes a negative correlation and green denotes a positive correlation. Weak correlations ($r < 0.3$) are shown in the complete correlation matrix Fig. S2. Illustrations of GDD_{15}, GDD_{95} and FH were taken from Schürch *et al.* (2018).

Linkage disequilibrium and population structure

Prior to MTA analysis we evaluated population structure and LD. Principal component analysis of the marker genotypes revealed no distinct substructure in the investigated population. The biplot of the first two principal components showed no apparent clusters, with the first component explaining 8% and the second component explaining 3.3% of the variation in the population (Fig. S5). This is consistent with prior work using the same population (Kollers *et al.*, 2013; Yates *et al.*, 2018). On average across all chromosomes, LD decayed below an r^2 of 0.2 at a distance of 9 MB. There was however considerable variation in this threshold among the single chromosomes (Table S2).

Association study

Genome-wide association results differed markedly depending on the applied model. Using a MLM with kinship matrix and PCA as covariates resulted in no significant MTA for any trait (Fig. S3). In contrast, the GLM using the haplotype method yielded 2949 significant

Table 2: Marker-trait associations for temperature response, vigour, GDD_{15}, GDD_{95} and final canopy height, including p-value, allelic effect estimate and minor allele frequency.

Trait	SNP	Chr	Position	p-value	effect	maf
$slp_{GR\sim T}$	wsnp_Ex_c1597_3045682	1B	688'283'256	1.68E-06	-4.90E-05	0.19
	CAP7_c10839_300	4B	533'724'424	4.12E-06	-4.10E-05	0.24
	IAAV7104	5D	553'678'522	9.63E-06	-4.87E-05	0.13
$int_{GR\sim T}$	RAC875_s109189_188	2B	248'149'774	5.10E-07	0.000133	0.42
	Ku_c63300_1309	4B	21'556'672	2.72E-06	-0.00023	0.10
	Kukri_rep_c68594_530	4D	12'773'259	7.45E-09	-0.00018	0.40
	Kukri_c6477_696	5D	423'502'809	3.94E-07	-0.00016	0.21
GDD_{15}	wsnp_Ex_c12447_19847242	1D	416'456'386	1.91E-06	5.680002	0.46
	Tdurum_contig47508_250	2A	754'339'235	1.30E-06	7.757529	0.21
	Kukri_c55381_67	3A	648'868'234	1.38E-06	-8.27442	0.17
	Excalibur_c74858_243	5B	13'190'663	2.50E-08	-6.49833	0.47
GDD_{95}	Excalibur_c49597_579	5A	521'934'666	1.30E-06	-5.483	0.42
	Excalibur_c74858_243	5B	13'190'663	6.08E-07	-5.14378	0.47
	Tdurum_contig44115_561	5B	669'897'388	2.39E-07	-8.48015	0.13
	RAC875_c38693_319	7B	740'056'880	2.92E-06	6.287669	0.20
FH	Excalibur_c85499_232	1A	582'219'427	2.22E-06	0.02035	0.11
	BS00089734_51	2B	150'200'409	3.76E-07	0.018447	0.16
	Kukri_c49280_230	3A	20'134'735	3.88E-08	0.029134	0.08
	Tdurum_contig64772_417	4B	26'491'482	4.58E-09	0.034734	0.07
	RAC875_rep_c105718_585	4D	25'989'162	1.17E-11	-0.02371	0.38
	BS00036421_51	4D	32'347'318	1.06E-06	-0.01463	0.37
	RAC875_c8231_1578	5A	613'588'253	6.47E-07	0.014219	0.43
	wsnp_Ku_rep_c71232_70948744	5A	679'663'586	1.80E-09	-0.02029	0.47
	Excalibur_rep_c72561_141	5B	34'040'001	3.65E-07	-0.03066	0.05
	BS00109560_51	5B	556'182'591	1.49E-08	-0.01766	0.46
	BS00022120_51	6A	396'301'470	2.21E-10	-0.02386	0.24

MTA for $\alpha < 0.05$ and 1846 MTA for $\alpha < 0.001$ respectively. However, investigation of the respective QQ-plots showed large *P*-value inflation in the haplotype method whereas the *P*-values were slightly deflated when using the MLM approach (Fig. S3, Fig. S4). In contrast, with FamCPU the QQ-plots (Fig. 5) showed no *P*-value inflation, except for some markers. This pattern is expected, if population structure is appropriately controlled. Therefore, FarmCPU was chosen to be the most appropriate method for the given data, despite identifying less significant MTA.

As a positive control we compared our final height data and associated markers with data made by Zanke *et al*. (2014b). Final canopy height correlated strongly between the two studies ($r = 0.95$), which is in accordance with the high heritability of the trait. In this study, we found 11 significant MTA for final height (Table 2, Fig. 5). Zanke *et al.* (2014b).

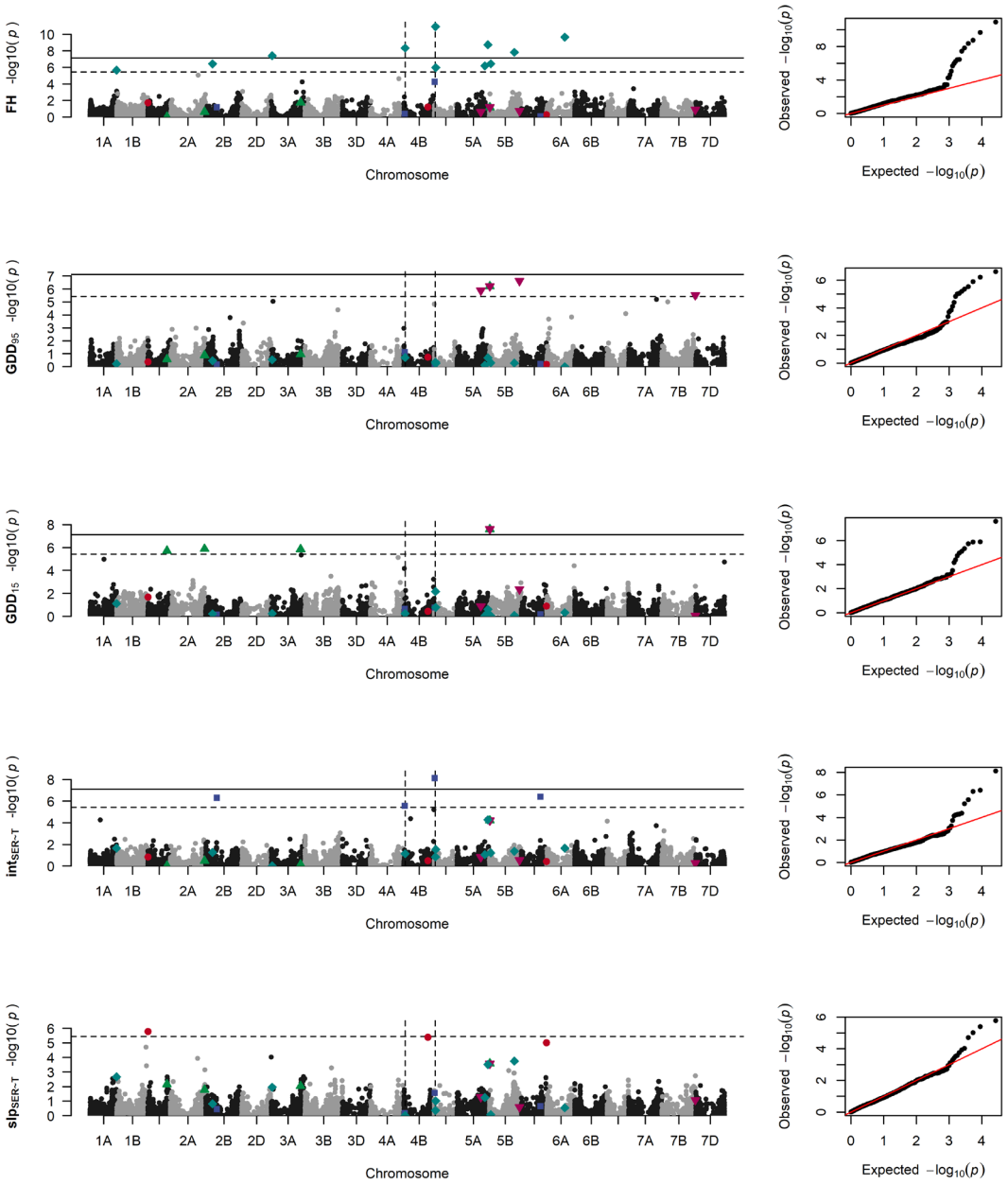

Fig. 5: Manhattan plots and quantile-quantile plots depicting the GWAS results using FarmCPU for final height (FH), growing degree days until start (GDD_{15}) and end (GDD_{95}) of stem elongation; vigour-related intercept ($int_{GR\sim T}$) and temperature-related slope ($slp_{GR\sim T}$) of stem elongation in response to temperature. Horizontal lines mark the Bonferroni corrected significance threshold for $P < 0.05$ (dashed line) and $P < 0.001$ (solid line). Dashed vertical lines mark the position of *Rht-B1* and *Rht-D1* on chromosome 4B and 4D, respectively. Significant marker trait associations for $slp_{GR\sim T}$ (red dots), $int_{GR\sim T}$ (blue squares), GDD_{15} (green up-facing triangles), GDD_{95} (purple down-facing triangles) and FH (turquois diamonds) are highlighted in all manhattan plots.

reported 280 significant MTA for final height across several environments. Of these, only marker RAC875_rep_c105718_585 on chromosome 4D overlapped with the MTA found in this study. However, by considering flanking markers, we found that of the remaining ten significant MTA for final height, six were in LD with MTA found by Zanke *et al.* (2014b; Table S3). The significant MTA found for FH in this study are near known genes controlling FH. For example, Tdurum_contig64772_417, is 4 MB upstream of *Rht-B1* and RAC875_rep_c105718_585, is 7 MB downstream of *Rht-D1* on their respective group 4 chromosomes.

Temperature-response loci are independent of vigour loci

For $slp_{SER\sim T}$ we detected one significant (LOD = 5.77) MTA on chromosome 1B (wsnp_Ex_c1597_3045682) and two almost significant (LOD = 5.39 / LOD = 5.02) MTA on chromosomes 4B (CAP7_c10839_300) and 5D (IAAV7104), respectively (Fig. 5). All associated markers for $slp_{SER\sim T}$ yielded small but significant allelic effects ranging from -0.049 mm $°C^{-1}d^{-1}$ to -0.041 mm $°C^{-1}d^{-1}$ (Table 2). The GWAS for $int_{SER\sim T}$ yielded four significant MTA on chromosomes 2B, 4B, 4D and 5D respectively (Table 2, Fig. 5). Start and end of SE yielded four MTA each (Table 2, Fig. 5).

Comparing the GWAS results for temperature-response, vigour, final height, GDD_{15} and GDD_{95} revealed no common quantitative trait loci (QTL) between $slp_{SER\sim T}$ and any other trait. Only one marker (Excalibur_c74858_243) was significantly associated with both GDD_{15} as well as GDD_{95}. The lack of overlap, of MTA, between temperature-response, vigour and timing of critical stages indicate they are genetically independent. However,

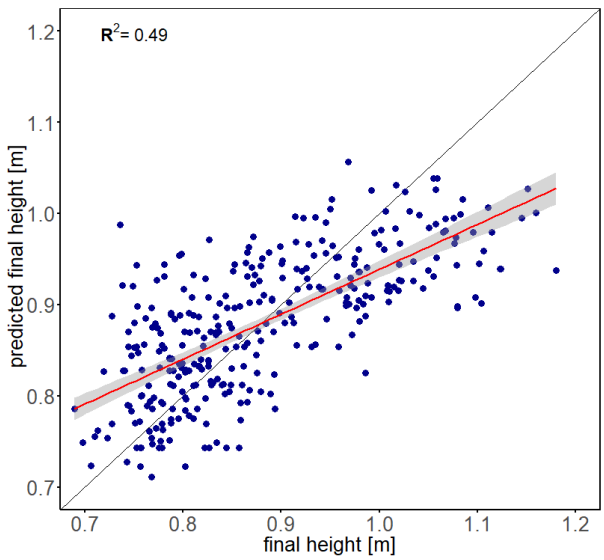

Fig. 6: Prediction of final height using the SNP alleles of significantly associated QTL for temperature response, vigour, start and end of stem elongation as predictors with the linear model: FH = QTL $slp_{SER\sim T}$ + QTL $int_{SER\sim T}$ + QTL GDD_{15} + QTL GDD_{95}.

there is a genetic connection between vigour and FH on the one hand and between the start and end of stem elongation on the other.

To identify potential causative genes underlying the QTL, we searched the reference genome annotation around the respective QTL intervals. For temperature-response we found an increased presence of genes or gene homologues involved in the flowering pathway, *i.e. EARLY FLOWERING 3, FRIGIDA* and *CONSTANS* (Table 3). Around the QTL associated with vigour the annotation showed genes associated with growth (*i.e. GRAS, CLAVATA, BSU1*, Argonaute) as well as developmental progress (*i.e.* Tesmin/TSO1-like CXC domain, *BEL1*, *AGAMOUS* (Table 4). Importantly, we found *GAI-like protein 1* 6MB upstream of marker Kukri_rep_c68594_530, which we identified as *Rht-D1* by blasting the *Rht-D1* sequence (GeneBank ID AJ242531.1) against the annotated reference genome.

Vigour, temperature-response and the timing of SE affect final height

The phenotypic correlations show a strong connection between temperature-response, vigour and FH as well as weaker connections between GDD_{15}, GDD_{95} and FH. In order to examine this interdependency on a genetic level, we used a linear model to predict FH with the SNP alleles of the QTL for $slp_{SER\sim T}$, $int_{SER\sim T}$, GDD_{15} and GDD_{95} as predictors. The model was able to predict FH with an accuracy $R^2 = 0.49$, with significant contributions by QTL of all three traits (Fig. 6, Table 5).

Table 3: Selected putative candidate genes for the intercept of temperature response from the IWGSC reference genome annotation.

Chr	SNP [Position]	r.start	r.end	Gene	description	distance
chr1B	wsnp_Ex_c1597_3045682 [688'283'256]	688'282'509	688'286'431	TraesCS1B01G480600	winged-helix DNA-binding transcription factor family protein	747
		688'352'414	688'354'696	TraesCS1B01G480700	HMG-Y-related protein A	-69'158
		687'710'716	687'719'885	TraesCS1B01G480100	Argonaute	572'540
		687'128'952	687'135'442	TraesCS1B01G479200	Zinc finger protein CONSTANS	1'154'304
		687'078'233	687'084'562	TraesCS1B01G479000	Zinc finger protein CONSTANS	1'205'023
		686'928'468	686'931'886	TraesCS1B01G478700	Zinc finger protein CONSTANS	1'354'788
		686'749'516	686'755'405	TraesCS1B01G478100	WD-repeat protein, putative	1'533'740
		685'645'287	685'649'392	TraesCS1B01G477400	Early flowering 3	2'637'969
chr4B	CAP7_c10839_300 [533'724'424]	537'474'959	537'479'867	TraesCS4B01G266000	Protein FRIGIDA	-3'750'535
		541'363'317	541'365'139	TraesCS4B01G267700	Protein upstream of flc	-7'638'893
		542'582'729	542'583'265	TraesCS4B01G268300	MADS transcription factor	-8'858'305
chr5D	IAAV7104 [553'678'522]	554'357'761	554'360'305	TraesCS5D01G544800	FRIGIDA-like protein, putative	-679'239
		554'467'487	554'472'596	TraesCS5D01G545100	Transducin/WD-like repeat-protein	-788'965
		556'226'523	556'234'480	TraesCS5D01G548800	Transducin/WD-like repeat-protein	-2'548'001

Table 4: Selected putative candiate genes for vigour ($int_{SER\sim T}$) of temperature response from the IWGSC reference genome annotation.

Chr	SNP [Position]	r.start	r.end	Gene	description	distance
chr2B	RAC875_s109189_188 [248’149’774]	243'569'388	243'571'100	TraesCS2B01G239400	GRAS transcription factor	4'580'386
chr4B	Ku_c63300_1309 [21’556’672]	21'187'173	21'192'244	TraesCS4B01G028500	Tesmin/TSO1-like CXC domain-containing protein	369'499
		20'005'649	20'008'978	TraesCS4B01G026600	Argonaute family protein	1'551'023
		19'740'974	19'744'058	TraesCS4B01G026200	WD40 repeat-like protein	1'815'698
		23'404'428	23'408'188	TraesCS4B01G031300	BHLH family protein, putative, expressed	-1'847'756
		23'818'506	23'822'972	TraesCS4B01G032000	Protein UPSTREAM OF FLC	-2'261'834
		18'162'363	18'165'744	TraesCS4B01G025500	Homeobox protein BEL1 like	3'394'309
		18'091'908	18'093'975	TraesCS4B01G025400	BEL1-like homeodomain protein	3'464'764
		17'229'197	17'236'874	TraesCS4B01G024000	Argonaute protein	4'327'475
		17'017'132	17'019'148	TraesCS4B01G023300	AGAMOUS-like MADS-box transcription factor	4'539'540
		26'335'682	26'336'740	TraesCS4B01G036600	BRI1 suppressor 1 (BSU1)-like 3	-4'779'010
		26'824'399	26'827'490	TraesCS4B01G037200	WD-repeat protein, putative	-5'267'727
		15'427'017	15'431'870	TraesCS4B01G021500	basic helix-loop-helix (bHLH) DNA-binding superfamily protein	6'129'655
		15'259'656	15'263'139	TraesCS4B01G021200	basic helix-loop-helix (bHLH) DNA-binding superfamily protein	6'297'016
		15'146'117	15'150'854	TraesCS4B01G021100	Basic helix loop helix (BHLH) DNA-binding family protein	6'410'555
		14'710'395	14'711'057	TraesCS4B01G020800	Protein FAR1-RELATED SEQUENCE 5	6'846'277
		28'413'432	28'414'112	TraesCS4B01G041000	sensitive to freezing 6	-6'856'760
		29'673'211	29'674'674	TraesCS4B01G042500	Fantastic four-like protein	-8'116'539
chr4D	Kukri_rep_c68594_530 [12’773’259]	12'700'119	12'703'878	TraesCS4D01G028900	BHLH family protein, putative, expressed	73'140
		13'096'296	13'096'966	TraesCS4D01G029600	CLAVATA3/ESR (CLE)-related protein 25	-323'037
		13'196'859	13'200'535	TraesCS4D01G029700	Protein UPSTREAM OF FLC	-423'600
		11'364'404	11'369'466	TraesCS4D01G026100	Tesmin/TSO1-like CXC domain-containing protein	1'408'855
		10'746'363	10'750'251	TraesCS4D01G024300	Argonaute protein	2'026'896
		10'684'336	10'690'389	TraesCS4D01G024100	Argonaute family protein	2'088'923
		10'254'979	10'257'683	TraesCS4D01G023600	WD40 repeat-like protein	2'518'280

		15'768'990	15'772'059	TraesCS4D01G034500	WD-repeat protein, putative	-2'995'731
		9'495'616	9'501'619	TraesCS4D01G022600	Homeobox protein BEL1 like	3'277'643
		9'443'778	9'445'575	TraesCS4D01G022500	BEL1-like homeodomain protein 1	3'329'481
		9'069'403	9'071'423	TraesCS4D01G021100	MADS-box transcription factor	3'703'856
		16'584'271	16'584'948	TraesCS4D01G038400	sensitive to freezing 6	-3'811'012
		8'777'205	8'779'670	TraesCS4D01G020300	Growth-regulating factor	3'996'054
		8'149'046	8'151'425	TraesCS4D01G019200	basic helix-loop-helix (bHLH) DNA-binding superfamily protein	4'624'213
		8'135'666	8'137'454	TraesCS4D01G019100	basic helix-loop-helix (bHLH) DNA-binding superfamily protein	4'637'593
		8'010'719	8'012'446	TraesCS4D01G018800	basic helix-loop-helix (bHLH) DNA-binding superfamily protein	4'762'540
		7'992'104	7'995'445	TraesCS4D01G018700	basic helix-loop-helix (bHLH) DNA-binding superfamily protein	4'781'155
		17'765'786	17'767'021	TraesCS4D01G039900	Fantastic four-like protein	-4'992'527
		18'781'062	18'782'933	TraesCS4D01G040400	GAI-like protein 1 **(Rht-D1)**	-6'007'803
		6'703'246	6'703'509	TraesCS4D01G015200	SAUR-like auxin-responsive protein family	6'070'013
		6'699'039	6'699'458	TraesCS4D01G015100	SAUR-like auxin-responsive protein family	6'074'220
		6'682'318	6'682'602	TraesCS4D01G015000	SAUR-like auxin-responsive protein family	6'090'941
		6'663'820	6'664'131	TraesCS4D01G014900	SAUR-like auxin-responsive protein family	6'109'439
		6'461'624	6'462'688	TraesCS4D01G013800	BRI1 suppressor 1 (BSU1)-like 3	6'311'635
		19'169'377	19'171'147	TraesCS4D01G040600	Protein FAR1-RELATED SEQUENCE 5	-6'396'118
		6'017'847	6'023'948	TraesCS4D01G012800	Protein FAR1-RELATED SEQUENCE 5	6'755'412
		4'128'933	4'133'919	TraesCS4D01G008400	WD-repeat protein, putative	8'644'326
		21'775'252	21'776'785	TraesCS4D01G046200	CONSTANS-like zinc finger protein	-9'001'993
chr5D	Kukri_c6477_696 [423’502’809]	423'858'756	423'860'766	TraesCS5D01G334100	Armadillo repeat only	-355'947
		421'503'514	421'504'332	TraesCS5D01G329500	HVA22-like protein	1'999'295
		426'296'827	426'301'957	TraesCS5D01G337800	WD-repeat protein, putative	-2'794'018
		429'289'426	429'292'023	TraesCS5D01G341000	CONSTANS-like zinc finger protein	-5'786'617
		416'787'868	416'788'986	TraesCS5D01G325300	Protein Mei2	6'714'941
		416'625'946	416'628'639	TraesCS5D01G325200	Protein Mei2	6'876'863
		415'622'032	415'622'615	TraesCS5D01G323500	Auxin-responsive protein	7'880'777

Table 5: Type II analysis of variance of the linear model FH = QTL $slp_{SER\sim T}$ + QTL $int_{SER\sim T}$ + QTL GDD_{15} + QTL GDD_{95}.

QTL	SNP	Sum Sq	Df	F value	Pr(>F)	
$Slp_{SER\sim T}$1_1B	wsnp_Ex_c1597_3045682	0.021	1	3.364	6.76E-02	
$Slp_{SER\sim T}$2_4B	CAP7_c10839_300	0.062	1	9.862	1.86E-03	**
$Slp_{SER\sim T}$3_5D	IAAV7104	0.114	1	18.055	2.87E-05	***
$Int_{SER\sim T}$1_2B	RAC875_s109189_188	0.018	1	2.828	9.37E-02	
$Int_{SER\sim T}$2_4B	Ku_c63300_1309	0.122	1	19.318	1.54E-05	***
$Int_{SER\sim T}$3_4D	Kukri_rep_c68594_530	0.428	1	67.968	5.25E-15	***
$Int_{SER\sim T}$4_5D	Kukri_c6477_696	0.001	1	0.157	6.92E-01	
GDD_{15}1_1D	wsnp_Ex_c12447_19847242	0.052	1	8.313	4.22E-03	**
GDD_{15}2_2A	Tdurum_contig47508_250	0.075	1	11.970	6.19E-04	***
GDD_{15}3_3A	Kukri_c55381_67	0.002	1	0.298	5.85E-01	
GDD_{15}4_5B/GDD_{95}2_5B	Excalibur_c74858_243	0.050	1	8.013	4.96E-03	**
GDD_{95}1_5A	Excalibur_c49597_579	0.057	1	9.010	2.91E-03	**
GDD_{95}3_5B	Tdurum_contig44115_561	0.012	1	1.985	1.60E-01	
GDD_{95}4_7B	RAC875_c38693_319	0.002	1	0.326	5.68E-01	
	Residuals	1.887	300	NA	NA	

3.4 Discussion

In this study we present a method to measure temperature response during stem elongation of wheat using high throughput phenotyping of canopy height in the field. The results show a highly heritable genotype-specific ambient temperature response of wheat which affects both growth and timing of the developmental key stages. We modelled temperature-response in a simple linear framework with the intercept estimated at the temperature of zero correlation to the slope. This allowed for the decomposition of growth dynamics into a genotype-specific vigour component and temperature-response component. Thereby we could assess interdependence between vigour and temperature-response to plant height and the timing of developmental key stages.

Linear models were used before to describe wheat growth response to temperature for leaf elongation (Nagelmüller *et al.*, 2016), canopy cover (Grieder *et al.*, 2015) as well as stem elongation rate (Slafer & Rawson, 1995a). Others proposed the use of a more complex, Arrhenius type of function to account for decreasing growth rates at supra optimal temperatures (Parent & Tardieu, 2012). Wheat has its temperature-optimum at around 27 °C (Parent & Tardieu, 2012). As temperatures in the measured growth intervals during stem elongation did not exceed 25 °C and given the temporal resolution of the data, a simple linear model is justified (Parent *et al.*, 2018).

The results of the correlation analysis show a clear connection between FH and temperature-response ($slp_{SER\sim T}$) as well as between FH and vigour ($int_{SER\sim T}$). This is consistent with part i) and ii) of our hypothesis: Final height can be described as a function of temperature-independent growth processes and as a function of temperature-response during SE. Importantly, among all components, the temperature-response was a major driver of final height and also had a strong influence on the timing. Temperature-response delayed the beginning of stem elongation leading to a later start and end of the whole phase. This finding might appear counter intuitive: given the assumption that plants develop faster under higher ambient temperatures a more responsive genotype should develop faster compared to a less responsive one. Slafer and Rawson (1995b) reported an accelerated development towards floral transition with increasing temperatures up to 19°C whereas higher temperatures slowed development. In that respect, a more responsive genotype would experience a stronger delay of floral transition under warm temperatures.

In terms of their correlation to FH, the effects of the timing of start and end of stem elongation (part iii) of the initial hypothesis) are less distinct. Final height was more a function of faster growth than duration of growth, especially since genotypes with a strong temperature-response have a shorter duration of SE. However, the timing of start and end of stem elongation was linked with temperature-response. Based on this result and the according correlations, it would appear that temperature-response influences FH directly as well as indirectly by mediating start and end of stem elongation.

The question, whether these trait correlations are due to pleiotropic effects will substantially impact the breeding strategy (Chen & Lübberstedt, 2010). If these effects are pleotropic, they have a huge impact on breeding as they indicate that temperature-response, timing and height are to a large degree determined by the same set of genes. Alternative explanations are linkage and population structure. As the examined traits are major drivers of adaptation to the different regions of Europe we anticipate a very strong selection for both, temperature response as well as timing of critical stages. The GABI wheat panel is made of wheat varieties from different regions of Europe. Even if there is no apparent population structure at neutral markers, there may be a strong population structure at selected loci with strong effect on local adaptation. However, pleiotropy between height and flowering time is known for maize and rice, supporting the hypothesis of pleiotropy here. The *DWARF8* gene of maize encoding a DELLA protein is associated with height and flowering time (Lawit *et al.*, 2010) and strongly associated with climate adaptation (Camus-Kulandaivelu *et al.*, 2006, p.). The rice *GHD7* locus has a strong effect on number of days to heading, number of grains per panicle, plant height and stem growth (Xue *et al.*, 2008). To further examine the relationship among the different traits we consider the following GWAS analysis using stringent correction of population structure.

The GWAS results indicate an independent genetic control of final height, temperature response and the timing of critical stages. Whereas vigour and FH as well as start and end of SE appear to be partly linked. Yet, final height could be predicted with surprising

accuracy using the QTL for temperature response, vigour, start and end of SE which reflects the correlations found in the phenotypic data.

Previous studies investigating the control of developmental key stages in wheat with respect to temperature generally adopted the concept, that after fulfilment of photoperiod and vernalisation, *Eps* genes act as fine tuning factors independent of environmental stimuli (Kamran *et al.*, 2014; Zikhali & Griffiths, 2015). Temperature, apart from vernalisation is thought to generally quicken growth and development independent of the cultivar (Slafer & Rawson, 1995b; Porter & Gawith, 1999; Slafer *et al.*, 2015). A genotype-specific temperature effect on the duration of different phases was not considered (Takahashi &Yasuda 1971, Slafer & Rawson 1995c). It was however reported, that photoperiod effects vary depending on temperature (Slafer & Rawson, 1995d). Under long days, Hemming *et al*. (2012) reported faster development and fewer fertile florets under high compared to low temperatures. Temperature-dependent effects were also found for different *Eps* QTL (Slafer & Rawson, 1995d; Gororo *et al.*, 2001). It has previously been suggested, that *Eps* effects could be associated with interaction effects between genotype and temperature fluctuations (Slafer & Rawson, 1995d; van Beem *et al.*, 2005).

The mechanisms of ambient temperature sensing and its effects on growth and development are not yet well understood (Sanchez-Bermejo & Balasubramanian, 2016). However, important findings regarding ambient temperature effects on flowering time as well as on hypocotyl elongation have come from the model species *Arabidopsis thaliana* (Wigge, 2013). With respect to these two traits, Sanchez-Bermejo and Balasubramanian (2016) reported distinct genotypic differences in temperature-sensitivity. According to their results, the flowering pathway genes *FRIGIDA (FRI)*, *FLOWERING LOCUS C (FLC)* and *FLOWERING LOCUS T (FT)* are major candidate genes for ambient temperature mediated differences in flowering time (Sanchez-Bermejo & Balasubramanian, 2016). In the present study, we found *FRI* homologues near two of the three QTL for temperature-response. *FRI* and *FLC* acts as main vernalisation genes in *A. thaliana* (Johanson *et al.*, 2000; Amasino & Michaels, 2010). In wheat, these genes are not yet well described. However, *FLC* orthologues were found to act as flowering repressors regulated by vernalisation in monocots (Sharma *et al.*, 2017).

Another promising candidate gene for temperature response found near the QTL on chromosome 1B is *EARLY FLOWERING 3* (*ELF3*). In *Arabidopsis*, *ELF3* was found to be a core part of circadian clock involved in ambient temperature response (Thines & Harmon, 2010). In Barley, *ELF3* was shown to be involved in the control of temperature dependent expression of flowering time genes (Ejaz & von Korff, 2017). A mutant *ELF3* accelerated floral development under high ambient temperatures while maintaining the number of seeds (Ejaz & von Korff, 2017). Furthermore, *ELF3* has been reported as a candidate gene for *Eps1* in Triticum monococcum (Alvarez *et al.*, 2016).

One important aspect we could not address in the current study is the interaction of genotype specific temperature response with vernalisation and photoperiod (Slafer &

Rawson, 1995d; Gol *et al.*, 2017; Kiss *et al.*, 2017). It also remains unclear if and to which extent temperature response varies across different developmental phases and how temperature-response relates to other environmental stimuli such as vapour pressure deficit or radiation. Nevertheless, the results of this study present valuable information towards a better understanding of temperature response in wheat and may be of great importance for breeding. Temperature-response could provide a breeding avenue for local adaptation as well as the control of plant height.

With the recent advancements in UAV-based phenotyping techniques, the growth of canopy cover and canopy height can be measured using image segmentation and structure from motion approaches (Bareth *et al.*, 2016; Aasen & Bareth, 2018; Roth *et al.*, 2018a). Thus, temperature-response can be investigated during the vegetative canopy cover development (Grieder *et al.*, 2015) and during the generative height development as demonstrated here. It can also be assessed in indoor platforms (e.g. Parent & Tardieu, 2012) and the field using leaf length tracker (Nagelmüller *et al.*, 2016) measuring short-term responses of leaf growth to diurnal changes in temperature. Combining this information may greatly improve our understanding about the genetic variation in growth response to temperature.

3.5 Conclusion

Modern phenotyping platforms hold great promise to map the genetic factors driving the response of developmental processes to environmental stimuli. To the best of our knowledge, this is the first experiment dissecting the stem elongation process into its underlying components: temperature-dependent elongation, temperature-independent vigour and elongation duration. The independent loci detected for these traits, suggest that it is possible to select them independently. The detected loci may be used to fine tune height and the beginning and end of stem elongation as they explain a substantial part of the overall genotypic variation. With increases in automation, growth processes may be monitored in the field on a daily basis or even multiple times per day. This will increasing the precision in assessing genotype responses to the fluctuation in meteorological conditions and quantifying the relationship of these responses to yield. Remote sensing by means of unmanned aerial vehicles in combination with photogrammetric algorithms will allow to measure these traits in breeding nurseries. We believe that this is paving the road for a more informed selection to climate adaptation within individual growing seasons.

Acknowledgements

We sincerely thank Hansueli Zellweger for managing and nursing our field experiments. We further thank the members of the ETH crop science and the ETH molecular plant breeding groups, especially Michelle Nay and Beat Keller, for many fruitful discussions. We also thank Martina Binder for doing the correlation analysis between the final height data of this study and the data made by Zanke *et al*. (2014b) in the framework of her MSc-Thesis. We would like to thank Marion Röder (IPK Gatersleben) for supply of the GABI wheat panel including genetic information. Finally, we thank the anonymous reviewers for

their helpful comments and suggestions. This work was supported by the Swiss National Foundation (SNF) in the framework of the project PhenoCOOL (project no. 169542).

4 Understanding wheat physiological and phenological phases linked with environmental interactions

Martina Binder[a,b,*], Lukas Kronenberg[a,*], Andreas Hund[a], Bruno Studer[b], Achim Walter[a], Steven Yates[b]

[a] Crop Science, Institute of Agricultural Sciences, ETH Zürich, 8092 Zurich, Switzerland
[b] Molecular Plant Breeding, Institute of Agricultural Sciences, ETH Zürich, 8092 Zurich, Switzerland
[*]Contributed equally to this work

This chapter is adapted from the master thesis of Martina Binder (2019), co-supervised by the author of this thesis; who contributed significantly to the drafting of the research question, the selection of genotypes, the design of the experiment and supervision of data analysis.

Abstract

Wheat production is impaired by changing climate. Furthermore, a stagnation in wheat yields was observed in recent years. It was proposed, that altering the sensitivity to environmental stimuli such as temperature and photoperiod could be used as a breeding strategy to improve wheat adaptation and optimize the timing of phasic development. A recent study showed that wheat has a highly heritable growth response to temperature during stem elongation and that this trait is correlated with the timing of critical stages and final height. The aim of the current study was to test whether temperature response in the vegetative phase corresponds to temperature response in the reproductive phase under field conditions and whether genotypes show the same temperature response under controlled conditions. Further, we investigated how temperature response corresponds with the timing of floral transition and analysed, whether reduced height genes affect temperature response. Temperature response of leaf elongation measured under controlled conditions showed a high correlation ($R^2 = 0.58$) with temperature response during stem elongation in the field. Furthermore, a low temperature response during stem elongation was correlated with an earlier floral transition compared to high responsive genotypes. However, temperature response of leaves measured in the field did neither correlate with temperature response measured in the greenhouse, nor with temperature response during stem elongation in the field. We hypothesise that this might be due to the difference in temperature range between the experiments. However, further research is needed to elucidate the relationship between temperature response in the vegetative and the reproductive phase in wheat.

4.1 Introduction

Wheat (*Triticum aestivum spp.*) is an important staple crop for food security. As changing climate impairs wheat production, wheat cultivars must be adapted to new conditions. In addition, a growing world population must be fed (Tilman *et al.*, 2011). However, a stagnation of yields in wheat production has been observed in several countries over the last years (Calderini & Slafer, 1998; Ray *et al.*, 2012; Schauberger *et al.*, 2018). Nevertheless, it is unlikely that yield potential has been reached (Schauberger *et al.*, 2018).

One of the most important achievements in the last century was the introduction of the reduced height (*Rht*) genes in wheat breeding (Hedden, 2003). These are located on the short arms of chromosomes 4B (*Rht-B1*) and 4D (*Rht-D1*). The dwarfing alleles *Rht-B1b* and *Rht-D1b* make the plant insensitive to the growth hormone gibberellin (GA; Allan *et al.*, 1959; Gale & Youssefian, 1985; Peng *et al.*, 1999). As a result, these plants are smaller, which prevents lodging and increases the harvest index (Hedden, 2003). However, the *Rht* genes are also associated with side effects. It was shown that *Rht-B1* and *Rht-D1* have negative pleiotropic and epistatic effects on many important wheat traits such as reduced disease resistance (Baltazar *et al.*, 1990; Srinivasachary *et al.*, 2008; Nicholson *et al.*, 2008), postponed heading date (Mo *et al.*, 2018), and reduced grain quality traits (Casebow *et al.*, 2016). Currently, *Rht-B1* and *Rht-D1* are widely used in breeding programs (Gale & Youssefian, 1985; Ellis *et al.*, 2002). Since the discovery of the unfavourable effects of *Rht-B1* and *Rht-D1,* researchers have been searching for alternative *Rht* genes. To date, 25 *Rht* genes have been discovered from which only *Rht-B1* and *Rht-D1* are GA insensitive (Mo *et al.*, 2018). Different combinations of *Rht* genes have been proposed depending on the desired height reduction and the targeted environment (Mo *et al.*, 2018).

Alternative strategies to further increase wheat yields have been proposed in the context of physiological breeding, *i.e.* in the fine tuning of developmental patterns and developmental stages which are determinant for yield potential (Slafer *et al.*, 2015). In wheat, the critical phase for yield formation coincides with stem elongation (SE) between floral transition and anthesis (Slafer *et al.*, 2015). Floral transition marks the switch from vegetative to vegetative development, when the shoot apex differentiates from producing leaf primordia to producing spikelet primordia (Trevaskis *et al.*, 2007a; Kamran *et al.*, 2014). The formation of the terminal spikelet at the shoot apex marks the end of floral transition, determining the final number of spikelets per spike (Slafer *et al.*, 2015). During SE, floret primordia are initiated at the spikelets, which reach the state of fertile florets at anthesis or are aborted during SE (Slafer *et al.*, 2015). The number of fertile florets at anthesis and thus the number of grains per spike largely determine yield (Fischer, 1985; Whitechurch *et al.*, 2007). A higher number of fertile florets at anthesis could be obtained by a prolonged SE duration due to more dry matter accumulation by the spikes (Slafer *et al.*, 1996; Whitechurch *et al.*, 2007; Gonzalez-Navarro *et al.*, 2016). The major abiotic factors influencing SE duration are temperature and photoperiod (Slafer *et al.*, 2015). Altering the sensitivity to photoperiod has often been proposed to manipulate SE duration and thus increase yield (e.g. Slafer *et al.*, 2001; González *et al.*, 2003c; Pérez-Gianmarco *et al.*,

2018). The effect of temperature is much less investigated – apart from cardinal temperatures or temperature sums for different phases, only few studies have dealt with temperature response on wheat development at developmental phases or phases of the vegetation period other than those relevant for vernalisation(Slafer & Rawson, 1994; Atkinson & Porter, 1996; Fischer, 2011).

In a preceding study we reported a highly heritable growth response to temperature in stem elongation of 328 wheat genotypes across three years in the field (Kronenberg *et al.*, 2019). Temperature response correlated with the start of SE, SE duration and final height. Other studies reported genotypic differences in growth response to temperature for canopy cover (Grieder *et al.*, 2015) and leaf elongation (Nagelmüller *et al.*, 2016). The results of Kronenberg et al. (2019) imply that temperature response might be exploited as a breeding trait. According to the correlations, selecting for a low temperature response would presumably result in earlier genotypes with a longer stem elongation phase and reduced height (Kronenberg *et al.*, 2019). However, the phenotyping of temperature response during SE is time consuming, as it requires frequent height measurements throughout the SE phase (Kronenberg *et al.*, 2017, 2019). In contrast, temperature response of leaf elongation can be measured with high throughput in the field (Nagelmüller *et al.*, 2016) as well as under controlled conditions (Yates *et al.*, 2019) with comparably little effort. Wheat leaves grow for approximately one week and growth can be measured accurately on a scale of millimetres per hour (Nagelmüller *et al.*, 2016). Measuring leaf elongation rate (LER) in response to temperature would therefore facilitate the screening for temperature response and increase throughput, especially if done in controlled conditions. However, it is unclear, whether the genotype ranking in temperature response is stable across the different developmental stages. It is, for example known, that the cardinal temperatures change across developmental changes (Porter & Gawith, 1999). Furthermore it is not clear how well temperature response measured under controlled conditions translates to the field, as is often the case with results from controlled conditions (Poorter *et al.*, 2016)

Based on these considerations, the objective of this study was to:

i) Investigate the comparability of temperature response between leaf growth in the vegetative phase and stem elongation in the reproductive phase under natural field conditions,
ii) compare temperature response of leaf growth measured in the greenhouse in non-vernalised plants to temperature response of leaf and stem elongation in the field,
iii) determine the exact time point of floral transition (terminal spikelet stage) in the field and outline genotypic differences in the time point of the transition from the vegetative to the reproductive phase and its connection to temperature response and
iv) check possible interaction with photoperiod (*Ppd*) and reduced height (*Rht*) genes,

in order to gather a deeper understanding of growth response to temperature and its interactions with phenology in wheat.

4.2 Materials and methods

Plant material

A total of eleven genotypes distributed in three groups were selected from the panel used by Kronenberg *et al*. (2017, 2019) based on their temperature response during SE (Fig. 1D). The groups comprised genotypes from the population extremes (group 1 with low temperature response: CH CLARO, TORONTO, SEMOAFOR, MARKSMAN; group 3 with high temperature response: TAMARO, ROMANUS, OSTAKA STREZELECKA, RYWALKA) and the population centre (average temperature response: RUNAL, WINNETOU, FASTNET).

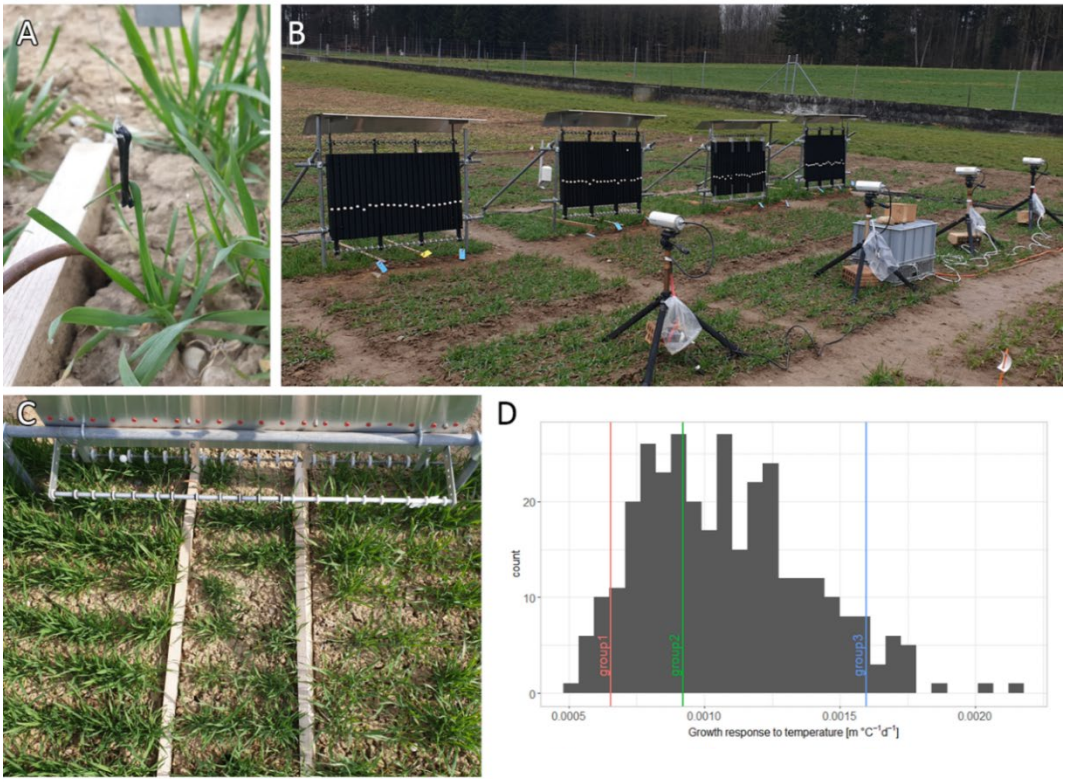

Fig. 1: Setup of the leaf growth measurements in the field using the leaf length tracker (LLT, Naglemüller et al, 2016). A: Hairpin attached to the youngest leaf of the growing wheat plant. **B:** LLT-Panels with white beads moving upwards as the wheat leaves grow. In front of each panel, a camera was installed that tracked bead displacement of the beads. **C:** Backside of the LLT showing the segmentation of the plot in three micro plots. **D:** Histogram showing the distribution of temperature response (3-year best linear unbiased predictors) during stem elongation (SE) among 328 genotypes. Vertical lines represent the means of the three resp. four genotypes assigned to the respective group. Group 1: low temperature response in SE, group 2: average temperature response in SE and group 3: high temperature response in SE.

Leaf length tracking in the field

Leaf elongation rates (LER) were measured in the field from mid-February to beginning of April 2019 using the leaf length tracker (LLT) system described by Nagelmüller *et al*. (2016). The installation follows the principle of an auxanometer. Briefly, the youngest leaf was attached to a hairpin to which a thread was attached (Fig. 1A). The thread was guided over three deflection pulleys along an aluminium panel and held tight with a counter weight (20 g). On the front side of the panel, a white bead was attached to the thread, which moved upwards on the panel as leaves elongated (Fig. 1B). Displacement of the beads was recorded through images taken by cameras placed in front of the panels. Pictures were taken every 120 seconds and bead displacement was extracted using a custom computer application (see Nagelmüller *et al.*, 2016 for details).

The plants were grown in four small plots at the ETH research station for plant sciences Lindau-Eschikon ('Eschikon'; 47.449°N, 8.682°E, 520 m a.s.l.; soil type, gleyic cambisol; sowing date, 17th October 2018). The plots (0.9 m x 1 m) contained three genotypes each (Table 1). One additional genotype, CH Nara, was added to the fourth plot to also have complete ground cover in this plot. This genotype was omitted from analysis. and were sown by hand. Consequently, sowing density was not exact and could not be determined. The plots were ploughed (26.9.2018) and worked with a rotary harrow (16.10.2018) before sowing. The plots were fertilized with dolomite (55% $CaCO_3$, 35% $MgCO_3$, 400 kg/ha, 24.1.2019,) potash (60% K, 200 kg/ha, 24.1.2019), boron-ammonium nitrate (26% N, 200 kg/ha, 27.2.2019), superphosphate (46% P, 200 kg/ha, 27.2.2019) and sprayed with the herbicide Herold SC (18.10.2018, 0.6 l/ha). In the previous season, sugar beet was grown on the plots.

Table 1: Experimental set-up of the genotypes grown in small plots for the leaf length tracker experiment.

Genotype	Group	Comments	Plot
CH CLARO	Group 1	low growth response to temperature in stem elongation	1
TAMARO	Group 3	high growth response to temperature in stem elongation	1
TORONTO	Group 1	low growth response to temperature in stem elongation	1
RUNAL	Group 2	middle growth response to temperature in stem elongation	2
ROMANUS	Group 3	high growth response to temperature in stem elongation	2
SEMAFOR	Group 1	low growth response to temperature in stem elongation	2
WINNETOU	Group 2	middle growth response to temperature in stem elongation	3
FASTNET	Group 2	middle growth response to temperature in stem elongation	3
OSTKA STRZELECKA	Group 3	high growth response to temperature in stem elongation	3
RYWALKA	Group 3	high growth response to temperature in stem elongation	4
MARKSMAN	Group 1	low growth response to temperature in stem elongation	4
CH NARA	-	not analysed, needed to cover the whole plot space	4

We assigned the genotypes randomly to one of the four plots, where they were grown in stripes of 0.3 m x 1 m (Table 1). In each plot, we installed a LLT. To avoid disturbance of the experiment, the LLTs were not moved during the experiment. Therefore, we measured only leaves of two plant rows of the plots. Normally, we attached the youngest plant leaves of the main shoot with a leaf length of 0.5 to 5 cm in the same row for one week and then used the next leaf for the following week of measurement (Fig. 1C).

We assigned two beads of each LLT panel as controls to account for non-growth dependent movement of the beads. They were equipped with a thread in the same way as the other beads, except that the thread was fixed with a nail into the soil instead of being attached to a leaf. The camera-tracked side of the LLTs was oriented towards north-east in order to minimize shading of the growing wheat plants and glare on the camera.

Air temperature was measured at 10 cm above ground with CS215 sensor (Campbell Scientific Ltd., Loughborough, UK) and shielded with a 10 plate unaspirated radiation shield (RAD10, Campbell Scientific Ltd., Loughborough, UK).

We measured LER during a period of seven consecutive weeks, beginning on Monday the 19th of February 2019 at 6 pm and ending on Monday the 8th of April 2019 at 8 am. On average, we tracked six leaves for each genotype every week (min. four leaves) for the whole measuring period. Measurements failed for genotype CH CLARO for week 2 and for genotype TORONTO for weeks 1 and 2 due to stormy weather.

LER was modelled with respect to temperature using a linear model. For each leaf, temperature response was estimated according to eq. 1,

$$LER_i = a_i * T + b + e \qquad \text{Eq. 1}$$

where LER_i is the LER of each individual leaf (i = 1,…,447), the slope estimator a_i of the linear motel for the ith genotype is the temperature response, T is the temperature, b is the model intercept and e is the residual error. As we had an un-replicated strip design, we had to use the groups for further statistical analysis. In order to test for significant differences between the groups, we used ANOVA and Tukey HSD post hoc test using a linear mixed model following eq. 2,

$$a_i = \mu + g_j + p_k + ps_{kt} + psw_{ktu} + e \qquad \text{Eq. 2}$$

Where a_i derives from eq.3, μ is the overall mean, g_j is the fixed group effect (j = 1,2,3), and p_k is the fixed plot effect (k = 1,2,3,4). As random terms, we used plot to genotype (ps_{kt}, t = 1,…11) interaction and plot, genotype, week (psw_{ktu}, u = 1,…,7) interaction. The parameter e is the residual error.

Leaf length tracking in the greenhouse

For the leaf growth measurements in the greenhouse, we used the "monocot envirotyping unit" (MEU) which was recently developed at ETH and is not published yet (Yates *et al.*, manuscript in preparation). This phenotyping platform is also based on an auxanometer principle, but instead of optical tracking of a bead attached to the string, the movement of the string is analysed by the torsion of the roller that is connected to a rotary voltage transducer linked to a computer.

Leaf growth measurements were done in a greenhouse at Agroscope Reckenholz in Zürich, Switzerland (47°25'41"N 8°31'00"E). Plants were grown from the 2nd of May 2019 until the 5th of June 2019 in a nursery. The seeds were sown in pots (75 mm x 75 mm x 85 mm) containing 85 g dry weight soil (Migros Kitchen Scale, Model 7039.208 (J18)). The soil was a 84:16 (v/v) mixture of organic and inorganic components ("Containererde für Stauden und Kübelpflanzen", Ökohum gmbh, Herrenhof, Switzerland). In each pot, 10 seeds were sown. The pots containing the growing wheat plants were watered twice a day by flooding the table for fifteen minutes. The plants were fertilized with liquid fertilizer in the first and second week after emergence (Wuxal Universaldünger, Maag/Syngenta, Dielsdorf, Switzerland). The macronutrient content of a fertilizer application was equivalent to 37 kg N/ha, 37 kg/ha P_2O_5, 28 kg/ha K_2O. The plants were treated against mildew (20.5.2019, *Folicur* (Tebuconazole 0.125 g/l, Trifloxystrobin 0.125g/l, COMPO Jardin AG)) and against aphids (23.5.2019, 0.05g/l Acetamiprid, COMPO Jardin AG). Day length was extended from 6 am to 10 pm with high pressure sodium lamps. The lamps were turned off when air temperature exceeded 23°C or sunlight intensity was higher than 500 Wm^{-2}.

The wheat plants were grown for three weeks in the nursery and then transferred to the MEU to measure LER for one week. Greenhouse temperature was influenced by the outside air temperature and ranged from 20 °C to 41 °C. Day length was extended by high pressure sodium lamps from 12 am to 10 pm. The lamps were switched off when solar radiation and air temperature exceeded 600 Wm^{-2} resp. 35 °C. Before putting the pots on the phenotyping platform, soil was watered until it reached retention capacity. The genotypes were distributed over four MEU frames with 16 measuring stations each. We had an incomplete randomized block design with five replicates of each genotype distributed over four MEU. We ensured that a complete replication was measured on each MEU. The experimental setup was repeated three times. The youngest leaf of each plant (leaf no. 4) was attached to a hairpin to measure LER. We completed three weeks of measurements in total from the 23th of May until the 12th of June. We watered the pots on the MEU as needed, such that the plants did not experience water stress.

On average four tracked leaves of each genotype for each week (min. three leaves) were available for further calculations. Measurements above 35 °C and with less than 40% soil water content were excluded from the analysis. Temperature response was calculated

according to eq. 3. To test for significant differences among the groups, we used ANOVA and Tukey HSD post hoc test using a linear mixed model following eq. 3.

$$a_i = \mu + g_j + l_k + w_u + e \qquad \text{Eq. 3}$$

Where GRT_i derives from eq. 3, μ is the overall mean, g_j is the fixed group effect (j = 1, 2, 3), l_k is the fixed position of the platform (k = 1,…,4), w_u (u = 1, 2, 3) is the fixed time point of measurement and e is the residual error.

To calculate genotypic best linear unbiased estimates (BLUEs), we replaced group with genotype in eq.5. These genotypic BLUEs were then correlated to the 3 years BLUEs of temperature response data from the SE phase made by Kronenberg *et al.* (2019).

Dissection of apex meristems

The plants for meristem dissection were grown in plots with a size of 1.7 by 1.25 m at the ETH research station at Eschikon close (approx. 50 m) to the plants used for leaf growth measurements in the field. Sowing was done with a density of 400 seeds/m^2. Before wheat, buckwheat was grown on the plots. The plots were ploughed (26.9.2018) and worked with a rotary harrow (16.10.2018) before sowing. Fertilisation and plant protection was done as described above

We dissected the apex meristem of the same genotypes, which were used in the leaf growth experiments grown in the field from the 21th March 2019 to the 29th April 2019, to determine the terminal spikelet stage. The meristems were dissected three times a week under a microscope (OLYMPUS, model SZX-ILLB200) and photographed with a SONY 3CCD colour video camera (Model DXC-950P, analySIS pro 5.1 Olympus Soft Imaging Solution GmbH). For each genotype, the meristems of three to four plants were dissected at each time point (with the exception of the 21th March 2019 when only half of the genotypes were dissected). The apex development stage was rated visually following Gardner *et al*. (1985). The genotypes were considered as fully reproductive when terminal spikelet (stage 8, Gardner *et al.*, 1985) was reached and were then not further dissected. For further calculations, a minimum of one and a maximum of five rated growth meristems for each genotype at each time point were available.

To test for significant differences between the groups we calculated ANOVA following a linear mixed model according to eq. 4.

$$q_i = g_j + d_o + gd_{jo} + sd_{to} + e \qquad \text{Eq. 4}$$

Where q_i (i = 1,…,460) is the score of development of each replicate of each genotype at each date, g_j is the fixed group effect (j = 1,2,3), d_o is the fixed effect of the date of dissection (o = 1,…,15) and gd_{jo} is the group x date interaction. As random terms, we used the genotype x date interaction (sd_{to}, t = 1,…11) and e is the residual error.

Due to the strong interdependencies reported by Kronenberg *et al*. (2019), we tested for synergistic effects of *Rht* and *Ppd* genes on the reported traits: temperature response during

SE ($slp_{SER\sim T}$), start of SE (GDD_{15}), end of SE (GDD_{95}) and final height (Kronenberg *et al.*, 2019). To do so, we used genetic information available for the GABI wheat panel of the reduced height genes *Rht-B1*, *Rht-D1*, *Rht-24* (Kollers *et al.*, 2013; Würschum *et al.*, 2017) and the photoperiod sensitivity gene *Ppd-D1* (Kollers *et al.*, 2013). We tested the effects of the genes on the traits with the linear model according to Eq. 5,

$$Y_i = \mu + c(g_n + g_n \dots g_n) + e \qquad \text{Eq. 5}$$

where Y_i is the BLUE of the ith trait (i = $slp_{SER\sim T}$,GDD_{15},GDD_{95},FH), g_n is *Rht-B1*, *Rht-D1*, *Rht24* or *Ppd-D1* alone or in either combination of the four genes, and e is the residual error. We had the genetic information of these four genes available for 126 genotypes.

All statistical analyses were computed with *R* (R Core Team, 2015). The linear models (Eq. 5) were computed using the R-package *lsmean* (Lenth, 2016) and the mixed linear models (Eq. 1 – 4) were calculated with R-package *asreml* (Butler, 2018).

4.3 Results

The temperature response of leaf elongation among the three groups measured in the field differed significantly between group two and three ($P < 0.05$) over the measurement period (Fig. 2A). In contrast, there were no significant differences between group one and two ($P > 0.05$) and group one and three ($P > 0.05$). This result is opposite to what we would have expected. Based on the temperature response during stem elongation, we would have expected a significantly lower temperature response of group one compared to group three, with group two in between. The ranking among the three groups was constant over the seven weeks of measurement except for week three where the ranking of group one changed with respect to group two and three (Fig. 2A). Temperature response increased for all groups over the seven weeks such that temperature response had almost doubled in the last week compared to the first week. Interestingly, the variation in weekly mean temperature was relatively constant across the duration of the experiment, with weekly mean temperatures ranging from 5.1°C to 6.3 °C from week two to week seven and a mean temperature of 4.1 °C in the first week. The overall mean temperature across all seven weeks was 5.7 °C.

In the greenhouse, temperature response did not increase over the duration of the experiment. This might be due to the controlled environment and because we always measured the fourth leaf in all genotypes and replications. The mean temperature over the three weeks was 30 °C. Temperature response also differed between the three groups but the ranking among groups across the duration of the experiment was less constant (Fig. 2B). Group three showed the highest temperature response followed by group one and group two in the first and the third week. In the second week, the group ranking matched the expected ranking based on temperature response during stem elongation. Across all

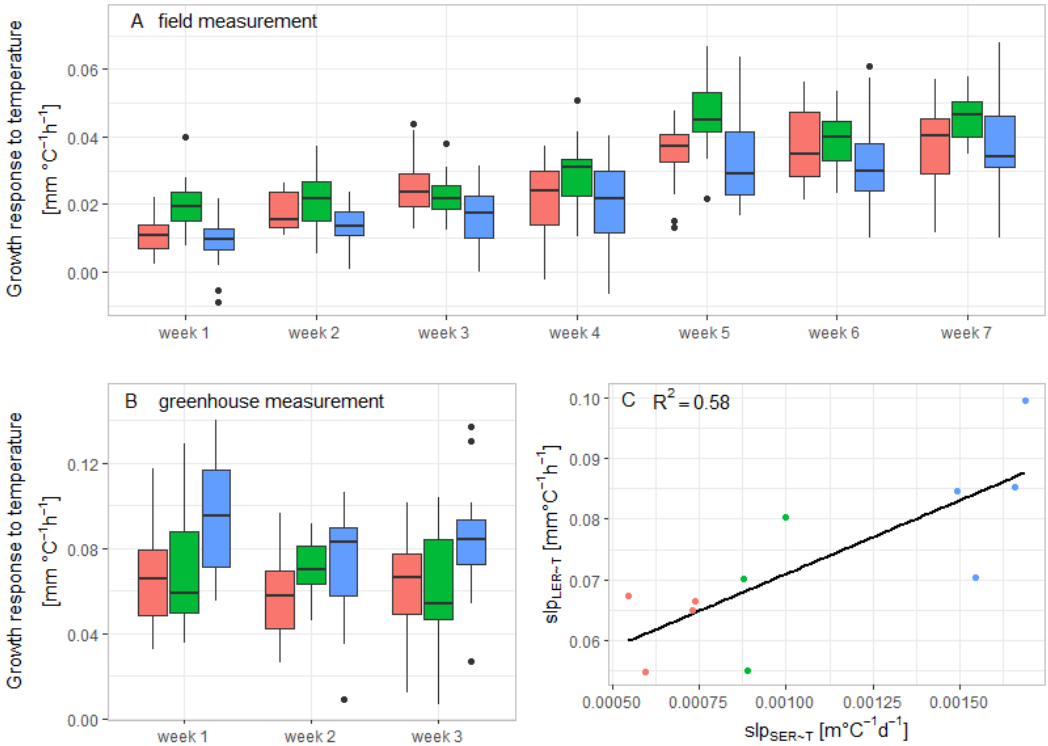

Fig. 2: Leaf growth response to temperature among three temperature response groups in the field and in the greenhouse. A: Temperature response of leaves grown in the field experiment (February to April 2019). **B:** Temperature response of leaves grown in the greenhouse in three consecutive weeks (May to June 2019). **C:** Correlation between temperature response of leaf elongation measured in the greenhouse ($slp_{LER\sim T}$) and temperature response of stem elongation ($slp_{SER\sim T}$) in the field. Individual points represent best linear unbiased estimates of eleven genotypes, colors represent the temperature response group (red = low $slp_{SER\sim T}$, green = average $slp_{SER\sim T}$, blue = high $slp_{SER\sim T}$).

three weeks, no significant differences in temperature response were found between group one and group two ($P > 0.05$).

Temperature response of leaf elongation in the greenhouse matches temperature response of stem elongation in the field

The ranking of the groups changed when temperature response of leaf elongation was measured in the greenhouse compared to the field. In the greenhouse, temperature response differed significantly between group one and group three ($P < 0.01$) as well as between group two and group three ($P < 0.01$). This result is expected based on the placement of the groups in the stem elongation temperature response distribution of the population (Fig. 2B, Fig. 1D): The group ranking of temperature response during leaf elongation matched the group ranking of temperature response during stem elongation. Surprisingly, even the ranking of single genotypes was very similar (Fig. 2C). We used a linear model to regress the genotypic BLUEs of the greenhouse leaf elongation experiment against the genotypic BLUEs for temperature response in stem elongation from Kronenberg *et al*. (Kronenberg *et al.*, 2019). The model yielded a unexpectedly high correlation ($R^2 = 0.58$), indicating that

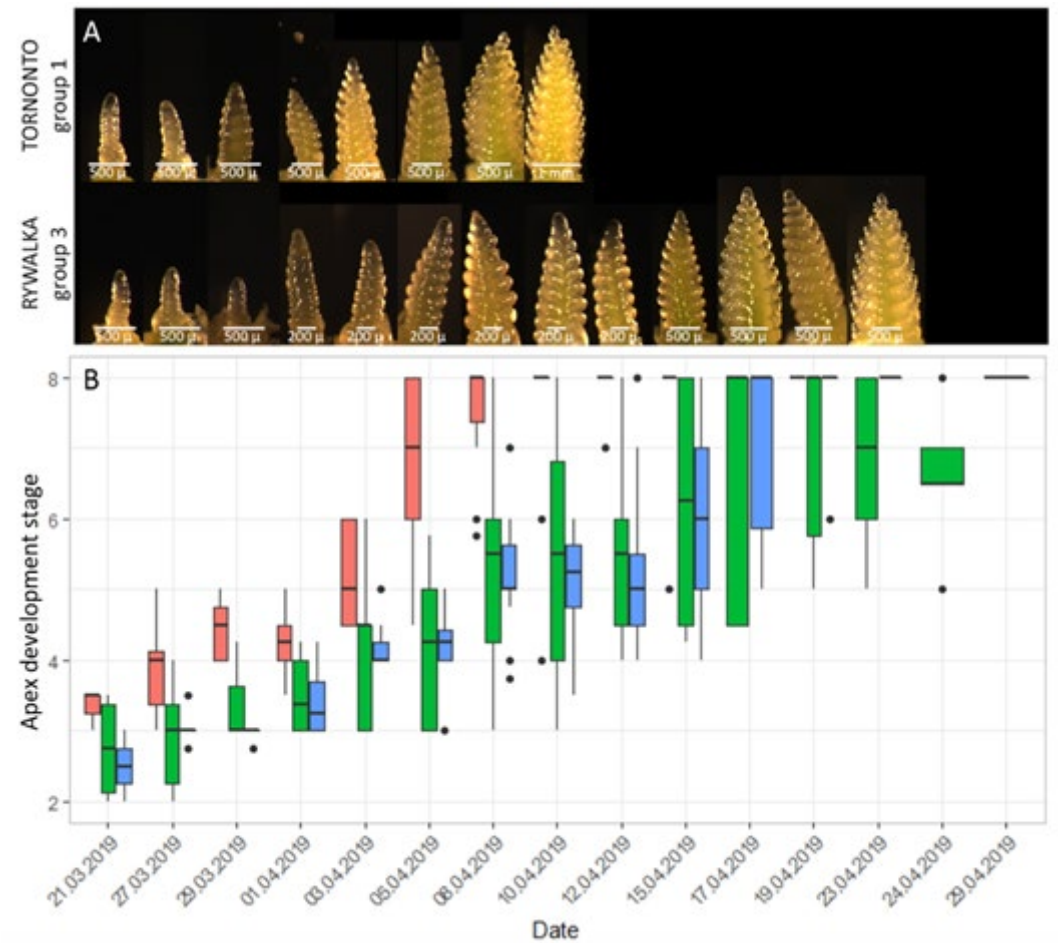

Fig. 3: Transition of the apex meristem from the vegetative to the reproductive stage. A: Pictures show development from genotype TORONTO (group one, low temperature response in stem elongation) and RYWALKA (group three: high temperature response in stem elongation). **B:** Shoot apex development stage following Gardner et al. (1985) for the three temperature response groups (red = low temperature response in SE, green = average response in SE, blue = high response in SE).

temperature response in un-vernalised leaves is comparable to temperature response in stem elongation

Temperature response of population extremes correlates with floral transition

Based on the correlation between start of SE and temperature response during SE (r = 0.63) reported by Kronenberg *et al*. (2019), we evaluated the timing of floral transition among the three temperature response groups by dissecting the shoot apex (Fig. 3A). Based on group median, group one finished transition on the 10th of April 2019, hence one week before group three (Fig. 3B). On the scale of population extremes, this validates the correlation between temperature response and the start of SE as well as GDD_{15} as proxy measure thereof reported by Kronenberg *et al*. (2019). All genotypes of group two and three finished transition by the 23rd April 2019, except genotype WINNETOU (group two)

that was very inhomogeneous in its development. It finished transition the latest, on the 29th April 2019.

The three Rht genes and Ppd-D1 explain a part of the genetic variability between genotypes

Finally, we wanted to investigate whether pleiotropic effects of *Rht* genes and *Ppd-D1* might explain the correlation pattern among temperature response during SE ($slp_{SER\sim T}$), final height (FH), start of SE (GDD_{15}), and end of SE (GDD_{95}). Therefore, where possible, we statistically tested for the effect of these genes, alone and in combination, on the traits. We found that the combination of *Rht-B1, Rht-D1, Rht-24* and *Ppd-D1* explained a considerable part of the variation for all traits ($0.24 \leq R^2 \leq 0.69$, Table 2). For final height, *Rht-D1* explained the largest part of the variation ($R^2 = 0.41$) whereas *Rht-B1* only explained 6%, indicating that *Rht-B1* diversity is small in the population. The combination of all *Rht* genes explained 69% of the variation in final height. Different combinations of *Rht* genes explained a considerable amount variation in temperature response ($0.19 \leq R2 \leq 0.51$) whereas the effect of *Ppd-D1* alone was small ($R^2 = 0.05$). Surprisingly, the effect of Ppd-D1 on GDD_{15} and GDD_{95} was small ($R^2 = 0.06$ and $R^2 = 0.17$, respectively). Also in combination with *Rht* genes, the explained proportion of the variance was small ($R^2 < 0.24$).

Table 2: Effects of *Rht* genes and *Ppd-D1* on final height (FH), start of stem elongation (GDD_{15}), end of stem elongation (GDD_{95}) and temperature response ($slp_{SER\sim T}$). Numbers (R^2, $P < 0.01$) explain how much of the genetic variability is explained by the genes. The four genes were tested for their synergistic effect for each combination.

Rht-B1	*Rht-D1*	*Rht-24*	*Ppd-D1*	FH	GGD_{15}	GGD_{95}	$slp_{SER\sim T}$
Rht-B1				0.06			0.07
	Rht-D1			0.41	0.14		0.26
		Rht-24		0.21		0.06	0.13
			Ppd-D1		0.06	0.17	0.05
Rht-B1	*Rht-D1*	*Rht-24*	*Ppd-D1*	0.69	0.24	0.22	0.52
	Rht-D1	*Rht-24*	*Ppd-D1*	0.53	0.23	0.22	0.39
		Rht-24	*Ppd-D1*	0.21		0.21	0.17
Rht-B1		*Rht-24*		0.24		0.07	0.19
Rht-B1		*Rht-24*	*Ppd-D1*	0.24		0.2	0.2
Rht-B1	*Rht-D1*		*Ppd-D1*	0.64	0.24	0.19	0.51
Rht-B1			*Ppd-D1*		0.07	0.16	0.09
Rht-B1	*Rht-D1*			0.64	0.19		0.49
Rht-B1	*Rht-D1*	*Rht-24*		0.69	0.19	0.08	0.51
	Rht-D1	*Rht-24*		0.5	0.14		0.32
	Rht-D1		*Ppd-D1*	0.45	0.24	0.19	0.35

4.4 Discussion

In this study, we measured growth response to temperature of single wheat leaves in the field and in the greenhouse. The aim was to investigate, whether temperature response of leaf growth in the vegetative phase corresponds to temperature response of stem elongation in the reproductive phase. Further, we wanted to test, whether temperature response measured under controlled conditions are comparable to measurements in the field.

Interestingly, the group ranking found for temperature response during stem elongation changed when temperature response of leaves was measured in the field. Furthermore, temperature response during leaf elongation in the field increased over time and there was a tendency for greater increase in the group that was less responsive during SE in the first weeks. Previous studies have already shown genotypic differences for leaf growth (Cao & Moss, 1989; Nagelmüller *et al.*, 2016). Likewise, differences in temperature response between genotypes and between multiple developmental phases have been reported (Angus *et al.*, 1981; Slafer & Rawson, 1994, 1995c). However, the aforementioned studies were conducted with only few genotypes. Although we conducted our study also with only eleven genotypes, these genotypes represent a wide genetic variability since they were selected as the population extremes of a large set of more than 300 genotypes showing large variation in temperature response during stem elongation (Kronenberg *et al.*, 2019). Consequently, our data showed that there are genotypic differences in temperature response. The rank changes appeared to occur across different developmental phases. In line with this, Grieder *et al*. (2015) have observed that genotypes with high growth rates at low temperatures had lower growth rates at high temperature in the vegetative phase and vice versa. They have concluded that growth at low temperature comes with a certain cost of genetic adaptation.

The temperature response ranking of leaf elongation in the greenhouse did not match the ranking of leaf elongation in the field. There are several possible reasons for this. First of all, greenhouse data in general often does not predict field data accurately with a mean R^2 of 0.26 as reviewed in Poorter *et al*. (2016). The ratio between the daily amount of light and temperature received is smaller under controlled conditions (Poorter *et al.*, 2016). Also plant density, water and nutrient availability and available rooting volume often differs markedly compared to the field (Poorter *et al.*, 2016). Another reason for the changed group ranking could be that we did not use vernalized plants in the greenhouse for the measurements, whereas the field measurements were performed in early spring, when plants were fully vernalised. Finally, the different temperature ranges to which the plants were exposed in the two environments might be the reason for the alteration in the group ranking. In the field, the mean temperature of the seven weeks (5.7 °C) was much closer to the minimum temperature for leaf growth, which is at -1 °C, compared to the temperature range experienced by the plants in the greenhouse. The temperature response ranking of leaf elongation in the greenhouse was similar during the SE phase in the field not only on the group, but also on the genotypic level. We did not expect such a good fit between greenhouse and field data for two different developmental phases. This result supports the

hypothesis, that the difference in temperature range could have caused the rank change between stem elongation and leaf elongation in the greenhouse on the one hand and leaf elongation in the field on the other hand. The optimum temperatures for leaf growth and SE are 22 °C and 20.3 °C, respectively (*as reviewed in* Porter & Gawith, 1999). Therefore, leaf elongation in the greenhouse and SE experienced temperatures closer to the optimum whereas leaf elongation in the field was near the temperature minimum.

Interestingly, the temperature response of leaf elongation in the field almost doubled during the measuring period for all groups even though weekly mean temperature changed by only a few degrees. A change in temperature sensitivity over time (Slafer & Rawson, 1994) and an increase in base temperature has already been reported (Slafer & Rawson, 1995c). In our case, an increase in the mean temperature seems not to be the driving factor for the increase in temperature response. Therefore, we hypothesize that other environmental conditions could have triggered this change, such as increasing solar radiation and day length. Furthermore, the biomass of the growing plant increases with ongoing development and, therefore, more resources become available.

Even though leaf growth response to temperature did not correspond to temperature response in the greenhouse, the field data could still hold valuable information in a breeding context, as leaf growth response to temperature is a good indicator for early vigour (Grieder *et al.*, 2015). Furthermore, high growth response to temperature results in faster canopy cover and, therefore, weed suppression (Coleman *et al.*, 2001). The rank change in genotype specific temperature response between different temperature ranges has to be investigated further. It seems as if growth response to temperature in the greenhouse could be used to screen wheat plants for their temperature response during SE. The correlation with floral transition and with final height indicate that temperature response could be used to simultaneously breed for earliness and reduced height. However, the data should be validated by measuring temperature response in different temperature ranges in a controlled environment. If the temperature response of different genotypes is dependent only on the temperature irrespective of their developmental phase, then screening must be done in the right temperature range.

Plant height correlated positively with temperature response during SE in the data used in this study (Kronenberg *et al.*, 2019). Keyes *et al*. (1989) have found that the growth rate was a negative linear function of the number of *Rht* genes in leaf elongation. Other authors found that growth rate in SE was reduced in dwarf varieties. (Youssefian *et al.*, 1992b) have shown that growth rate in SE was reduced in lines carrying dwarf alleles genes. Furthermore, it was shown that the relative growth rate of the flag leaf was decreased by *Rht-B1c* and *Rht-D1b* (King *et al.*, 1983). These findings raise the question whether temperature response is a pleiotropic effect of dwarf genes. However, the GWAS results from Kronenberg *et al*. (2019) indicate, that temperature response is under independent genetic control. The fact that the three major *Rht* genes combined explained 51% of the variation in temperature response might be explained by the above-discussed reduction in growth rate due to *Rht* genes. Alternatively, as our results imply a connection between

temperature response and earliness, the correlation between final height and temperature response might be partly be due to co selection for earliness and reduced height in European elite cultivars.

4.5 Conclusion

Overall, we could show that genotypes changed in their responsiveness to temperature between the vegetative and reproductive phase in the field, which was also reflected in the time points they finished transition between these two phases. It is not known, which physiological mechanism caused this change in responsiveness to temperature, but it might indicate that temperature response depends on the ambient temperature range. We could show that the temperature response of stem elongation is accessible by measuring the temperature response of leaves grown in the greenhouse under warm ambient temperatures. New phenotyping platforms, that allow leaf length tracking with reasonable replicate numbers, make temperature response as a trait measurable in the greenhouse in an easy and efficient way. Further investigation of the physiological response of plant growth to temperature should be carried out in the future. Such studies should be performed in controlled conditions and they should analyse plant growth in different organs, temperature ranges and developmental stages. If the leaf growth response to temperature could be reproduced in controlled conditions at low temperatures, this could clarify the question whether temperature response changes due to low temperatures.

Acknowledgement

We sincerely thank Norbert Kirchgessner and Hansueli Zellweger for their help in overhauling the LLT system. Further, we thank Hansueli Zellweger for maintaining and nursing the field and Norbert Kirchgessner for the improvements in the LLT analysis software. We also thank Gustavo A. Slafer (University of Lleida) for his valuable input concerning the meristem dissections and Marion Röder (IPK Gatersleben) for supply of the GABI wheat panel including genetic information. This work was supported by the Swiss National Foundation (SNF) in the framework of the project PhenoCOOL (project no. 169542).

5 Diel temperature regime markedly affects gene expression, carbohydrate metabolism and diel leaf growth in soybean

Lukas Kronenberg[a], Steven Yates[b], Shiva Ghiasi[c], Lukas Roth[a], Michael Friedli[a], Michael Ruckle[b], Roland Werner[c], Flavian Tschurr[a], Melanie Binggeli[a], Nina Buchmann[c], Bruno Studer[b] and Achim Walter[a]

[a] Crop Science, Institute of Agricultural Sciences, ETH Zürich, 8092 Zurich, Switzerland
[b] Molecular Plant Breeding, Institute of Agricultural Sciences, ETH Zürich, 8092 Zurich, Switzerland
[c] Grassland Sciences, Institute of Agricultural Sciences, ETH Zürich, 8092 Zurich, Switzerland

Abstract

Plants have evolved to grow under prominently fluctuating environmental conditions. In controlled conditions, temperature is often set to artificial, binary regimes with a constant value at day and a constant value at night. Here, we investigated how such a diel (24 h) temperature regime affects leaf growth, carbohydrate metabolism and gene expression, compared to a temperature regime with a field-like gradual increase and decline throughout 24 h. We found that leaf growth shows different times of peak activity under the two treatments that cannot be explained intuitively. Also, diel patterns of starch and sucrose as well as expression of 5'042 genes differed between treatments. The binary temperature regime induced a daytime synchronization of genes controlling cell division, amongst other findings. The results show that the coordination of a wide range of metabolic processes is markedly affected by the diel variation of temperature.

5.1 Introduction

Leaf growth, gene expression and plant metabolism are tightly coupled to the environment by internal oscillators such as the circadian clock (McClung, 2001; Nozue *et al.*, 2007; Farré, 2012; Ruts *et al.*, 2012). By controlling gene expression and metabolic processes, the circadian clock enables plants to synchronize their metabolism with external stimuli, thus optimizing photosynthesis, growth, survival and competitive advantage (Green *et al.*, 2002; Dodd *et al.*, 2005; Caldeira *et al.*, 2014). Environmental factors such as light, temperature, water or nutrient availability affect leaf growth (Pantin *et al.*, 2011, 2012). Rapid changes of these factors can potentially alter the short-term, diel (24 h) pattern of leaf growth. It was reported frequently that leaves of dicot plants show pronounced diel growth fluctuations that are repetitive, but largely independent of the diel temperature regime (Bunce, 1977; Nozue *et al.*, 2007; Walter *et al.*, 2009; Poiré *et al.*, 2010). In contrast, leaf growth of monocot plants has often been reported as tightly linked to diel variations of the temperature regime (Gallagher, 1979; Sadok *et al.*, 2007; Nagelmüller *et al.*, 2016; Yates *et al.*, 2019).

Over decades, plant physiological studies have been performed under controlled conditions in climate chambers. There, environmental factors are typically set to a regime that deviates markedly from that in the field. Light intensity, humidity and temperature are often controlled in a rather binary, step-wise way and not in gradually fluctuating regimes similar to what would be found in the field. With respect to temperature, climate chamber studies often apply day-night temperature differences of less than 6 °C in a binary (constant day/constant night temperatures) regime (Poorter *et al.*, 2016). It is unclear, whether this feature affects growth, metabolism and gene expression – and if yes, to which extent.

Based on the recent development of a method to analyse dicot leaf growth in the field and in the growth chamber (Mielewczik *et al.*, 2013), it became obvious that diel patterns of dicot leaf growth might differ markedly when analysed either in the field or in controlled conditions. Differences in the organization of the leaf growth zone between monocots and dicots might favour the special significance of this effect in leaves of dicot plants (Nelissen *et al.*, 2016). In monocots, the zones of cell division and of cell expansion are clearly separated. The dividing cells of monocots are situated close to the ground and are surrounded by the sheath of older leaves, which protects them from some environmental fluctuations (Allard & Nelson, 1991; Brégard & Allard, 1999). In contrast, dicot leaves show cell division and cell expansion in tissue that is exposed to the sunlight (Avery, 1933; Poethig & Sussex, 1985) and thereby to a very different microclimate compared to the protected growth zone of monocot, graminoid leaves. The buffering effect of the ground also benefits rosette or rosette-like dicot species such as *Arabidopsis thaliana* or seedlings of *Nicotiana tabacum*. The difference between monocot and dicot plants becomes more pronounced in species with a less prostrate growth habit, with leaves situated several cm above ground. Therefore, leaves of plants such as soybean (*Glycine max*) would be better suited to analyse the influence of differing temperature regimes on dicot leaf growth and metabolism.

The aim of this study is to test the hypothesis that the environmental perception mechanisms of the plant, such as the circadian clock, are sensitive to not only the absolute value of temperature perceived, but that the pattern of temperature to which a growing leaf is exposed to affects the underlying metabolism and gene expression that times growth processes in *Glycine max*.

5.2 Results

Diel leaf growth in field grown soybean follows temperature

In a preliminary experiment, we measured relative growth rate (RGR) of leaves of field-grown soybean and compared it to measurements performed in controlled conditions with a binary temperature regime. The diel growth pattern observed in the field differed considerably from the growth pattern observed under binary controlled conditions. In the field, relative growth rate (RGR) mirrored the increasing temperature with a maximum in the mid-afternoon and minimum growth at night (Fig. 1 a). In contrast, RGR observed in a binary temperature regime displayed the reported pattern for soybean growth, where growth rate reaches a maximum towards the end of the night period, and a minimal growth rate is observed in the mid-afternoon (Fig. 1 b; Friedli & Walter, 2015). Such patterns were also observed in *Arabidopsis thaliana* (Pantin *et al.*, 2011) or seedlings of *Nicotiana tabacum* (Walter *et al.*, 2009; Poiré *et al.*, 2010). In order to test whether the observed pattern from the field could be reproduced under controlled conditions, we performed a second preliminary experiment. There, we grew plants in a dynamic temperature-controlled environment, where the diel temperature mimicked the temperatures experienced in the field. We found that under the simulated field conditions, leaf RGR reached a maximum in the afternoon, as was observed in the field (Fig. S1 a). This growth pattern immediately switched back to maximum RGR at end-of-night, when the temperature was changed to a classic non-dynamic, binary regime (see Day 3 in Fig. S1 a).

A binary temperature regime induces a peak of leaf growth in the early morning

Based on these results, we set up an experiment under controlled conditions with two temperature treatments: The first treatment was binary (Bi), where the temperature was set to a constant 21 °C/17 °C day/night temperature regime. In the second treatment, temperature was set to a gradually (Gr) fluctuating diel time course, simulating the diel temperature observed in field conditions.

The leaf growth measurements showed pronounced differences in diel RGR patterns between the treatments (Fig. 2 a). Plants in the Bi treatment had a maximum RGR at the beginning of the day. Then, RGR gradually declined towards the dark period, but a second maximum was observed in the middle of the night. In contrast, the growth pattern in the Gr treatment resembled the one observed in the field. RGR peaked in the afternoon and then gradually declined towards the end of the day, with no increase in RGR at night. These contrasting patterns became increasingly apparent when the diel trend (*i.e.* seasonal) was extracted through time series decomposition (Fig. S2 b).

In the Bi treatment with constant day and night temperatures, there was no apparent connection between RGR and temperature (Fig. 2 b). In contrast, the Gr treatment with a field-like temperature cycle showed a diel growth pattern highly correlated with temperature (Fig. 2 c). Beyond this observation we modelled RGR within each treatment using a simple growth model based on temperature, vapour pressure deficit, light and the leaf size / age (eq.1; Nagelmüller *et al.*, 2018). In the Gr treatment the model was able to predict RGR with an accuracy of R^2 = 0.64 (Fig. S3 a), with significant effects of temperature, light and leaf size (Table 1). In comparison, the model performed poorly in the Bi treatment (R^2 = 0.27, Fig. S3 b), where only leaf size showed a significant effect (Table 1). Because absolute leaf size is finite, RGR decreased as leaves aged in both treatments. However, the decline was greater and more linear in the Bi treatment in the first half of the experiment compared to the Gr treatment (Fig. S2 c).

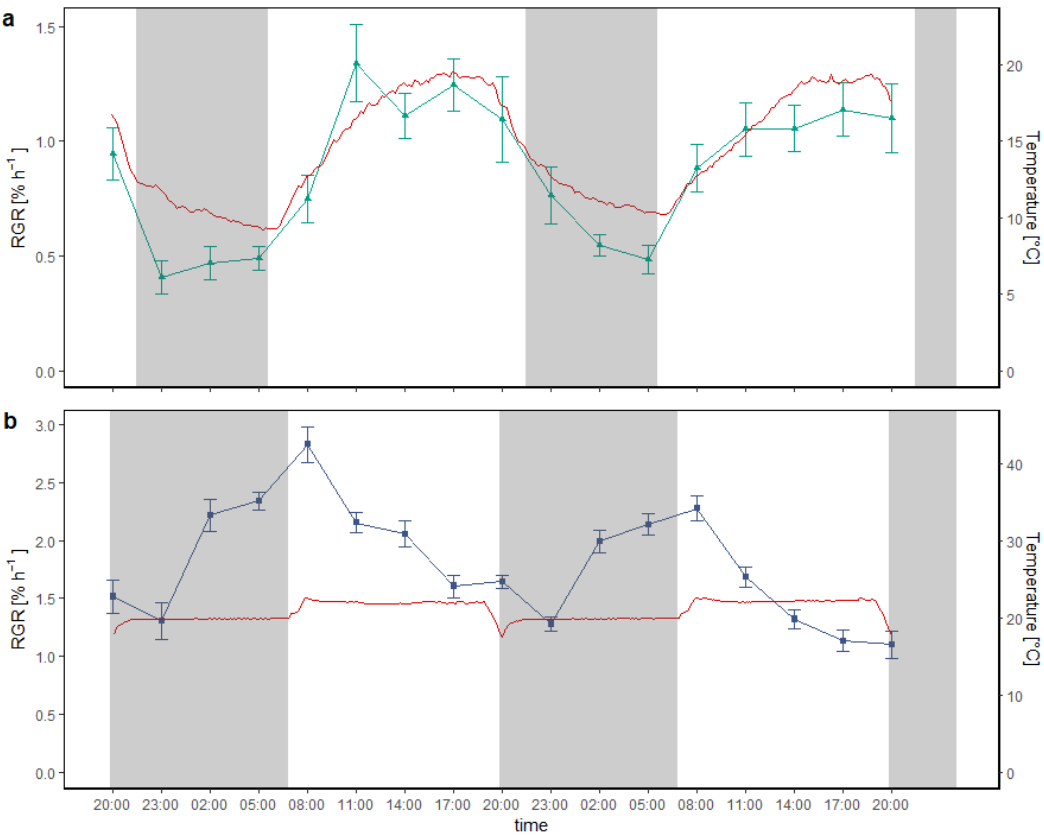

Fig. 1: Diurnal growth pattern of soybean leaves in the field and under controlled conditions. **a:** Green triangles and error bars show the mean relative growth rate (RGR; $\%h^{-1}$) and standard error (SE) of n = 12 soybean leaves grown in the field. **b**: Blue squares and error bars show mean RGR ± SE of n = 6 soybean leaves grown under controlled conditions in a binary temperature regime with constant day and night temperatures. RGR was captured every 90s and aggregated to 3 h average per leaf. The solid red lines show the air temperature in the field (**a**) and under controlled conditions (**b**), and shaded areas indicate the dark period. Data for b was adapted from figure S4 of Friedli & Walter (2015), with kind permission of Wiley.

Temperature, relative humidity (RH), vapour pressure deficit (VPD) and light were monitored throughout the experiment (Fig. S4). The temperature sum was similar for the Bi and Gr treatments, but due to technical limitations of growth chamber control, plants in the Bi treatment experienced a slightly higher temperature sum of 76.5 °Cd compared to 72.0 °Cd in the Gr treatment, due to a difference of 1.13 °C in daily mean temperature. Accordingly, total leaf growth was lower in the Gr treatment (198 % ± 6.6 % SE) compared

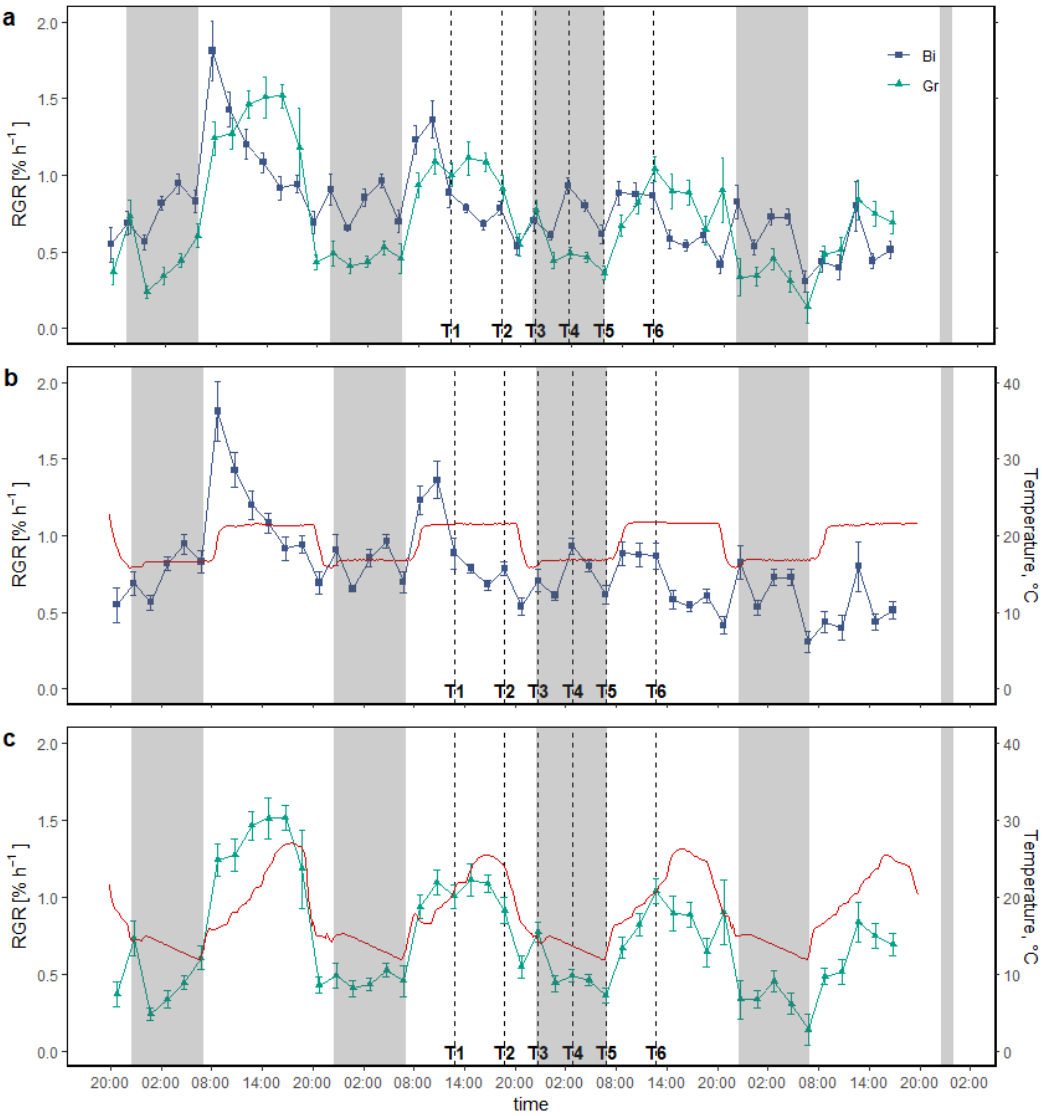

Fig. 2: Diurnal growth pattern of soybean leaves under contrasting temperature conditions. a Shows the relative growth rate (RGR; $\%h^{-1}$) under binary diurnal temperature conditions (Bi, blue squares) and gradient temperature regime (Gr, green triangles). **b** Illustrates the RGR under Bi conditions in relation to temperature (solid red line) and **c** the RGR in the Gr treatment in relation to temperature. RGR data was aggregated to 2 h. Mean ± SE is shown for n = 9 replicates per treatment. Shaded grey areas indicate the dark period and vertical black dashed lines indicate the sampling time points (T1-T6) for RNA-seq and carbohydrate analysis.

to the Bi treatment (212 % ± 7.5 % SE). However the difference was not statistically significant ($P = 0.195$).

Diel fluctuations of starch and soluble sugars feed carbohydrates into the expanding tissue

In order to investigate if the observed differences in growth are aligned with corresponding fluctuations in the leaf carbohydrate content, we measured the concentrations of starch, glucose, fructose and sucrose (mg $g_{drymatter}^{-1}$; Fig. 3 a-b, Fig. S5 a-c) in the leaves at each sampling time point (T1-T6; Table S1). The first sampling time-point (T1) was at 12:45 pm on the second day of the experiment, which coincided with mid-morning in the subjective time of day in the experiment. T2 was six hours later in the subjective afternoon, followed by T3 at 10:45 pm just after subjective dusk. T4 was in the middle of the night followed T5 before the subjective dawn at 06:45 am. The last sampling (T6) was done 24 hours after T1. In addition, to determine the effects of temperature on carbon dynamics in

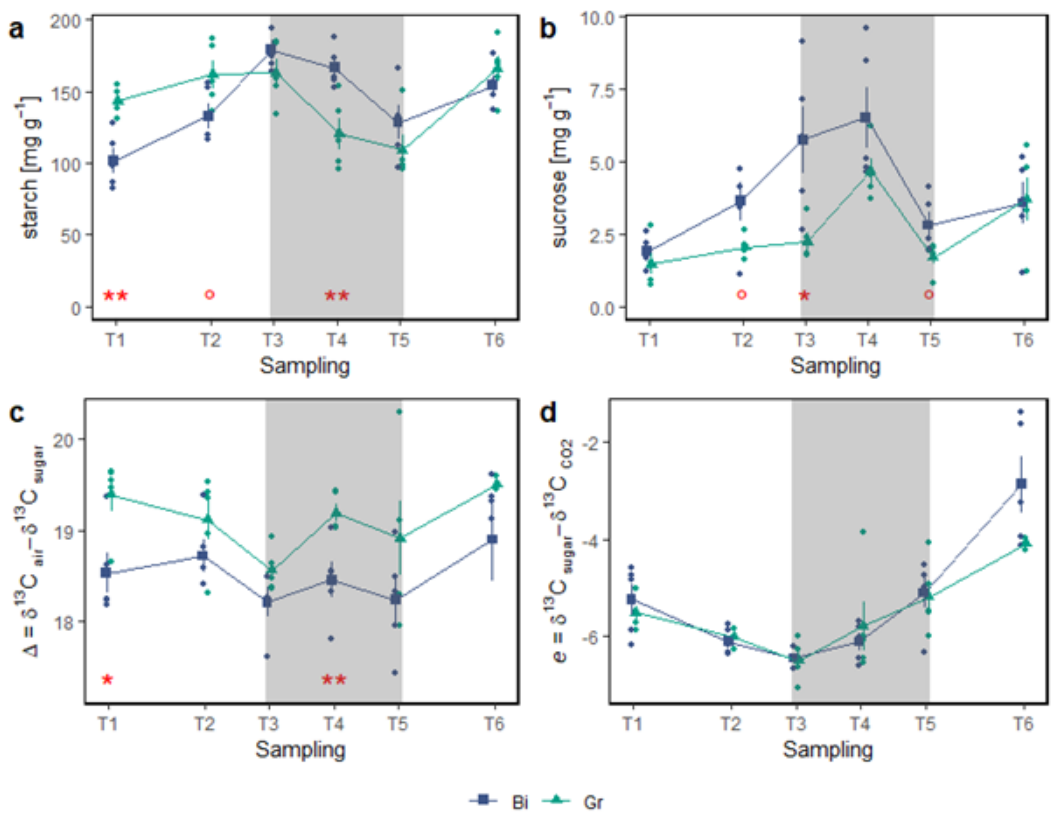

Fig. 3: Leaf concentration of starch (a) and sucrose (b) as well as carbon isotope discrimination (Δ, c) and apparent isotope fractionation (*e*, d) at the respective sampling time points (T1-T6). Blue squares and green triangles show the mean of n = 5 samples for the respective treatment and time point (Bi = binary temperature regime, blue squares; Gr = gradient temperature regime, green triangles). Blue and green dots show individual measurement points of the respective treatment and error bars indicate the standard error. Red stars and dots indicate significant differences between the treatments (*** = $P < 0.001$, ** = P 0.01, * = $P < 0.05$, ° = $P < 0.1$) and shaded areas indicate the dark period.

the leaves, we conducted carbon isotope analysis of plant bulk, carbohydrates and respired CO2 (Fig. S5 d-g).

Table 1: ANOVA table of the growth model applied to each treatment (Bi, Gr) individually to predict relative growth rate based on temperature (T), vapour pressure deficit (VPD), light (L) and square root of the leaf area (A, *see* Eq. 1).

Predictor	Df	Sum Sq	Mean Sq	F value	Pr(>F)	
Gr: Gradually fluctuating temperature regime						
T	1	2.756001	2.756001	60.44055	1.16E-09	***
VPD	1	0.071798	0.071798	1.574574	0.216482	n.s.
L	1	0.340348	0.340348	7.464004	0.009167	**
$\sqrt{A}$	1	0.677035	0.677035	14.84773	0.000393	***
Residuals	42	1.915139	0.045599			
Bi: Binary temperature regime						
T	1	0.092802	0.092802	1.559247	0.218691	n.s.
VPD	1	0.110277	0.110277	1.852845	0.180712	n.s.
L	1	0.000643	0.000643	0.010809	0.91769	n.s.
$\sqrt{A}$	1	1.061198	1.061198	17.83003	0.000127	***
Residuals	42	2.499732	0.059517			

In the Bi treatment, starch increased rapidly throughout the day (T1-T3), decreased during the night (T3-T5) and increased again until the final sampling time point (T6; Fig. 3 a). In the Gr treatment, the afternoon increase (T2-T3) of starch was less pronounced compared to the Bi treatment. The decrease during the night was comparable for Gr and Bi treatments, and in the morning (T6) the value of ca. 150 mg g-1 was reached again (Fig. 3 a). Overall, leaves in the Bi treatment showed a higher amplitude of fluctuation. For both treatments, starch was not depleted completely at the end of the night. For sucrose, a more rapid increase and overall accumulation was observed during the afternoon in the Bi treatment compared to the Gr treatment (Fig. 3 b). Sucrose was not completely depleted at the end of the night, either, and values observed at T6 were somewhat higher than those at T1. For glucose and fructose, no significant differences between the treatments were observed. Both carbohydrates fluctuated in a similar pattern throughout the diel cycle (Fig. S5 a-b). The total soluble sugars content was higher in the Bi treatment during the night than in the Gr treatment (Fig. S5 c).

Accumulation and storage of carbon as starch and sucrose during the afternoon in the Bi treatment is consistent with the reduced afternoon RGR in this treatment. This observation is consistent with photosynthates being utilized less for growth processes during the afternoon compared to the Gr treatment (Gibon *et al.*, 2004, 2009; Graf *et al.*, 2010; Stitt & Zeeman, 2012). At night, sucrose concentration decreased in the Bi treatment, which is consistent with it being used for increased RGR at night. In both treatments, carbohydrate concentrations increased from T1 to T6 (from one day to the next), reflecting the transition of the growing leaf from a sink to a source organ (Pantin *et al.*, 2011; Ruts *et al.*, 2012;

Pilkington *et al.*, 2015). In the course of leaf ontogeny, there is increasing water competition between growth and transpiration, leading to a switch from metabolic to hydraulic control of leaf expansion (Pantin *et al.*, 2011; Ruts *et al.*, 2012). Limited growth capacity coupled with more photosynthetic tissue thereby turns older leaves into a net source for carbon which is stored as starch (Pantin *et al.*, 2011; Ruts *et al.*, 2012; Pilkington *et al.*, 2015). Overall, these results are in accordance with the role of starch metabolism as the balance between growth and carbon supply in both treatments (Sulpice *et al.*, 2009; Graf *et al.*, 2010; Ruts *et al.*, 2012).

Our isotope analysis showed a consistent ^{13}C enrichment in the leaves of plants grown in Bi regime compared to Gr (Fig. S5 d-g). In order to have a better insight into plant carbon metabolism, we calculated carbon isotope discrimination (△ ; Farquhar *et al.*, 1982) as well as post-photosynthetic carbon isotope fractionation (e; Ghashghaie *et al.*, 2003). Results showed higher discrimination (△) in plants grown in the Gr condition compared to Bi (Fig. 3 c). Since there was no difference in *e* between plants (Fig. 3 d), it can be concluded that the differences observed in $\delta^{13}C$ of bulk, sugars, starch and that of respired CO_2 (Fig. S5 d-g) are a result of carbon isotope discrimination that takes place during the photosynthesis, during which CO_2 is assimilated into sugars. Changes in VPD and temperature ranges (Fig. S4 a-c) did not support higher △ observed in Gr condition, as shown by earlier studies (Sharifi & Rundel, 1993; Cornwell *et al.*, 2018). However, studies by Troughton and Card (1975) and Körner *et al.* (1991) showed positive dependencies of △ to increasing temperature, as observed in our study (see Fig. 3 c). Dependence of △ on temperature and not on VPD in this study conveys a difference in the carbon assimilation process between these two conditions that could well be related to the differences observed earlier in the concentration analysis.

Differences in diel temperature pattern cause differences in gene expression

Given the differences in RGR and metabolite accumulation patterns between the two treatments, we wanted to determine whether growth was repressed or growth phases differently partitioned due to metabolic processes. Or alternatively, if diurnal growth changed due to altered endogenous rhythmicity in response to the temperature treatments. To investigate this, we performed RNA-seq and subsequent differential gene expression analysis of leaves sampled at the time points T1-T6 (Fig. 2, Table S1).

Comparison of pairwise treatments at each time point identified 5’042 unique differentially expressed (DE) genes. The number of DE genes varied across time points, with T3 having the least (n = 97, Table 2) and T6 having the most (n = 2’469) DE genes. Overlap in DE genes among time points is illustrated in Fig. 4 a. To get a holistic overview of the samplings and treatments we subjected the differentially expressed genes to a principle component analysis (PCA). Broadly, the first two components (together explaining 56% of the variation) represent a clock, with sampling times distributed clockwise (Fig. 4b). Moreover, the two treatments cluster together. The first principle component (explaining 36% of the variation) mostly discriminates between day (T1, T2, and T6, negative on the

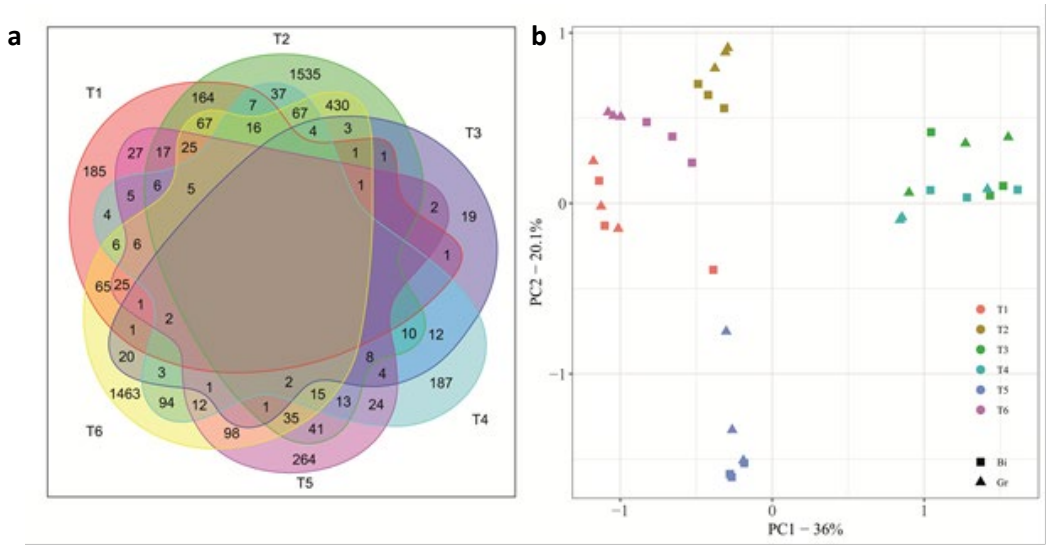

Fig. 4: Distribution of differentially expressed (DE) genes between samples and time points. a: Venn diagram showing the number of unique DE genes per time point and the number of common DE genes between time points. **b:** Principal component analysis using the correlation matrix of DE genes per sample (n = 3), time point (T1-T6, see colour legend) and treatment (squares = binary (Bi), triangles = gradient (Gr) diurnal temperature regime).

x-axis) and night (T3 and T4, positive on the x-axis), whereas the second principle component mostly discriminated T5 (between day and night). Thus, whilst there are perturbations of gene expression the overall transcriptome profiles are diurnal and conserved between treatments.

Table 2: Number of differentially expressed (DE) genes per sampling time point (T1-T6).

TP	DE genes count
T1	638
T2	2511
T3	97
T4	550
T5	640
T6	2469
total	6905
unique total	5042

We then looked for changes in biological processes between the two treatments. Instead of comparing single time points, we clustered the expression profiles using a 4x4 self-organizing map (SOM, Fig. S6). Using gene ontology (GO) term enrichment analysis, we found many biological processes were differentially regulated in the clusters. Here we found clusters enriched for growth (clusters 1,3 and 10) cell division (clusters 4 and 8), carbon metabolism (cluster 2), photosynthesis (clusters 5, 6 and 11), and circadian rhythm

(clusters 12 and 16). Some clusters show inconsistent expression patterns between T1 and T6 (*i.e.* clusters 7, 14 and15) in the Bi treatment. A possible explanation for this effect could be leaf aging from one day to the next, which is also represented by the markedly declining growth rate (Fig. S2 c).

A binary temperature regime caused a synchronization of cell division

The SOM clustering yielded two distinct clusters enriched with genes associated with different processes in the cell cycle (Fig. S6; clusters 4 and 8). Together, 253 genes contained at least one GO term related to cell division processes, presenting a broad spectrum of molecular functions. All of these genes were over-expressed in the Bi treatment at T2 (Fig. 5 a), coinciding with minimal growth after the growth peak in the early morning. In contrast, the expression of these genes was random in the GR treatment. This indicates a synchronization of cell division in the leaf cells in the binary temperature regime. Thus,

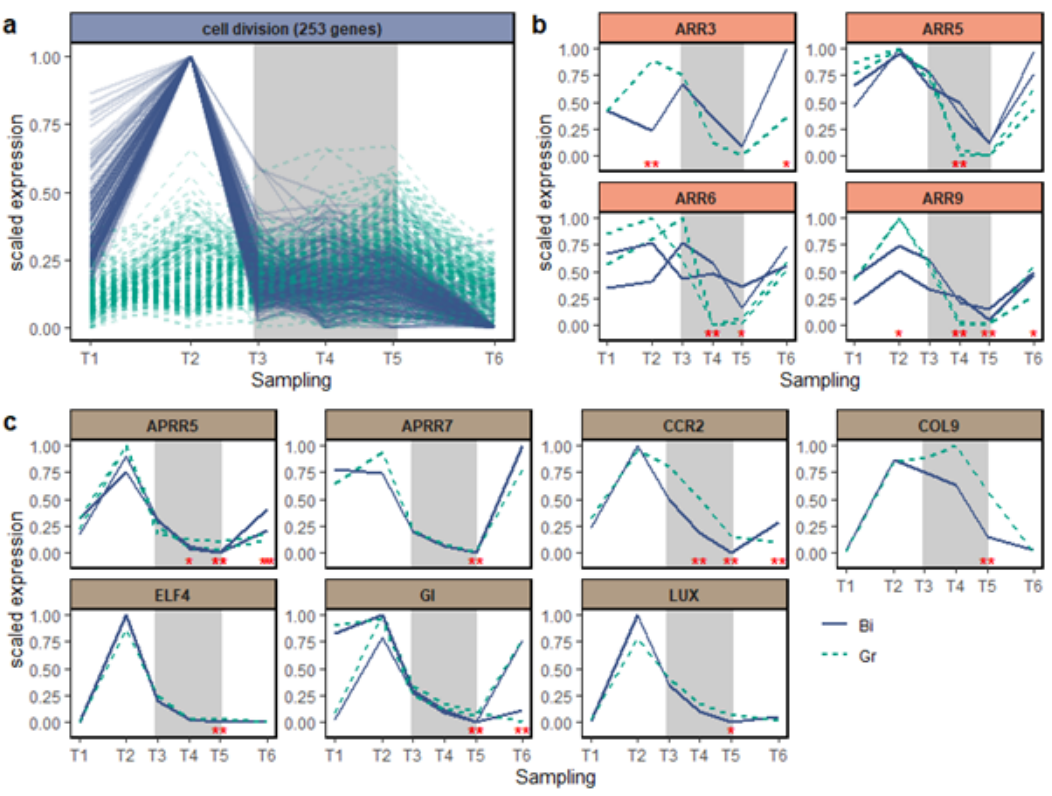

Fig. 5: Expression profiles of differentially expressed genes enriched in specific gene ontology terms from gene groups clustered by a self-organizing map. Expression of all time points (T1-T6) was scaled between 0 and 1 for every gene. **a:** Genes associated with cell division upregulated at T2 in the Bi treatment. **b:** Circadian clock-associated genes upregulated in the Bi temperature treatment in the dark period. **c:** Circadian clock-associated genes upregulated in the Gr temperature regime in the dark period. Time points with significant differential expression are indicated with * ($P < 0.05$), ** ($P < 0.01$) and *** ($P < 0.001$). The shaded areas indicate the dark period. Genes were selected form the self-organizing map clusters 4 and 8 for a and from clusters 12 and 16 for **b** and **c** (see Fig. S6).

this might explain the decrease in RGR in the Bi treatment as cells were undergoing division and not expansion. The synchronization of cell cycle was unexpected as we found no reports of naturally occurring cell division synchronization in higher plants. Yet, synchronization of cell cycle has been observed in algae, cyanobacteria and other unicellular organisms, which is controlled by the circadian clock (Mittag, 2001; Mori & Johnson, 2001; Yang *et al*., 2010; de Winter *et al*., 2013).

Temperature treatments affect expression of different regulatory elements associated with the circadian clock

Given the tentative link between the circadian clock and cell division, we then examined the clusters with enrichment of clock-associated genes. Clusters 12 and 16 contained a number of circadian clock genes which were upregulated at night, depending on the treatment (Fig. S6). At night (T4, T5), type-A Response Regulators (*ARR5*, *ARR6* and ARR9) were upregulated in the Bi treatment coinciding with the night growth peak in this treatment (Fig. 5 b). *ARR3* and *ARR9* on the other hand were downregulated at T2 coinciding with the decline in RGR and with the upregulated cell division in the Bi treatment at this time point. Given the type-A response regulators negatively regulate the response to the phytohormone cytokinin (To *et al*., 2004), this might explain the cell division synchronisation. Because cytokinin plays a key role in plant growth, morphogenesis and cell division (Werner *et al*., 2001).

In the Gr treatment with more natural temperature fluctuations, a number of circadian clock genes were upregulated at night when temperatures were low (Fig. 5 c). These were namely the morning loop genes *PSEUDO-RESPONSE REGULATOR 5* (*APRR5*) and *APRR7*, the evening components *EARLY FLOWERING* 4 (*ELF4*), *LUX ARRHYTHMO* (*LUX*) and *GIGANTEA* (*GI*), and the clock regulated genes *COLD CIRCADIAN RHYTHM AND RNA BINDING 2* (*CCR2*) and *CONSTANS-LIKE 9* (*COL9*). *PRR5* and *PRR7* as well as *ELF4* and *LUX* are important components of the temperature compensation mechanism in the *Arabidopsis thaliana* circadian clock (Salomé *et al*., 2010; Jones *et al*., 2019). Together with *ELF3*, *ELF4* and *LUX* were reported to regulate the diurnal gating of hypocotyl elongation, peaking at dawn, in *Arabidopsis thaliana* (Nusinow *et al*., 2011). The clock also mediates diurnal starch turnover, with increased starch accumulation in mutants lacking GI (Eimert *et al*., 1995; Izawa *et al*., 2011; Ruts *et al*., 2012).

5.3 Discussion

In this study, we measured growth of soybean leaves in high temporal resolution in the field and under controlled conditions. The first important finding was that diel growth pattern measured in the field was profoundly different from what is expected based on findings from controlled conditions. In the field, plants did not show the expected growth peak at night, instead RGR closely followed temperature. We were then able to reproduce the observed growth pattern in the field under controlled conditions by mimicking a natural temperature regime. Not only did this alter the diel growth pattern but resulted in clear differences in metabolism and timing of cell division. Temperature effects were not

detectable in the Bi regime but became apparent in the Gr regime even though average temperature was kept similar in both treatments. Together, the data presented here allow for new insight on interplay between carbon metabolism, growth and gene expression in response to ambient temperature.

It is known from studies with starch-free mutants that the carbohydrate status has a direct impact on the amplitude and phasing of diel leaf growth patterns (Wiese *et al.*, 2007). Mutants that cannot store carbohydrates produced, via photosynthesis, during the afternoon show a higher growth rate during this time of the day. Whereas at night, they are depleted in energy and carbohydrates for cell wall synthesis which inhibits growth (Wiese *et al.*, 2007). Similar shifts in pattern are seen here, demonstrating the tight connection between diel fluctuations of carbohydrate concentrations and diel leaf growth patterns. Moreover, the diel growth patterns fit with the gene expression data. The synchronization of genes involved in cell division in the late afternoon implicates that at this time of the day, the remaining cell division activity of the soybean leaf takes place in the Bi treatment (also: *APRR* and other activities are aligned with this). This phase is then followed by a later phase of cell expansion, leading to the observed peak of leaf growth activity during the night. In the Gr treatment though, cell division activity is spread out during the diel cycle and mirrors that of the temperature course. Thus, it appears that in dicots, growth is more temperature driven than regulated by the circadian clock – at least under natural temperature regimes. This is in agreement with findings from the monocot *Brachypodium distachyon*, where growth follows temperature despite clear circadian gene expression (Matos *et al.*, 2014).

Both temperature and light are important factors for a 'realistic' behaviour of plant growth and metabolism under controlled conditions. Annunziata *et al*. (2017) demonstrated, that diel carbon and nitrogen metabolism were significantly altered, when *Arabidopsis* plants were grown in sunlight compared to binary or sinusoidal artificial illumination. Similar effects on metabolism and gene expression where shown with respect to temperature (Annunziata *et al.*, 2018). Our study confirms these results and directly links this to leaf growth showing the manifold effect of temperature on plant function. Moreover the clock appears to synchronize cell division in the late afternoon. Broadly the core clock is retained regardless of temperature regime, but some elements are recruited for this synchronization. The results suggest that when plants experience a natural diel temperature cycle, similar to that in the field, their leaf growth follows that of temperature. Yet, under a binary temperature regime, the circadian clock plays a prominent role in leaf expansion.

Together, these results have important implications for further investigations into plant metabolism, plant-environment interaction, and the genetic control thereof. If the aim is to understand or predict how plants develop in natural environments, climate conditions set to a more realistic regime could lead to results that are more transferrable. State of the art growth cabinets allow mimicking natural conditions in greater extent compared to the current study. Digital controllers, lights, and sensors allow for precise, real-time, and dynamic control of temperature, humidity, and light (Cruz *et al.*, 2016). In contrast, specific

processes (e.g. cell division in the current study) may become more accessible under binary or steady state settings. Thus, applying binary or steady state settings for one or multiple variables could be beneficial to study processes isolated from the effects of these environmental variables.

Acknowledgement

We thank Brigitta Herzog for her support in planting and nursing the seedlings used for the controlled condition experiments in this study and Hansueli Zellweger who maintained and nursed the field experiments. Further, we thank Norbert Kirchgessner for his support with the analysis software Martrack Leaf. This work was supported by the Swiss National Foundation (SNF) in the framework of the project PhenoCOOL (project no. 169542).

5.4 Material and methods

In preliminary experiments, leaf growth in soybean (*Glycine max* (L.) Merrill, variety Gallec) was measured in the field in 2014 and under controlled conditions in 2015. Based on these results, the main experiment presented in this study was performed also under controlled conditions in 2017.

Preliminary field experiment 2014

Measurements of field-grown soybean were conducted at the research station for plant science of ETH Zurich in Eschikon, Lindau (Switzerland) in 2014. The setup for the leaf growth measurements were arranged as described in detail in Mielewczik *et al.* (2013) and Friedli & Walter (2015) with the exception of two modifications. First, white beads on a black background were used instead of black beads on a white background. By the exchange of the colour of the beads and the background, disturbing shades almost never occurred which resulted in a markedly improved tracking rate. Second, weatherproof closed-circuit television (CCTV) cameras (Lupusnet HD - LE934, CMOS sensor, maximal resolution of 1920 × 1080 pixels, Lupus-Electronics® GmbH, Germany) were used to take images in the field. These cameras have an internal infrared lighting, enabling to take images also during the night. Images are saved automatically on an exchangeable micro SD card. Thus, no computer was needed in the field for image storage as it was necessary for the measurements reported in Mielewczik *et al.* (2013) and measurements could also be conducted during rainy periods. The measurements were performed on the youngest fully unfolded trifoliate leaf in six plants simultaneously over a period of four weeks between June 20 and July 21 2014. Data from 12 independent leaves grown under comparable weather conditions were combined in one weekly time course. Relative growth rate (RGR) was captured every 90 seconds and data were aggregated to 3 h-mean values.

Preliminary growth cabinet experiments 2015: simulated field conditions and switch to binary temperature regime

Soybean plants [*Glycine max* (L.) Merrill, variety 'Gallec'] were inoculated with 'HiStick® Soybean Inoculant' (Becker Underwood Limited, UK) and grown in QuickPot™ trays (88 cm^3 per seedling, Herkuplast Kubern GmbH, Germany) filled with a sterilized substrate (Substrat1, Klasmann-Deilmann GmbH, Germany) that was autoclaved at 121 °C for 30 minutes prior to sowing. After 18 days, seedlings were transferred to clay pots (12 cm in diameter) filled with a mixture by weight of 2/3 'sterile Landerde' (RICOTER Erdaufbereitung AG, Switzerland) and 1/3 fire-dried quartz sand (0.7-1.2 mm, Carlo Bernasconi AG, Switzerland). After transplantation, plants were grown in a climate chamber (Conviron, Winnipeg, Canada) with climate parameters (temperature, relative humidity, temporal cycle of light intensity) set to average conditions of six successive days (21.-26. June 2014) recorded during growth measurements in the field in 2014. In this setting, the temperature changed from 26 °C during the light period to 15-12 °C during the dark period. Relative humidity (RH) was 60% during the light period and 80% during the dark period and a light/dark photoperiod of 15.3:8.7 h was applied. Plants were watered three times per week to ensure unlimited water supply and new plants were grown for each measurement campaign.

One day before measurements started, plants were transferred to a second climate chamber of identical type. There, the leaf area growth of terminal leaflets of the second to the fourth trifoliate leaf (TL2 - TL4) was measured on six plants simultaneously for around one week. The climate chamber was set to mimic field conditions as described above for the first 2.5 days of the leaf growth measurements. Then, the climate parameters were switched to a binary regime as used in Friedli & Walter (2015) and kept until the end of the experiment. Temperature was constant at 24 °C during the light period and at 20 °C during the dark period, respectively. RH was set to 60% during the light and the dark period and a light/dark photoperiod of 13:11 h was applied.

Comparison of binary temperature regime and simulated field conditions (2017)

In the preliminary experiments, the plants experienced different daily mean temperatures and photoperiods depending on the respective experiment. In order to exclude this possible bias, we conducted a third experiment with two diurnal temperature treatments, in which mean temperature and photoperiod were the same.

Both treatments had the same photoperiod regime with 16 h light / 8 h dark period. For 1 h around the change from light to dark and vice versa, light intensity was gradually decreased or increased, respectively, to simulate dusk and dawn. While maintaining the same temperature sum, the treatments differed in the diurnal temperature regime. In the first treatment (Bi), temperature was set to a binary regime at constant 21 °C during the light and 17 °C during the dark period, respectively (Fig. 2B). In the second treatment, temperature was set to a gradually fluctuating diurnal pattern (Gr) such as plants experience

in the field. Temperature was set to reach a minimum of 13 °C at the end of the night and then it gradually reached the maximum of 27 °C in the early afternoon (Fig. 2C).

Plants were cultivated as described above for 2015 and grown in the same climate chambers, which were set to the Bi conditions. After 14 days, seedlings were transferred to clay pots and then grown under the respective treatment (Bi or Gr) until the measurement and sampling period at second trifoliate leaf stage.

Leaf growth measurements and phenotypic data analysis

In all experiments, leaf growth was measured as described in Mielewczik *et al.*, (2013) and Friedli & Walter (2015). In short, young and most recently unfolded terminal leaflets were fixed separately in a metal frame by gluing five strings to the margin of the leaflets and tautening them over a second metal ring with 10 g lead weights. White plastic beads (8 mm in diameter) were threaded onto the strings close to the margin of the leaflets to serve as artificial landmarks for the later tracking. On top of each leaflet, a monochrome CMOS camera (DMK 23GP031, maximal resolution of 2592 × 1944 pixels, The Imaging Source Europe GmbH, Bremen, Germany) with a narrow bandpass interference infrared filter (940 nm) was installed. To allow image acquisition during the dark period, a ring with six infrared light-emitting diode (LED) clusters (940 nm) was installed and a black background was placed under the leaf for an optimal contrast of the images for the later tracking of the white beads. Images of each leaflet were taken every 90 s (120 s in 2017) for around one week until the measurements of fresh plants started.

In the 2017 experiment, growth analysis was supplemented with carbohydrate and gene expression analysis. Thus, samplings of the second trifoliate leaves of independent plants were taken at six time points within 24 h between day two and three for subsequent carbohydrate (n = 5) and gene expression analysis (n = 3). Sampling time points were T1 = mid-morning, T2 = mid-afternoon, T3 = after sunset, T4 = middle of the night, T5 = before sunrise and T6 = mid-morning (Fig. 2, Table S1). Leaf size and RGR was recorded every two minutes following Mielewczik *et al.* (2013) and subsequently aggregated to 2 h intervals. The experiment was repeated twice from 2017-02-28 until 2017-03-04 (RGR measurement of n = 4 plants) and from 2017-03-16 until 2017-03-20 (RGR measurement of n = 5. Plants. Growth data of both iterations was combined resulting in n = 9 replicates per treatment. Carbohydrate and gene expression analysis was performed with only the samples from the first iteration.

Relative growth rate (RGR, mean of n = 9 replicates per treatment; $\%h^{-1}$) for every time point (t) was modelled using a linear model with temperature (T; °C), vapour pressure deficit (VPD; kPa), light (L; MJ m^{-2}) and leaf area (A; px) as independent variables with the respective parameter estimates $\beta_{1:4}$ following (Nagelmüller *et al.*, 2018):

$$RGR_t = \beta_0 + \beta_1 \cdot T_t + \beta_2 \cdot VPD_t + \beta_3 \cdot L_t + \beta_4 \cdot \sqrt{A_t} + \varepsilon \qquad \text{Eq. 1.}$$

Leaf area was included as an age factor to account for the decline in RGR over time. All statistical analyses were performed in the R environment (R Core Team, 2018).

Quantification of starch and water-soluble sugars

Starch, sucrose, fructose and glucose content was quantified as described in (Ruckle *et al.*, 2017, 2018): Leaves were flash-frozen using liquid nitrogen directly at the respective sampling time point (T1-T6). Samples were then lyophilized and biomass was recorded as lyophilised leaf weight. The lyophilised leaves were homogenized into powder using a Mixer Mill MM 400 (Retsch, Haan, Germany). Water-soluble carbohydrates were then extracted from 10 mg of the powder with ethanol washes. Starch was digested with α-amylase and amyloglucosidase (Sigma-Aldrich, St. Louis, MO, USA). Glucose, fructose and sucrose were quantified based on enzymatic conversion of NADP to NADPH. NADPH was quantified by light absorption at 340 nm using an Enspire© plate reader (Perkin Elmer, Waltham, MA, USA).

$\delta^{13}C$ values of respired CO_2

In order to measure carbon isotope composition of dark respired CO_2 ($\delta^{13}C_R$), plants were placed for 30 minutes in the dark to avoid the light enhanced dark respiration (LEDR) period (Duranceau *et al.*, 1999; Atkin *et al.*, 2000; Tcherkez *et al.*, 2003; Barbour *et al.*, 2007). One fully developed leaf was cut and placed immediately into a gas tight Tedlar® bag (Keyka Ventures, USA) according to Barbour *et al*. (2011) and Barthel *et al*. (Barthel *et al.*, 2014). The bag was flushed several times with synthetic CO_2-free air (20% O_2 and 80% N_2, Pangas, Switzerland) until a CO_2 free atmosphere was measured by an infrared gas analyser (LI-820, LI-COR, USA). The bag afterwards was kept in the dark for approximately one hour and the air was sampled with a gas-tight syringe (BD Plastipak, Switzerland) and transferred into a 12 mL evacuated gas-tight glass vial ("Exetainer", Labco, England). The $\delta^{13}C$ value of dark respired CO_2 ($\delta^{13}CO_2$) was measured with a modified Gasbench II as described by Zeeman *et al*., (2008) coupled to a DeltaplusXP isotope ratio mass spectrometer (IRMS, ThermoFisher, Germany). In addition, the $\delta^{13}C$ value of atmospheric CO_2 ($\delta^{13}C_{air}$) in the climate chamber with Bi condition was 10.0 ‰ ± 0.38 ‰ (SD) and atmospheric CO_2 in the climate chamber with Gr condition was 10.42 ‰ ± 0.14 ‰ (SD). Atmospheric CO_2 was collected 3 months after the experiment was done. However, due to air conditioning, climate chamber air is always in equilibrium. Seasonality effects of air $\delta^{13}CO_2$ are therefore negligible.

$\delta^{13}C$ values of bulk organic matter, sugar and starch

Leaves that were not used for CO_2 collection were freeze-dried and ground. From these samples 2 mg was weighed in Sn capsules (5 x 9 mm, Saentis, CH) for $\delta^{13}C$ analysis of bulk leaf organic material ($\delta^{13}C_{bulk}$) with a Flash EA 1112 Series elemental analyzer (ThermoFisher, Germany) coupled to a DeltaplusXP IRMS via a ConFlo III as described by Brooks *et al*. (2003) and Werner *et al*. (1999).

Extraction of carbohydrates for isotopic analysis was performed according to Lehmann *et al*. (2015). Briefly, 100 mg freeze-dried plant material were weighed in 2 mL reaction tubes. 1.5 mL 85 °C deionized water was added to prevent enzymatic activities. These samples were incubated for 30 min at 85 °C in a water bath. After centrifugation for 2 min at 10000 *g*, the supernatant and the remainder (pellet) were separated and kept for sugar and starch extraction, respectively. 1 mL of the supernatant was added to a column filled with a cation exchanger (Dowex 50WX8, hydrogen form, 100-200 mesh, Sigma Aldrich, CH), that was placed above a second column filled with an anion exchanger (Dowex 1X8, chloride form, 100-200 mesh, Sigma Aldrich, CH). The neutral sugar fraction was eluted with 30 mL deionized water. The sugars were then frozen, freeze dried, re-dissolved in deionized water and stored at -20 °C for further use. Starch was enzymatically isolated from the pellet according to standard protocols (Wanek *et al.*, 2001; Richter *et al.*, 2009). The pellet was washed several times using an MCW solution (methanol/chloroform/deionized water, 12/5/3, v/v/v) and deionized water and dried overnight. On the second day, the starch was re-solubilized in water and gelatinized at 100 °C for 15 min and afterwards broken down to sugars at 85°C for 2 hours using the heat resistant α-amylase (EC 3.2.1.1, Sigma-Aldrich, CH) and filtered from sugars with centrifugation filters (Vivaspin 500, Sartorius, Germany). For $\delta^{13}C$ measurements, aliquots from the starch-derived sugar ($\delta^{13}C_{starch}$) and sugar ($\delta^{13}C_{sugar}$) were pipetted into Sn capsules, dried in an oven at 60 °C, and analysed with the EA-IRMS coupling as described above.

Carbon isotope discrimination and apparent isotope fractionation

In order to calculate carbon isotope discrimination (△), $\delta^{13}C$ of sugars as the first product of photosynthesis was subtracted from $\delta^{13}C$ of the climate chamber air as the source of CO_2 following Farquhar *et al*. (1982):

$$\triangle = (\delta^{13}C_{air} - \delta^{13}C_s)$$

In addition, the apparent isotope fractionation was calculated following Ghashghaie *et al*. (2003):

$$e = (\delta^{13}C_R - \delta^{13}C_s)$$

RNA extraction and analysis

Total RNA from all samples was extracted with Trizol (Agilent Technologies, Santa Clara, CA, USA) as described by the manufacturer. Then quality was checked using the Agilent TapeStation system. The samples were sequenced using Illumina HiSeq 4000 at the Functional Genomics Center Zurich (Zurich, Switzerland). The sequence reads were mapped to the NCBI *Glycine max* genome v2.0.39 (Schmutz *et al.*, 2010) using TopHat (v.2.1.1; Trapnell *et al.*, 2009) with Bowtie2 (v2.2.3; Langmead & Salzberg, 2012). Gene expression was calculated using cufflink (v.2.1.1) with the cuffdiff program (Trapnell *et al.*, 2012) using the Glycine_max_v2.0.39.gff3 annotation data (Schmutz *et al.*, 2010).

To investigate the differences between treatment, comparisons between Bi and Gr treatments were made per time point to avoid non-specific circadian regulated genes. Genes were defined as differentially expressed when their expression changed 2-fold and was significant (adjusted *P*-value < 0.05). Differentially expressed genes of both treatments across all time-points were subjected to a principal component analysis (PCA) in order to obtain an overview of the relationships between samplings and treatments. In order to favour expression dynamics rather than abundance driven clustering, the PCA was performed using the sample-time-point correlation matrix.

Expression profiles of all DE genes across all time points were z-score normalized and clustered in a 4x4 Self Organizing Map (SOM) using the R kohonen package (Wehrens & Kruisselbrink, 2018). Functional groups were identified by performing a gene ontology enrichment analysis with fisher's exact test on each cluster using R TopGO (Alexa & Rahnenfuhrer, 2018).

6 General discussion

6.1 High throughput phenotyping techniques deliver access to the investigation of dynamic traits

Plant growth is an important indicator of adaptation and fitness, as it is responsive to many environmental covariates, among which temperature is one of the most relevant. The results of the previous four chapters of this thesis show, that high throughput phenotyping technologies are suitable for capturing growth in a temporal resolution and accuracy to make it accessible as a dynamic trait. Environmental adaptation is a major challenge for plant breeding in order to maintain stable and high yields in various environments (Slafer & Araus, 2007; Araus *et al.*, 2008). This challenge will become even more important with global climate change. Global temperature increase may shift boundaries of current mega-environments for crop production (Ortiz *et al.*, 2008). Furthermore, weather extremes such as heat, drought or flooding are predicted to become more frequent and more severe in the future (Porter & Semenov, 2005; Ray *et al.*, 2015; Mäkinen *et al.*, 2018). Dynamic response to abiotic stress may therefore become a key trait for future crop improvement through physiological breeding (Hund *et al.*, 2019).

For field-grown wheat Grieder *et al.* (2015) showed, that genotypes differ for their temperature-response of canopy cover development during winter. Using terrestrial laser scanning (TLS) in a high throughput field phenotyping-platform, we were able to show the same for height development during wheat stem elongation. Furthermore, we were able to measure this in a number of genotypes and at a temporal resolution high enough to perform a genome wide association study. Thus, we were able to investigate the genetic basis for temperature response during stem elongation. In soybean, it would be possible to investigate temperature response of canopy cover growth or canopy height increase with the same methods as used in wheat. Soybean canopy cover can be accurately measured using digital imaging (Purcell, 2000; De Bruin & Pedersen, 2009) and canopy height can be measured using terrestrial laser scanning (Friedli *et al.*, 2016b). However, in the scope of this thesis, the focus in soybean was on single leaf growth dynamics in response to temperature. Using the method developed by Mielewczik *et al.* (2013) we could show clear temperature effects on diel leaf growth dynamics, as described in chapter five. However, we were not able to detect significant genotypic differences in growth response to temperature when diel leaf growth dynamics were measured in three genotypes in the field (Braun, 2017). Although allowing for very high temporal resolution in growth measurements, the applied method is very low in throughput. The total number of leaves we were able to measure simultaneously in the field with the current setup was limited to nine. Hence, we had only three replicates per genotype, which is only a third of the replicates we had when measuring diel leaf growth under controlled conditions. Measurements in the field are subjected to increased disturbance due to wind, rain and varying illumination. With only tree replicates, the statistical power was insufficient to prove significant differences among varieties. Hence, potential genetic variation in

temperature response of field grown soybean remains to be further investigated with more suitable methods.

Although successful within the respective cases, the methods used by Grieder *et al*. (2015) and Kronenberg *et al*. (2017, 2019) to measure temperature response in the field both have major drawbacks: The former is cheap and highly mobile and can thus be readily applied independent of budget and location. Nevertheless, being handheld, it lacks the throughput to be applied in large populations. The latter method is stationary and requires an expensive, high-tech phenotyping platform. Therefore, both methods are not readily applicable in large breeding experiments or multi-environment trials. Nevertheless, both methods supply a valuable proof of concept, which can be transferred to more adaptable platforms including phenomobiles and unmanned aerial vehicles (UAV). In recent years, UAVs have been increasingly adopted for field phenotyping endeavours. They are now capable of measuring plant height in the same accuracy range as TLS using structure from motion photogrammetric methods (Hund *et al.*, 2019). Furthermore, it is not only possible to retrieve canopy cover from UAV data but also leaf area index can be directly measured in high accuracy (Roth *et al.*, 2018a). This method could be a promising approach to investigate temperature response of soybean leaf growth in the field as indicated above. UAV are not only cost effective but also offer an outstanding throughput: a field of one hectare can be recorded within 20 minutes with a ground sampling resolution of 3 mm (Roth *et al.*, 2018b). This offers the opportunity for growth measurements in a resolution of once or even twice per day. Therefore, the technical basis is set to exploit dynamic growth response to temperature or other environmental covariates for physiological breeding.

6.2 Temperature response is a heritable trait affecting many aspects of plant development

It is well established that plants respond to temperature in all developmental phases and that warm ambient temperatures generally fasten growth and development (Slafer & Rawson, 1994, 1995a,d; Atkinson & Porter, 1996; Fischer, 2011; Slafer *et al.*, 2015). In agronomy and plant physiology, the length of developmental phases or the timing of important developmental stages is generally expressed in growing degree-days, in order to account for – or model the effect of – temperature (Bonhomme, 2000; Parent *et al.*, 2018). Following the concept of thermal time, it is assumed that there is a common response to temperature applicable to most developmental processes in crops (Parent *et al.*, 2018). Furthermore, Parent and Tardieu (2012) concluded based on an extensive meta-analysis, that there is no genetic source of variability for temperature response in crop species. However, genetic variability in temperature response has been reported for a number of plant species and processes throughout the literature (*see* Clavijo Michelangeli José A. *et al.*, 2016 *and references cited therein*), even though only a limited number of genotypes are usually compared.

In chapter three, we were able to show that there is ample genetic variability in wheat temperature response during stem elongation in a large set of European wheat varieties. Furthermore, the trait was highly heritable and connected to other important traits like final height, stem elongation duration and the beginning of stem elongation. As indicated by a genome wide association study, temperature response appears to be genetically independent of these traits. Putative candidate genes in the region of the associated QTL for temperature response are connected to the *Arabidopsis thaliana* flowering pathway. As stated numerous times throughout this thesis, the switch from vegetative to reproductive development and flowering time is of paramount importance for crop adaptation and yield.

Despite the advances in phenotyping, the remote capturing of developmental progress is not straightforward and we are not aware of existing best praxis protocols. In chapter two and three, we used GDD until 15% final height (GDD_{15}) as proxy measure for the timing of start of stem elongation and GDD_{95} for the end of stem elongation. While final height could be determined accurately, the exact timing of final height was more difficult to determine. As measurements were made in an interval of three to four days and the daily temperature sums are generally large towards the end of the season, a deviation in one measurement interval from the putative true date of final height would lead to great deviation in thermal time to final height. Therefore, GDD until 95% final height is the more accurate determinant of the timing of the end of stem elongation. A more generalized approach would be to fit a parametric model (i.e. logistic regression) to the canopy height data. Then final height would correspond to the asymptote and the lower and upper turning point could be interpreted as the start and end of stem elongation respectively. While the asymptotic determination of final height would possibly be less accurate than the visual determination as used in this thesis, the start and end of stem elongation would be determined less arbitrarily. However, such an approach was not possible in the framework of this thesis. In the first two seasons, canopy height measurements could only be performed successfully from April onwards due to technical problems with the measurement system. Therefore, it was not possible to model the start of stem elongation by applying a parametric model, as not enough height data before the start of stem elongation was available. Instead, we arbitrarily set GDD_{15} as threshold for the start of stem elongation; based on the visual comparison of the available canopy height data and corresponding growth stage ratings of the check varieties (varieties with multiple replications per lot used as check in the augmented design) in the field. Agronomically, the start of stem elongation (BBCH 31) is defined as the "ear 1cm stage", when the distance between first node and tillering node reaches a threshold of 1cm. Therefore, using a canopy height parameter as proxy for the start of stem elongation appears justified. Based on our data, there is a highly heritable ($H^2 > 0.8$) genotypic temperature sum requirement to reach

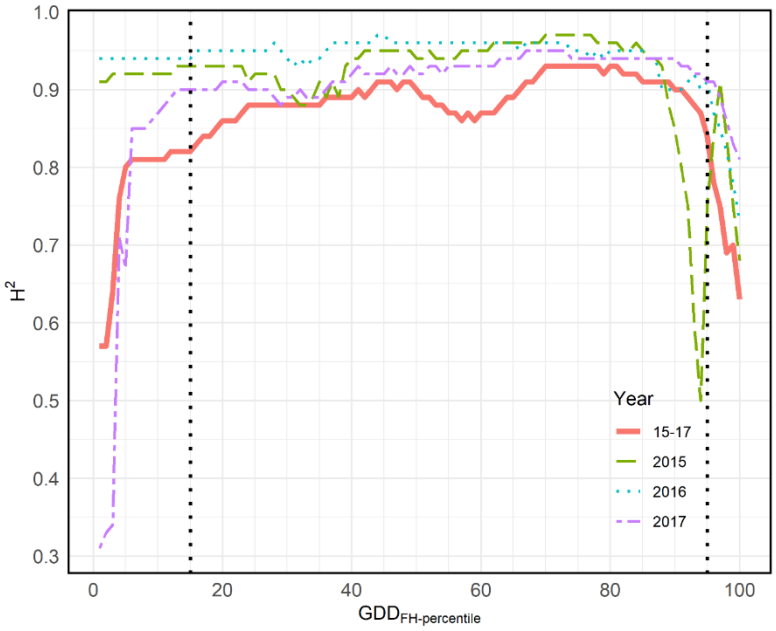

Fig. 1: Heritability of growing degree-day (GDD) requirement to reach a given final height (FH) percentile. Heritabilities for single years (2015, green dashed line; 2016, turquoise dotted line; 2017 , purple dot-dashed line) and heritability across all three years (15-17, solid red line) were calculated among the 228 genotypes present in all three years as described in chapter 3 (Eq. 3 – Eq. 5). The vertical black dotted lines indicate the 15th (GDD_{15}) and the 95th (GDD_{95}) final height percentile, which were used as proxies for start and end of stem elongation in this thesis.

any canopy height percentile between 5% and 95% of the genotype specific final height (Fig. 1). Therefore, even though GDD_{15} was set arbitrarily, it still yielded a confident genotypic ranking, which allowed the distinction between early and late varieties as shown for the population extremes (*see* Chapter two, Fig. 8*)*. The high heritabilities for GDD until respective final height percentiles (Fig. 1) indicate that height growth dynamics can be used as proxy measures for developmental progress.

Temperature response and the flowering pathway

To date, the genetic control of flowering is best understood in the model species *Arabidopsis thaliana* (Greenup *et al.*, 2009; Peng *et al.*, 2015; Blümel *et al.*, 2015), where more than 180 genes controlling flowering time have been identified (Peng *et al.*, 2015). In comparison, very little is known about the flowering pathway in wheat. We know that photoperiod (*Ppd*) and vernalisation (*Vrn*) genes mainly control flowering time in wheat, with earliness per se (*Eps*) genes acting as fine tuning factors (Fig. 2; Slafer *et al.*, 2015). Due to its large and complex genome and differences in the flowering pathways between monocots and dicots, the identification and molecular characterization of flowering time

genes and the translation of findings from *Arabidopsis* remains challenging (Peng *et al.*, 2015).

While photoperiod response appears to be partly conserved between *Arabidopsis* and cereals, the vernalisation pathways are different (Fig. 2; Greenup *et al.*, 2009). For example the wheat and barley *Vrn3* gene which induces flowering under long days is a homologue of the *Arabidopsis FLOWERING LOCUS T* photoperiod gene (Yan *et al.*, 2006; Distelfeld *et al.*, 2009) and the wheat *TaGI1* gene is a homologue of *GIGANTEA* which is involved in photoperiodic flowering (Zhao *et al.*, 2005). Vernalisation induced flowering in *Arabidopsis* is mainly mediated by *FLOWERING LOCUS C* (*FLC*) and *FRIGIDA* (*FRI*; Cockram *et al.*, 2007; Greenup *et al.*, 2009). In wheat, vernalisation response is mainly regulated by the genes *Vrn1* and *Vrn2* (Greenup *et al.*, 2009; Kamran *et al.*, 2014). Although homologues of *FLC* were recently found in wheat and their expression levels are connected to vernalisation, their role in the vernalisation pathway is less clear and remains to be further investigated (Sharma *et al.*, 2017). Apart from photoperiod and vernalisation response, flowering in *Arabidopsis* is delayed in cold conditions and accelerated by warm temperatures through the *SHORT VEGETATIVE PHASE* (*SVP*) gene in the thermo-sensitive flowering pathway (Greenup *et al.*, 2009). *SVP* controls *Arabidopsis* flowering time in response to ambient temperature by regulating the expression of *FLOWERING LOCUS T* (Lee *et al.*, 2007). In barley, *SVP*-like genes were found to influence spike development but not the timing of floral transition (Trevaskis *et al.*, 2007b).

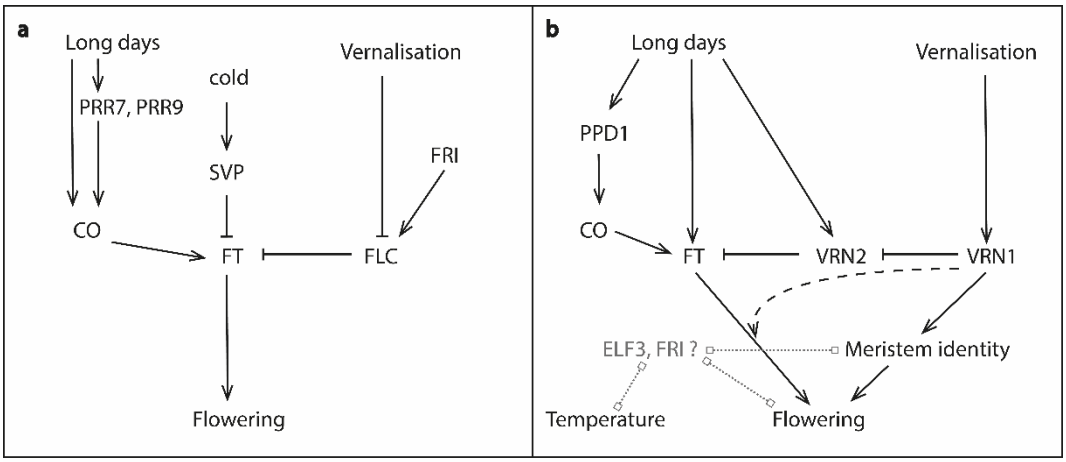

Fig. 2: A comparison of the (simplified) flowering pathway of *Arabidopsis thaliana* (a) and wheat (b). Flowering is promoted by long days and vernalisation in both species. While the photoperiod pathway is partly conserved, different genes mediate the vernalisation pathway in the two species. For gene abbreviations and descriptions, please refer to the text. Positive and negative regulatory actions are indicated by arrows and capped lines, respectively. The grey genes and grey dotted lines indicate speculative mechanisms based on the results of this thesis and the literature. The dashed arrow (**b**) indicates the effect of VRN1 after floral transition. The figure combines various aspects adapted from previously published gene models (Trevaskis *et al.*, 2007a; Hemming *et al.*, 2008; Greenup *et al.*, 2009; Jung & Müller, 2009b).

An earliness per se gene is involved in temperature response

A recent study in wheat showed an interaction between the earliness per se gene *Eps-D1* and ambient temperature which corresponded to different expression of a homologue of the *Arabidopsis* circadian clock gene *EARLY FLOWERING* (*ELF*) *3* (Ochagavia *et al.*, 2019). In chapter three, we directly measured temperature response during wheat stem elongation and identified *ELF3* as putative candidate gene for an associated QTL on chromosome 1B. Following Ochagavia *et al*. (2019), this indicates that growth response to temperature is connected to *Eps-B1* which is homologue to *Eps-D1*.

In wheat and barley, the effects of vernalisation and photoperiod have been well investigated. The role of the third group of genes in the wheat flowering pathway, the *Eps* genes, is less well understood (Zikhali & Griffiths, 2015). Broadly, *Eps* genes are considered to fine-tune flowering time independent of vernalisation or photoperiod (Bullrich *et al.*, 2002; Zikhali & Griffiths, 2015). In general *Eps* genes were thought to confer earliness independent of environmental stimuli (Snape *et al.*, 2001; Bullrich *et al.*, 2002; Zikhali & Griffiths, 2015) but interaction with temperature was also reported (Bullrich *et al.*, 2002; Appendino & Slafer, 2003; Ochagavía *et al.*, 2018). *Eps* genes have first been mapped in *Triticum monococcum* (Bullrich *et al.*, 2002) and *Hordeum vulgare* (Laurie *et al.*, 1995). In wheat, an *Eps* QTL was validated by Zikhali *et al.* (2014) on chromosome 1D and the most likely candidate gene was reported to be *ELF3* (Zikhali *et al.*, 2016). Furthermore, *ELF3* was also identified as candidate gene for the *Triticum monococcum Eps-A^{m}1* locus (Alvarez *et al.*, 2016) and associated with speed of reproductive development under high ambient temperature (Ejaz & von Korff, 2017). In *Arabidopsis*, *ELF3* is involved in light and ambient temperature response (Thines & Harmon, 2010). The recent results from Ochagavia *et al*. (2019) and Kronenberg *et al*. (2019) add additional evidence, that *ELF3* is involved in ambient temperature response in wheat.

A connection between temperature response and earliness was already indicated in the correlation analysis in chapter three. In chapter four, we could demonstrate that genotypes with a low temperature response in stem elongation had an earlier floral transition compared to high responsive genotypes. This result validates the relationship indicated by the correlation analysis in chapter three and gives additional support for *ELF3* as candidate gene for temperature response and earliness per se.

In chapter five, we found that the genes *ELF4, GIGANTEA (GI)* and *LUX ARRHYTHMO (LUX)* were differentially expressed in soybean leaves, depending on the diel temperature pattern. Together, *ELF3, ELF4* and *LUX* form the evening complex of the circadian clock which is involved in diurnal control of growth (Nusinow *et al.*, 2011) as well as in temperature compensation of the circadian clock (Jones *et al.*, 2019). GI is thought to be the major target of *ELF3* in the flowering pathway and its expression together with *ELF3* is temperature dependent in wheat (Ochagavia *et al.*, 2019). In *Triticum monococcum*, *LUX* was reported as a candidate gene for the thermo-sensitive *Eps-3A^m* locus (Gawroński *et al.*,

2014). Therefore, the same group of genes associated with temperature response and flowering in cereals appears to be involved in diurnal patterning of growth dynamics in response to temperature in soybean leaves. Notably, the difference in temperature applied in chapter five was subtle, with only the diel pattern but not daily mean temperatures being different between treatments. This implies that temperature response is very sensitive also to the pattern of received temperature even on a very short time scale. This is in agreement with the findings of Ochagavía *et al*. (2019) who stressed the importance of dynamic temperature conditions for the study of gene expression in connection with heading in wheat.

The results from chapter three and four of this thesis support the literature findings discussed above concerning the role of *ELF3* in temperature response of the wheat flowering pathway. It appears that temperature response is an important pathway in cereal flowering, which is comparable to the thermo-sensitive pathway in *Arabidopsis* in its effect on flowering time discussed above. Importantly, a possible role of *ELF3* in floral regulation by *SVP* has been suggested in *Arabidopsis* (Yoshida *et al.*, 2009), thus putatively connecting *ELF3* to the thermo-sensitive pathway in *Arabidopsis*. Our results suggest that temperature response of development towards flowering is directly measurable in stem elongation rates in wheat in the field. Furthermore, our results show that there is ample genetic variation in this trait, which might be exploited for improved local adaptation of wheat phasic development. In this context, the strong correlation between temperature response and final height may become important. Final height is not only important with respect to nitrogen fertilization and lodging, but is also correlated to other important traits. There is for example a positive correlation between final height and disease resistance due to negative pleiotropic effects of the *Rht-1* genes (Baltazar *et al.*, 1990; Srinivasachary *et al.*, 2008; Nicholson *et al.*, 2008). Reduced plant height also correlates with reduced rooting depth (Friedli *et al.*, 2019) which is important in connection with water availability. The question, whether the correlation between final height and temperature response is due to pleiotropy is therefore important in terms of breeding for local adaptation.

6.3 Temperature response across developmental stages, indoors and outdoors

Another important question in the exploitation of temperature response is whether the ranking of genotypes changes across different developmental stages. It is known that cardinal temperatures change across different stages (Porter & Gawith, 1999). As shown by Ochagavía *et al*. (2019), cardinal temperatures were affected by the respective *Eps* allele present in different near isogenic lines. Temperature response measured in leaf growth of genotype groups selected from the population extremes of the temperature response distribution, as shown in chapter four, delivered inconclusive results. Temperature response in vernalized leaves of the three groups measured at low temperatures in early spring did not correlate with temperature response of these groups in stem elongation. In contrast, temperature response of unvernalised leaves measured at warm temperatures in the

greenhouse was highly correlated with temperature response of stem elongation among genotypes of the extreme groups. This result was remarkable and unexpected. Often, findings from controlled conditions do not translate well to the field (Poorter *et al.*, 2016). Due to experimental restrictions, the results from chapter four do not allow direct conclusions. However, possible explanations for the observed relations between temperature response in leaf and stem elongation and relations between controlled conditions and the field are discussed below, based on findings from the relevant literature.

The most obvious explanation for the correlation between temperature response of leaf growth in the greenhouse and stem elongation in the field – and the reversed relationship for leaf growth in the field – is the perceived temperature range. The cardinal temperatures (minimum, optimum, maximum; ±SE) reported for leaf initiation (-1 ± 1.1 °C, 22 ± 0.4 °C, 24 ± 1 °C) are in a similar range compared to those for stem elongation (3 ± 0.4 °C, 20.3 ± 0.3 °C, >20.9 ± 0.2 °C) , as reviewed in Porter and Gawith (1999). In the greenhouse, the investigated leaves therefore grew at optimal to maximal temperatures, whereas in the field, they grew between minimum and optimum temperatures. As seen in chapter five the temperature range and diurnal pattern a plant is exposed to can drastically alter growth dynamics. However, temperature response could also change with the developmental progress, as cardinal temperatures do, and vernalisation effects might influence temperature response.

Considerations about vernalisation

In winter wheat, vernalisation not only confers flowering competence but also winter hardiness (Limin & Fowler, 2002; Fowler, 2008). Wheat responds to vernalisation at any developmental stage but the effects are most pronounced during the vegetative phase (Slafer & Rawson, 1994; Kamran *et al.*, 2014). Kiss *et al.* (2017) reported significant differences in expression levels of *Vrn1*, *Vrn2*, *Vrn3* and *Ppd1* in response to ambient temperature among groups of partially and fully vernalized genotypes with different photoperiod sensitivity. Furthermore, they reported significant genotype by temperature interactions in the timing of all developmental phases but most pronouncedly in the stem elongation phase (Kiss *et al.*, 2017). Depending on the allelic composition of *Vrn1*, its expression can be strongly affected by warm ambient temperatures, thus affecting vernalisation and reproductive development (Dixon *et al.*, 2019). Also, the expression of *Vrn2* is activated by warm temperatures during and after vernalisation in conjunction with photoperiod (Dixon *et al.*, 2019). Based on these findings, it can be assumed that also vernalisation genes and other genes in the flowering pathway are involved in the mediation of temperature response in wheat. Interestingly, this is supported by the findings of chapter three of this thesis. Although they were not statistically significant after rigid Bonferroni correction, we found two distinctive QTL associated with temperature response in close vicinity to *FRI* homologues. Despite their importance in the *Arabidopsis* vernalisation pathway, no clear homologues of *FRI* or *FLC* had been identified in temperate grasses (Yan *et al.*, 2006). Only recently, *FLC* homologues were identified in wheat as having a role in vernalisation (Sharma *et al.*, 2017; Consortium IWGSC *et al.*, 2018) and also high

confidence homologues of *FRI* were found (Consortium IWGSC *et al.*, 2018). We are not aware of any published work on *FRI* in wheat to date. The results of chapter three however indicate that *FRI* may be involved in temperature response during stem elongation in wheat. Together with the literature findings discussed above and with the results of chapter four, the effect of vernalisation in connection with ambient temperature response across developmental stages is a topic worth investigating further.

Considerations about photoperiod

Another important aspect, which needs to be considered with temperature response, is the influence of and potential interaction with photoperiod. Photoperiodism is widespread throughout the kingdoms of animals, plants and even fungi as the ability to coordinate critical developmental phases to favourable times of the year is advantageous (Jackson, 2009). In the long-day plants wheat and barley, flowering is repressed until a certain day length is reached. The photoperiod response gene *Ppd-1* mainly controls this response and the barley *Pph-H1* is most similar to the *Arabidopsis PRR7* pseudo response regulator (Turner *et al.*, 2005; Jackson, 2009). Early flowering through reduced photoperiod sensitivity was widely used in the green revolution to adapt varieties to a broader range of environments (Jackson, 2009).

In wheat, the duration of phenophases generally decreases as photoperiod increases and sensitivity to photoperiod is affected by temperature (Slafer & Rawson, 1996). Furthermore, interactions between genotype, photoperiod and temperature affect time to heading (Slafer & Rawson, 1995d). In this thesis, we did not specifically investigate photoperiod effects in relation to temperature response. Although the wheat cultivars used are of diverse geographic origin within Europe, most cultivars (85%) carried the photoperiod sensitive *Ppd-D1* allele. As seen in chapter four, no strong interaction with this gene and temperature response was detected in our data. For the *Ppd-A1* and *Ppd-B1*, no genotypic data was available as well as for 3 % of the *Ppd-D1* genotypes. Even though *Ppd-D1* is known to have the strongest effect, photoperiod sensitivity is quantitative depending on the allelic composition of *Ppd-D1*, *Ppd-A1* and *Ppd-B1* (Pérez-Gianmarco *et al.*, 2018). Thus, there might have been significant photoperiod effects on temperature response, which we could however not assess in the course of this thesis. A possible connection between photoperiod and temperature response is implied by the associated candidate gene *ELF3*. In *Arabidopsis*, *ELF3* acts as a repressor of light signals to the circadian clock as well as in temperature entrainment (Thines & Harmon, 2010) and is involved in photoperiodic flowering (Zagotta *et al.*, 1996). In barley, *ELF3* was reported to be involved in photoperiod response. Due to these possible interaction effects between temperature and photoperiod, the putative genotypic temperature sensitivities found in this thesis could be confounded with photoperiod effects. In order to account for genotype *x* photoperiod *x* temperature effects, experiments under controlled conditions are needed. By applying different combinations of temperature and photoperiod ranges, which reflect the range of photoperiod requirements found in the population, it should be possible to account for these interaction effects.

The results of chapter four indicate that phenotyping of leaf growth response to temperature under controlled conditions is a promising approach to investigate dynamic interactions between plant growth, phenology and environmental variables. The correlation between temperature response of leaf elongation indoors and stem elongation in the field is promising, even though the effects of vernalisation and temperature range need to be further investigated. The most important aspect of this correlation is that temperature response investigated under controlled conditions might be relatively readily transferrable to the field. This would allow for deeper investigations of photoperiod x vernalisation effects on temperature response and phenology, since these effects and their interactions are difficult to investigate in the field.

6.4 Complex traits can be investigated under controlled conditions, if the settings are right

The findings of this thesis offer interesting perspectives on the transferability between findings from controlled conditions and findings from the field. It is well known, that findings from growth cabinets and greenhouses are often not representative for processes in the field due to the artificial and limited conditions plants experience when grown in pots and under artificial light (Poorter *et al.*, 2016). Even though this is known, plants are still often grown in these very artificial settings to investigate physiology, genomic pathways and even response to environmental parameters or stress response. The reason for this is that a precise setting of certain environmental covariates in the field is impossible. Thus, both indoor and outdoor phenotyping have their strengths and weaknesses and a clear understanding of plant's responses to environmental stresses must be achieved by combining both indoor and outdoor phenotyping.

Investigations into diel growth fluctuations of dicot leaf growth under artificial conditions often indicated repetitive diel patterns independent of the temperature regime, which were thus attributed to endogenous control (Bunce, 1977; Nozue *et al.*, 2007; Walter *et al.*, 2009; Poiré *et al.*, 2010). Diel patterns of other processes such as carbon metabolism and their connection to growth processes were investigated under such conditions (for example: Gibon *et al.*, 2004; Rasse & Tocquin, 2006; Leonardos *et al.*, 2006; Cross *et al.*, 2006; Sulpice *et al.*, 2009) often neglecting the possible effect of more naturally fluctuating temperatures. The results from chapter five demonstrate the magnitude of effects simple diel temperature regimes can cause even if daily mean temperature remains the same: We observed differences in growth, carbohydrate metabolism and gene expression with a surprising synchronisation of cell division under constant day and night temperatures. Furthermore, setting a realistic diel temperature pattern allowed to replicate the observed diel leaf growth pattern in the field. The fact that the diel growth pattern readily changed to peak growth at night, when temperature settings were switched from a gradually fluctuating to a binary regime underlines the immediate effect temperature has on growth. Furthermore, the diel leaf growth pattern observed in field as well as in simulated field

conditions in chapter five resembles the diel pattern in soybean height growth reported by Friedli *et al*. (2016b), which also followed temperature.

Of course, there are good reasons for the application of constant day/night or extreme diurnal temperature settings. Simple temperature and light settings facilitate the comparison between studies and their replicability. In addition, the investigation of processes isolated from the effect of temperature may favour constant settings. However, if the aim is to understand or predict a plant's behaviour in the field, mimicking the environmental variables as realistic as possible may lead to results that are more reliable. These findings are supported by work performed by Annunziata *et al*. (2017, 2018) wo reported similar effects on carbon metabolism and gene expression when *Arabidopsis* was grown in more natural temperature conditions. Importantly, they also found significant differences in carbon and nitrogen metabolism between plants experiencing sunlight compared to artificial light conditions (Annunziata *et al.*, 2017). Modern growth cabinets allow for environmental settings closely and reproducibly mimicking conditions seen in the field (Cruz *et al.*, 2016). In the framework of this thesis, we did not investigate the influence of artificial illumination in our controlled condition experiments. However, it would be interesting to investigate the interactions between temperature response, photoperiod and light quality on plant growth and development. The results of chapter four and five of this thesis indicate, that a transfer of findings from controlled conditions to the field is facilitated through a more natural setting of environmental parameters in controlled condition studies. If this is the case, complex traits such as growth response to fluctuating environmental conditions can be investigated in detail under controlled conditions. The study of metabolism or gene expression is facilitated through replicable controlled environmental conditions. Furthermore, especially in Switzerland, investigations with genetically modified organisms underlie strong regulations, which makes field trials extremely expensive. The investigation of physiological pathways often depends on gene modifications, *i.e.* knockouts. Thus, controlled environment studies with environmental settings resembling the natural field conditions would be beneficial for a deeper understanding of crop physiology.

6.5 Could temperature response be a beneficial trait for plant breeding?

The usefulness of traits like temperature response or other traits related to the response to the environment depends on the applied breeding strategy. During the last decades, yield increases have stagnated in several crop species (Calderini & Slafer, 1998; Slafer *et al.*, 2001; Ray *et al.*, 2012; Schauberger *et al.*, 2018). In the past, pronounced increases in wheat yields were achieved by increasing the harvest index (HI) through the introduction of reduced height genes (Austin *et al.*, 1980; Miralles & Slafer, 2007). However, evidence suggests that the potential of further yield increase through an increase in HI is limited (Miralles & Slafer, 2007). Modern varieties have HIs close to 50% (Calderini *et al.*, 1999; Miralles & Slafer, 2007) and there has been no relevant progress in HI since the 1980s

(Reynolds *et al.*, 1999; Miralles & Slafer, 2007). Therefore, it might be difficult to further increase wheat yields by selecting for high yield potential alone (Slafer & Araus, 2007). Other reasons for the observed yield stagnation could be that breeding has not kept pace with the challenges of climate change and altered agricultural management (Brisson *et al.*, 2010; Hund *et al.*, 2019). A possible avenue to further increase yield and overcome the challenges of the changing climate lies in complementing traditional breeding strategies with physiological breeding (Slafer & Araus, 2007; Araus *et al.*, 2008; Reynolds & Langridge, 2016).

In traditional breeding, genetic improvement is sought through directly selecting for a primary trait, *i.e.* yield, in a diverse but generally favourable target environment (Ceccarelli & Grando, 1996; Araus *et al.*, 2008). The traditional breeding approach encompasses two main aspects: i) unspecified recombination of minor effect genes among elite germplasm and ii) the introduction of new genetic diversity, which is often associated with grain quality and disease resistance (Reynolds & Langridge, 2016). Yield is a complex, quantitative trait, which is characterized by low heritability and large genotype by environment interaction (G x E; Jackson *et al.*, 1996; Araus *et al.*, 2008). As G x E changes the composition of selected and rejected groups depending on the environment, G x E impedes response to selection (Cooper & DeLacy, 1994; Ceccarelli & Grando, 1996). Therefore, the performance of genotypes is evaluated by multi-environment testing at locations resembling the target population of environments in order to statistically account for G x E (Cooper & DeLacy, 1994). Hence, a physiological, mechanistic understanding of the underlying factors driving G x E, would facilitate the interpretation of these effects and thereby improve selection by means of physiological breeding (Araus *et al.*, 2008).

In physiological breeding, the primary trait (yield) is improved through indirect selection for secondary traits that are related to higher yield or improved performance under unfavourable conditions (Araus *et al.*, 2008). Grain yield can be described as a function of three efficiencies to use the available photosynthetic active radiation: light interception efficiency, radiation use efficiency (*i.e.* the efficiency to convert light energy into biomass) and harvest index (*i.e.* the efficiency of resource partition to the harvest organ; Reynolds *et al.*, 2009a; Hund *et al.*, 2019). These parameters and their interactions act cumulatively during the growing season and are themselves dependent on genotypic and environmental variables. In this context, physiological breeding aims at combining traits that indirectly define yield in a manner to tailor varieties that are well adapted to a certain environment and its biotic and abiotic constraints. Favorable traits that are complementary for a given target environment are accumulated through strategic trait-based crossing, thereby achieving cumulative gene action to improve yield (Reynolds *et al.*, 2009b; Reynolds & Langridge, 2016).

An often proposed physiological strategy to improve wheat yields is to adjust phasic development and thereby prolong stem elongation duration, which increases the number of grains per area (Slafer *et al.*, 1996; Miralles *et al.*, 2000; González *et al.*, 2003c; Slafer, 2003; Pérez-Gianmarco *et al.*, 2018). As seen in chapters three and four, temperature

response in wheat affects the timing of floral transition as well as stem elongation duration in wheat. Furthermore, when considering the correlations, a positive temperature response effect on stem elongation duration coincides with reduced final height. Therefore, temperature response in wheat might be exploited as a complementary trait in a physiological breeding context for local adaptation, especially when its high heritability is considered.

In the scope of this thesis, we were not able to screen for genotypic variability in soybean canopy cover or canopy height growth in response to temperature. However, this could be achieved with the methods discussed in chapter 6.1. In case there is heritable genotypic variability in these traits, it would be interesting to investigate how they correlate with cold tolerance, maturity group and flowering habit. Cold tolerance during the reproductive stage as well as early maturity are among the most important objectives in soybean breeding for cold climates (Schori *et al.*, 1993; Gass *et al.*, 1996; Ohnishi *et al.*, 2010; Copley *et al.*, 2018). Based on the findings of this thesis on temperature response in wheat and in soybean single leaf growth, similar effects between temperature response and development might be expected in soybean.

7 References

Aasen H, Bareth G. **2018**. Spectral and 3D Nonspectral Approaches to Crop Trait Estimation Using Ground and UAV Sensing. In: Thenkabail PS, Lyon JG, Huete A, eds. Hyperspectral Remote Sensing Of Vegetation. Biophysical and Biochemical Characterization and Plant Species Studies. 103-131.

Alexa A, Rahnenfuhrer J. **2018**. *topGO: Enrichment Analysis for Gene Ontology*.

Allan RE, Vogel OA, Craddock JC. **1959**. Comparative Response to Gibberellic Acid of Dwarf, Semidwarf, and Standard Short and Tall Winter Wheat Varieties 1. *Agronomy Journal* **51**: 737–740.

Allard G, Nelson CJ. **1991**. Photosynthate Partitioning in Basal Zones of Tall Fescue Leaf Blades. *Plant Physiology* **95**: 663–668.

Alvarez MA, Tranquilli G, Lewis S, Kippes N, Dubcovsky J. **2016**. Genetic and physical mapping of the earliness per se locus Eps-Am1 in Triticum monococcum identifies EARLY FLOWERING 3 (ELF3) as a candidate gene. *Functional & Integrative Genomics* **16**: 365–382.

Amasino RM, Michaels SD. **2010**. The Timing of Flowering. *Plant Physiology* **154**: 516–520.

Angus JF, Mackenzie DH, Morton R, Schafer CA. **1981**. Phasic development in field crops II. Thermal and photoperiodic responses of spring wheat. *Field Crops Research* **4**: 269–283.

Annunziata MG, Apelt F, Carillo P, Krause U, Feil R, Koehl K, Lunn JE, Stitt M. **2018**. Response of Arabidopsis primary metabolism and circadian clock to low night temperature in a natural light environment. *Journal of Experimental Botany* **69**: 4881–4895.

Annunziata MG, Apelt F, Carillo P, Krause U, Feil R, Mengin V, Lauxmann MA, Köhl K, Nikoloski Z, Stitt M, *et al.* 2017. Getting back to nature: a reality check for experiments in controlled environments. *Journal of Experimental Botany* **68**: 4463–4477.

Appendino ML, Slafer GA. **2003**. Earliness per se and its dependence upon temperature in diploid wheat lines differing in the major gene Eps-Am1 alleles. *The Journal of Agricultural Science* **141**: 149–154.

Araus JL, Cairns JE. **2014**. Field high-throughput phenotyping: the new crop breeding frontier. *Trends in Plant Science* **19**: 52–61.

Araus JL, Slafer GA, Royo C, Serret MD. **2008**. Breeding for Yield Potential and Stress Adaptation in Cereals. *Critical Reviews in Plant Sciences* **27**: 377–412.

Asseng S, Ewert F, Martre P, Rötter RP, Lobell DB, Cammarano D, Kimball BA, Ottman MJ, Wall GW, White JW, *et al.* 2015. Rising temperatures reduce global wheat production. *Nature Climate Change* **5**: 143–147.

Atkin OK, Evans JR, Ball MC, Lambers H, Pons TL. **2000**. Leaf Respiration of Snow Gum in the Light and Dark. Interactions between Temperature and Irradiance. *Plant Physiology* **122**: 915–924.

Atkinson D, Porter JR. **1996**. Temperature, plant development and crop yields. *Trends in Plant Science* **1**: 119–124.

Austin RB, Bingham J, Blackwell RD, Evans LT, Ford MA, Morgan CL, Taylor M. **1980**. Genetic improvements in winter wheat yields since 1900 and associated physiological changes. *The Journal of Agricultural Science* **94**: 675–689.

Avery GS. **1933**. Structure and Development of the Tobacco Leaf. *American Journal of Botany* **20**: 565–592.

Baltazar BM, Scharen AL, Kronstad WE. **1990**. Association between dwarfing genes 'Rht1' and 'Rht2' and resistance toSeptoria tritici Blotch in winter wheat (Triticum aestivum L. em Thell). *Theoretical and Applied Genetics* **79**: 422–426.

Barbour MM, Mcdowell NG, Tcherkez G, Bickford CP, Hanson DT. **2007**. A new measurement technique reveals rapid post-illumination changes in the carbon isotope composition of leaf-respired CO2. *Plant, Cell & Environment* **30**: 469–482.

Barbour MM, Tcherkez G, Bickford CP, Mauve C, Lamothe M, Sinton S, Brown H. **2011**. δ13C of leaf-respired CO2 reflects intrinsic water-use efficiency in barley. *Plant, Cell & Environment* **34**: 792–799.

Bareth G, Bendig J, Tilly N, Hoffmeister D, Aasen H, Bolten A. **2016**. A Comparison of UAV- and TLS-derived Plant Height for Crop Monitoring: Using Polygon Grids for the Analysis of Crop Surface Models (CSMs). *Photogrammetrie - Fernerkundung - Geoinformation* **2016**: 85–94.

Barthel M, Cieraad E, Zakharova A, Hunt JE. **2014**. Sudden cold temperature delays plant carbon transport and shifts allocation from growth to respiratory demand. *Biogeosciences* **11**: 1425–1433.

Bates D, Mächler M, Bolker B, Walker S. **2015**. Fitting Linear Mixed-Effects Models Using **lme4**. *Journal of Statistical Software* **67**.

Baxter B. **2013**. Plant acclimation and adaptation to cold environments. In: Temperature and Plant Development. John Wiley & Sons, Ltd, 19–48.

van Beem J, Mohler V, Lukman R, van Ginkel M, William M, Crossa J, Worland AJ. **2005**. Analysis of Genetic Factors Influencing the Developmental Rate of Globally Important CIMMYT Wheat Cultivars. *Crop Science* **45**: 2113–2119.

Bendig J, Bolten A, Bareth G. **2013**. UAV-based Imaging for Multi-Temporal, very high Resolution Crop Surface Models to monitor Crop Growth Variability. *PFG Photogrammetrie, Fernerkundung, Geoinformation*: 551–562.

Bieniawska Z, Espinoza C, Schlereth A, Sulpice R, Hincha DK, Hannah MA. **2008**. Disruption of the Arabidopsis Circadian Clock Is Responsible for Extensive Variation in the Cold-Responsive Transcriptome. *Plant Physiology* **147**: 263–279.

Blümel M, Dally N, Jung C. 2015. Flowering time regulation in crops—what did we learn from Arabidopsis? *Current Opinion in Biotechnology* **32**: 121–129.

Bonhomme R. 2000. Bases and limits to using 'degree. day'units. *European journal of agronomy* **13**: 1–10.

Borràs-Gelonch G, Rebetzke GJ, Richards RA, Romagosa I. 2012. Genetic control of duration of pre-anthesis phases in wheat (Triticum aestivum L.) and relationships to leaf appearance, tillering, and dry matter accumulation. *Journal of Experimental Botany* **63**: 69–89.

Braun P. 2017. Wie reagiert das Blattwachstum in Soja auf wechselnde Temperaturen? *Bachelor Thesis ETH Zurich.*

Brégard A, Allard G. 1999. Sink to source transition in developing leaf blades of tall fescue. *New Phytologist* **141**: 45–50.

Brisson N, Gate P, Gouache D, Charmet G, Oury F-X, Huard F. 2010. Why are wheat yields stagnating in Europe? A comprehensive data analysis for France. *Field Crops Research* **119**: 201–212.

Brooks PD, Geilmann H, Werner RA, Brand WA. 2003. Improved precision of coupled?13C and?15N measurements from single samples using an elemental analyzer/isotope ratio mass spectrometer combination with a post-column six-port valve and selective CO2 trapping; improved halide robustness of the combustion reactor using CeO2. *Rapid Communications in Mass Spectrometry* **17**: 1924–1926.

Bullrich L, Appendino M, Tranquilli G, Lewis S, Dubcovsky J. 2002. Mapping of a thermo-sensitive earliness per se gene onTriticum monococcum chromosome 1Am. *Theoretical and Applied Genetics* **105**: 585–593.

Bunce JA. 1977. Leaf Elongation in Relation to Leaf Water Potential in Soybean. *Journal of Experimental Botany* **28**: 156–161.

Busemeyer L, Mentrup D, Möller K, Wunder E, Alheit K, Hahn V, Maurer HP, Reif JC, Würschum T, Müller J, *et al.* 2013. BreedVision — A Multi-Sensor Platform for Non-Destructive Field-Based Phenotyping in Plant Breeding. *Sensors* **13**: 2830–2847.

Butler D. 2009. *asreml: asreml() fits the linear mixed model.*

Butler D. 2018. *asreml: Fits the Linear Mixed Model.*

Caldeira CF, Jeanguenin L, Chaumont F, Tardieu F. 2014. Circadian rhythms of hydraulic conductance and growth are enhanced by drought and improve plant performance. *Nature Communications* **5**: 5365.

Calderini DF, Reynolds MP, Slafer GA. 1999. Genetic gains in wheat yield and main physiological changes associated with them during the 20th century. In: Satorre EH, Slafer GA, eds. Wheat: Ecology and Physiology of Yield Determination. Food Products Press.

Calderini DF, Slafer GA. 1998. Changes in yield and yield stability in wheat during the 20th century. *Field Crops Research* **57**: 335–347.

Calviño P, Monzon J. **2009**. Chapter 3 - Farming Systems of Argentina: Yield Constraints and Risk Management. In: Sadras V, Calderini D, eds. Crop Physiology. San Diego: Academic Press, 55–70.

Camus-Kulandaivelu L, Veyrieras J-B, Madur D, Combes V, Fourmann M, Barraud S, Dubreuil P, Gouesnard B, Manicacci D, Charcosset A. **2006**. Maize Adaptation to Temperate Climate: Relationship Between Population Structure and Polymorphism in the Dwarf8 Gene. *Genetics* **172**: 2449–2463.

Cao W, Moss DN. **1989**. Temperature Effect on Leaf Emergence and Phyllochron in Wheat and Barley. *Crop Science* **29**: 1018–1021.

Casebow R, Hadley C, Uppal R, Addisu M, Loddo S, Kowalski A, Griffiths S, Gooding M. **2016**. Reduced Height (Rht) Alleles Affect Wheat Grain Quality (A Zhang, Ed.). *PLOS ONE* **11**: e0156056.

Cavanagh CR, Chao S, Wang S, Huang BE, Stephen S, Kiani S, Forrest K, Saintenac C, Brown-Guedira GL, Akhunova A, *et al.* 2013. Genome-wide comparative diversity uncovers multiple targets of selection for improvement in hexaploid wheat landraces and cultivars. *Proceedings of the National Academy of Sciences* **110**: 8057–8062.

Ceccarelli S, Grando S. **1996**. Drought as a challenge for the plant breeder. *Plant Growth Regulation* **20**: 149–155.

Chen Y, Lübberstedt T. **2010**. Molecular basis of trait correlations. *Trends in Plant Science* **15**: 454–461.

Chen D, Neumann K, Friedel S, Kilian B, Chen M, Altmann T, Klukas C. **2014**. Dissecting the Phenotypic Components of Crop Plant Growth and Drought Responses Based on High-Throughput Image Analysis. *The Plant Cell Online*: tpc.114.129601.

Chen L, Phillips AL, Condon AG, Parry MAJ, Hu Y-G. **2013**. GA-Responsive Dwarfing Gene Rht12 Affects the Developmental and Agronomic Traits in Common Bread Wheat. *PLoS ONE* **8**.

Clavijo Michelangeli José A., Sinclair Thomas R., Bliznyuk Nikolay. **2016**. Using an Arrhenius-type function to describe temperature response of plant developmental processes: inference and cautions. *New Phytologist* **210**: 377–379.

Cober ER, Stewart DW, Voldeng HD. **2001**. Photoperiod and Temperature Responses in Early-Maturing, Near-Isogenic Soybean Lines. *Crop Science* **41**: 721–727.

Cockram J, Jones H, Leigh FJ, O'Sullivan D, Powell W, Laurie DA, Greenland AJ. **2007**. Control of flowering time in temperate cereals: genes, domestication, and sustainable productivity. *Journal of Experimental Botany* **58**: 1231–1244.

Coleman RK, Gill GS, Rebetzke GJ. **2001**. Identification of quantitative trait loci for traits conferring weed competitiveness in wheat (Triticum aestivum L.). *Australian Journal of Agricultural Research* **52**: 1235.

Consortium (IWGSC) TIWGS, Investigators IR principal, Appels R, Eversole K, Feuillet C, Keller B, Rogers J, Stein N, Investigators I whole-genome assembly

principal, Pozniak CJ, *et al.* 2018. Shifting the limits in wheat research and breeding using a fully annotated reference genome. *Science* **361**: eaar7191.

Cooper M, DeLacy IH. **1994**. Relationships among analytical methods used to study genotypic variation and genotype-by-environment interaction in plant breeding multi-environment experiments. *Theoretical and Applied Genetics* **88**: 561–572.

Copley TR, Duceppe M-O, O'Donoughue LS. **2018**. Identification of novel loci associated with maturity and yield traits in early maturity soybean plant introduction lines. *BMC Genomics* **19**.

Cornwell WK, Wright IJ, Turner J, Maire V, Barbour MM, Cernusak LA, Dawson T, Ellsworth D, Farquhar GD, Griffiths H, *et al.* 2018. Climate and soils together regulate photosynthetic carbon isotope discrimination within C3 plants worldwide. *Global Ecology and Biogeography* **27**: 1056–1067.

Cross JM, Korff M von, Altmann T, Bartzetko L, Sulpice R, Gibon Y, Palacios N, Stitt M. **2006**. Variation of Enzyme Activities and Metabolite Levels in 24 Arabidopsis Accessions Growing in Carbon-Limited Conditions. *Plant Physiology* **142**: 1574–1588.

Cruz JA, Savage LJ, Zegarac R, Hall CC, Satoh-Cruz M, Davis GA, Kovac WK, Chen J, Kramer DM. **2016**. Dynamic Environmental Photosynthetic Imaging Reveals Emergent Phenotypes. *Cell Systems* **2**: 365–377.

De Bruin JL, Pedersen P. **2009**. New and Old Soybean Cultivar Responses to Plant Density and Intercepted Light. *Crop Science* **49**: 2225–2232.

Deery D, Jimenez-Berni J, Jones H, Sirault X, Furbank R. **2014**. Proximal Remote Sensing Buggies and Potential Applications for Field-Based Phenotyping. *Agronomy* **4**: 349–379.

Distelfeld A, Tranquilli G, Li C, Yan L, Dubcovsky J. **2009**. Genetic and Molecular Characterization of the VRN2 Loci in Tetraploid Wheat. *Plant Physiology* **149**: 245–257.

Dixon LE, Karsai I, Kiss T, Adamski NM, Liu Z, Ding Y, Allard V, Boden SA, Griffiths S. **2019**. VERNALIZATION1 controls developmental responses of winter wheat under high ambient temperatures. *Development* **146**: dev172684.

Dodd AN, Salathia N, Hall A, Kévei E, Tóth R, Nagy F, Hibberd JM, Millar AJ, Webb AAR. **2005**. Plant Circadian Clocks Increase Photosynthesis, Growth, Survival, and Competitive Advantage. *Science* **309**: 630–633.

Dornbusch T, Lorrain S, Kuznetsov D, Fortier A, Liechti R, Xenarios I, Fankhauser C. **2012**. Measuring the diurnal pattern of leaf hyponasty and growth in Arabidopsis – a novel phenotyping approach using laser scanning. *Functional Plant Biology* **39**: 860–869.

Duranceau M, Ghashghaie J, Badeck F, Deleens E, Cornic G. **1999**. δ13C of CO2 respired in the dark in relation to δ13C of leaf carbohydrates in Phaseolus vulgaris L. under progressive drought. *Plant, Cell & Environment* **22**: 515–523.

Eimert K, Wang SM, Lue WI, Chen J. **1995**. Monogenic Recessive Mutations Causing Both Late Floral Initiation and Excess Starch Accumulation in Arabidopsis. *The Plant Cell* **7**: 1703–1712.

Ejaz M, von Korff M. **2017**. The Genetic Control of Reproductive Development under High Ambient Temperature. *Plant Physiology* **173**: 294–306.

Ellis M, Spielmeyer W, Gale K, Rebetzke G, Richards R. **2002**. 'Perfect' markers for the Rht-B1b and Rht-D1b dwarfing genes in wheat. *Theoretical and Applied Genetics* **105**: 1038–1042.

Falconer DS, Mackay TFC. **1996**. *Introduction to Quantitative Genetics*. Essex, England: Benjamin Cummings.

Food and Agriculture Organization of the United Nations. 2017. *FAOSTAT Database.* Rome, Italy: FAO. Retrieved 2019-11-21 from http://www.fao.org/faostat/en/#data/QC

Farooq M, Bramley H, Palta JA, Siddique KHM. **2011**. Heat Stress in Wheat during Reproductive and Grain-Filling Phases. *Critical Reviews in Plant Sciences* **30**: 491–507.

Farquhar GD, O'Leary MH, Berry JA. **1982**. On the Relationship Between Carbon Isotope Discrimination and the Intercellular Carbon Dioxide Concentration in Leaves. *Functional Plant Biology* **9**: 121–137.

Farré EM. **2012**. The regulation of plant growth by the circadian clock. *Plant Biology* **14**: 401–410.

Fiorani F, Schurr U. **2013**. Future Scenarios for Plant Phenotyping. *Annual Review of Plant Biology* **64**: 267–291.

Fischer RA. **1985**. Number of kernels in wheat crops and the influence of solar radiation and temperature. *The Journal of Agricultural Science* **105**: 447–461.

Fischer RA. **2011**. Wheat physiology: a review of recent developments. *Crop and Pasture Science* **62**: 95–114.

Flink M, Pettersson R, Andrén O. **1995**. Growth dynamics of winter wheat in the field with daily fertilization and irrigation. *Journal of Agronomy and Crop Science* **174**: 239–252.

Fournier C, Andrieu B. **2000**. Dynamics of the Elongation of Internodes in Maize (Zea mays L.): Analysis of Phases of Elongation and their Relationships to Phytomer Development. *Annals of Botany* **86**: 551–563.

Fowler DB. **2008**. Cold Acclimation Threshold Induction Temperatures in Cereals. *Crop Science* **48**: 1147–1154.

Franklin KA. **2009**. Light and temperature signal crosstalk in plant development. *Current Opinion in Plant Biology* **12**: 63–68.

Friedli CN, Abiven S, Fossati D, Hund A. **2019**. Modern wheat semi-dwarfs root deep on demand: response of rooting depth to drought in a set of Swiss era wheats covering 100 years of breeding. *Euphytica* **215**: 85.

Friedli M, Kirchgessner N, Grieder C, Liebisch F, Mannale M, Walter A. **2016a**. Terrestrial 3D laser scanning to track the increase in canopy height of both monocot and dicot crop species under field conditions. *Plant Methods* **12**: 9.

Friedli M, Kirchgessner N, Grieder C, Liebisch F, Mannale M, Walter A. 2016b. Terrestrial 3D laser scanning to track the increase in canopy height of both monocot and dicot crop species under field conditions. *Plant Methods* **12**: 9.

Friedli M, Walter A. 2015. Diel growth patterns of young soybean (Glycine max) leaflets are synchronous throughout different positions on a plant. *Plant, Cell & Environment* **38**: 514–524.

Furbank RT, Tester M. 2011. Phenomics – technologies to relieve the phenotyping bottleneck. *Trends in Plant Science* **16**: 635–644.

Gale MD, Youssefian S. 1985. Dwarfing genes in wheat. In: Russel GE, ed. Progress in Plant Breeding 1. Butterworth, 1–35.

Gallagher JN. 1979. Field Studies of Cereal Leaf Growth I. INITIATION AND EXPANSION IN RELATION TO TEMPERATURE AND ONTOGENY. *Journal of Experimental Botany* **30**: 625–636.

Gardner JS, Hess WM, Trione EJ. 1985. Development of the Young Wheat Spike: A Sem Study of Chinese Spring Wheat. *American Journal of Botany* **72**: 548–559.

Gass T, Schori A, Fossati A, Soldati A, Stamp P. 1996. Cold tolerance of soybean (Glycine max (L.) Merr.) during the reproductive phase. *European Journal of Agronomy* **5**: 71–88.

Gaut BS, Long AD. 2003. The Lowdown on Linkage Disequilibrium. *The Plant Cell* **15**: 1502–1506.

Gawroński P, Ariyadasa R, Himmelbach A, Poursarebani N, Kilian B, Stein N, Steuernagel B, Hensel G, Kumlehn J, Sehgal SK, *et al.* 2014. A Distorted Circadian Clock Causes Early Flowering and Temperature-Dependent Variation in Spike Development in the Eps-3Am Mutant of Einkorn Wheat. *Genetics* **196**: 1253–1261.

Ghashghaie J, Badeck F-W, Lanigan G, Nogués S, Tcherkez G, Deléens E, Cornic G, Griffiths H. 2003. Carbon isotope fractionation during dark respiration and photorespiration in C3 plants. *Phytochemistry Reviews* **2**: 145–161.

Gibon Y, Bläsing OE, Palacios-Rojas N, Pankovic D, Hendriks JHM, Fisahn J, Höhne M, Günther M, Stitt M. 2004. Adjustment of diurnal starch turnover to short days: depletion of sugar during the night leads to a temporary inhibition of carbohydrate utilization, accumulation of sugars and post-translational activation of ADP-glucose pyrophosphorylase in the following light period. *The Plant Journal* **39**: 847–862.

Gibon Y, Pyl E-T, Sulpice R, Lunn JE, Höhne M, Günther M, Stitt M. 2009. Adjustment of growth, starch turnover, protein content and central metabolism to a decrease of the carbon supply when Arabidopsis is grown in very short photoperiods. *Plant, Cell & Environment* **32**: 859–874.

Gibson LR, Paulsen GM. 1999. Yield Components of Wheat Grown under High Temperature Stress during Reproductive Growth. *Crop Science* **39**: 1841–1846.

van Ginkel M, Reynolds MP, Trethowan R, Hernandez E. 2008. Complementing the Breeder's Eye with Canopy Temperature Measurements. In: International Symposium on

Wheat Yield Potential: Challenges to International Wheat Breeding. Mexico: CIMMYT, 134–135.

Gol L, Tomé F, von Korff M. **2017**. Floral transitions in wheat and barley: interactions between photoperiod, abiotic stresses, and nutrient status. *Journal of Experimental Botany* **68**: 1399–1410.

González FG, Slafer GA, Miralles DJ. **2002**. Vernalization and photoperiod responses in wheat pre-flowering reproductive phases. *Field Crops Research* **74**: 183–195.

González FG, Slafer GA, Miralles DJ. **2003a**. Floret development and spike growth as affected by photoperiod during stem elongation in wheat. *Field Crops Research* **81**: 29–38.

González FG, Slafer GA, Miralles DJ. **2003b**. Floret development and spike growth as affected by photoperiod during stem elongation in wheat. *Field Crops Research* **81**: 29–38.

González FG, Slafer GA, Miralles DJ. **2003c**. Grain and floret number in response to photoperiod during stem elongation in fully and slightly vernalized wheats. *Field Crops Research* **81**: 17–27.

Gonzalez-Navarro OE, Griffiths S, Molero G, Reynolds MP, Slafer GA. **2016**. Variation in developmental patterns among elite wheat lines and relationships with yield, yield components and spike fertility. *Field Crops Research* **196**: 294–304.

Gororo NN, Flood RG, Eastwood RF, Eagles HA. **2001**. Photoperiod and Vernalization Responses in Triticum turgidum × T. tauschii Synthetic Hexaploid Wheats. *Annals of Botany* **88**: 947–952.

Graf A, Schlereth A, Stitt M, Smith AM. **2010**. Circadian control of carbohydrate availability for growth in Arabidopsis plants at night. *Proceedings of the National Academy of Sciences* **107**: 9458–9463.

Granier C, Aguirrezabal L, Chenu K, Cookson SJ, Dauzat M, Hamard P, Thioux J-J, Rolland G, Bouchier-Combaud S, Lebaudy A, *et al.* 2006. PHENOPSIS, an automated platform for reproducible phenotyping of plant responses to soil water deficit in Arabidopsis thaliana permitted the identification of an accession with low sensitivity to soil water deficit. *New Phytologist* **169**: 623–635.

Green RM, Tingay S, Wang Z-Y, Tobin EM. **2002**. Circadian Rhythms Confer a Higher Level of Fitness to Arabidopsis Plants. *Plant Physiology* **129**: 576–584.

Greenup A, Peacock WJ, Dennis ES, Trevaskis B. **2009**. The molecular biology of seasonal flowering-responses in Arabidopsis and the cereals. *Annals of Botany* **103**: 1165–1172.

Grieder C, Hund A, Walter A. **2015**. Image based phenotyping during winter: a powerful tool to assess wheat genetic variation in growth response to temperature. *Functional Plant Biology* **42**: 387–396.

Grimm SS, Jones JW, Boote KJ, Hesketh JD. **1993**. Parameter Estimation for Predicting Flowering Date of Soybean Cultivars. *Crop Science* **33**: 137–144.

Hartmann A, Czauderna T, Hoffmann R, Stein N, Schreiber F. **2011**. HTPheno: An image analysis pipeline for high-throughput plant phenotyping. *BMC Bioinformatics* **12**: 148.

Hedden P. **2003**. The genes of the Green Revolution. *Trends in Genetics* **19**: 5–9.

Hemming MN, Walford SA, Fieg S, Dennis ES, Trevaskis B. **2012**. Identification of High-Temperature-Responsive Genes in Cereals. *Plant Physiology* **158**: 1439–1450.

Holman F, Riche A, Michalski A, Castle M, Wooster M, Hawkesford M. **2016**. High Throughput Field Phenotyping of Wheat Plant Height and Growth Rate in Field Plot Trials Using UAV Based Remote Sensing. *Remote Sensing* **8**: 1031.

Holzkämper A, Fossati D, Hiltbrunner J, Fuhrer J. **2015**. Spatial and temporal trends in agro-climatic limitations to production potentials for grain maize and winter wheat in Switzerland. *Regional Environmental Change* **15**: 109–122.

Hudson PS. **1934**. English wheat varieties II. Development of the wheat plant. *Zeitschriftfur Zuchtung*: 70–108.

Hund A, Kronenberg L, Anderegg J, Yu K, Walter A. **2019**. Non-invasive field phenotyping of cereal development. In: Ordon F, Friedt W, eds. Advances in breeding techniques for cereal crops. Cambridge UK: Buleigh Dodds Science Publishing.

Izawa T, Mihara M, Suzuki Y, Gupta M, Itoh H, Nagano AJ, Motoyama R, Sawada Y, Yano M, Hirai MY, *et al.* 2011. Os-GIGANTEA Confers Robust Diurnal Rhythms on the Global Transcriptome of Rice in the Field. *The Plant Cell* **23**: 1741–1755.

Jackson SD. **2009**. Plant responses to photoperiod. *New Phytologist* **181**: 517–531.

Jackson P, Robertson M, Cooper M, Hammer G. **1996**. The role of physiological understanding in plant breeding; from a breeding perspective. *Field Crops Research* **49**: 11–37.

Jansen M, Gilmer F, Biskup B, Nagel KA, Rascher U, Fischbach A, Briem S, Dreissen G, Tittmann S, Braun S, *et al.* 2009. Simultaneous phenotyping of leaf growth and chlorophyll fluorescence via GROWSCREEN FLUORO allows detection of stress tolerance in Arabidopsis thaliana and other rosette plants. *Functional Plant Biology* **36**: 902–914.

Johanson U, West J, Lister C, Michaels S, Amasino R, Dean C. **2000**. Molecular Analysis of FRIGIDA, a Major Determinant of Natural Variation in Arabidopsis Flowering Time. *Science* **290**: 344–347.

Jones MA, Morohashi K, Grotewold E, Harmer SL. **2019**. Arabidopsis JMJD5/JMJ30 Acts Independently of LUX ARRHYTHMO Within the Plant Circadian Clock to Enable Temperature Compensation. *Frontiers in Plant Science* **10**.

Jung C, Müller AE. **2009a**. Flowering time control and applications in plant breeding. *Trends in Plant Science* **14**: 563–573.

Jung C, Müller AE. **2009b**. Flowering time control and applications in plant breeding. *Trends in Plant Science* **14**: 563–573.

Junker A, Muraya MM, Weigelt-Fischer K, Arana-Ceballos F, Klukas C, Melchinger AE, Meyer RC, Riewe D, Altmann T. 2015. Optimizing experimental procedures for quantitative evaluation of crop plant performance in high throughput phenotyping systems. *Frontiers in Plant Science* **5**.

Kamran A, Iqbal M, Spaner D. 2014. Flowering time in wheat (Triticum aestivum L.): a key factor for global adaptability. *Euphytica* **197**: 1–26.

Kawahara Y, De M la B, Hamilton JP, Kanamori H, McCombie WR, Ouyang S, Schwartz DC, Tanaka T, Wu J, Zhou S, *et al.* 2013. Improvement of the Oryza sativa Nipponbare reference genome using next generation sequence and optical map data. *Rice (New York, N.Y.)* **6**: 4–4.

Keyes GJ, Paolillo DJ, Sorrells ME. 1989. The Effects of Dwarfing Genes Rht1 and Rht2 on Cellular Dimensions and Rate of Leaf Elongation in Wheat. *Annals of Botany* **64**: 683–690.

Kidokoro S, Watanabe K, Ohori T, Moriwaki T, Maruyama K, Mizoi J, Myint Phyu Sin Htwe N, Fujita Y, Sekita S, Shinozaki K, *et al.* 2015. Soybean DREB1/CBF-type transcription factors function in heat and drought as well as cold stress-responsive gene expression. *The Plant Journal* **81**: 505–518.

King RW, Gale MD, Quarrie SA. 1983. Effects of NORIN 10 and Tom Thumb Dwarfing Genes on Morphology, Physiology and Abscisic Acid Production in Wheat. *Annals of Botany* **51**: 201–208.

Kippes N, Debernardi JM, Vasquez-Gross HA, Akpinar BA, Budak H, Kato K, Chao S, Akhunov E, Dubcovsky J. 2015. Identification of the VERNALIZATION 4 gene reveals the origin of spring growth habit in ancient wheats from South Asia. *Proceedings of the National Academy of Sciences* **112**: E5401–E5410.

Kirby EJM. 1988. Analysis of leaf, stem and ear growth in wheat from terminal spikelet stage to anthesis. *Field Crops Research* **18**: 127–140.

Kirchgessner N, Liebisch F, Yu K, Pfeifer J, Friedli M, Hund A, Walter A. 2016. The ETH field phenotyping platform FIP: a cable-suspended multi-sensor system. *Functional Plant Biology* **44**: 154–168.

Kiss T, Dixon LE, Soltész A, Bányai J, Mayer M, Balla K, Allard V, Galiba G, Slafer GA, Griffiths S, *et al.* 2017. Effects of ambient temperature in association with photoperiod on phenology and on the expressions of major plant developmental genes in wheat (Triticum aestivum L.). *Plant, Cell & Environment* **40**: 1629–1642.

Kjaer KH, Ottosen C-O. 2015. 3D Laser Triangulation for Plant Phenotyping in Challenging Environments. *Sensors* **15**: 13533–13547.

Knight MR, Knight H. 2012. Low-temperature perception leading to gene expression and cold tolerance in higher plants. *New Phytologist* **195**: 737–751.

Kollers S, Rodemann B, Ling J, Korzun V, Ebmeyer E, Argillier O, Hinze M, Plieske J, Kulosa D, Ganal MW, *et al.* 2013. Whole Genome Association Mapping of Fusarium Head Blight Resistance in European Winter Wheat (Triticum aestivum L.). *PLOS ONE* **8**: e57500.

Körner C. **2003**. Carbon limitation in trees. *Journal of Ecology* **91**: 4–17.

Körner C. **2006**. Significance of Temperature in Plant Life. In: Morison JIL, Morecroft MD, eds. Plant Growth and Climate Change. Blackwell Publishing Ltd, 48–69.

Körner C. **2008**. Winter crop growth at low temperature may hold the answer for alpine treeline formation. *Plant Ecology & Diversity* **1**: 3–11.

Körner Ch, Farquhar GD, Wong SC. **1991**. Carbon isotope discrimination by plants follows latitudinal and altitudinal trends. *Oecologia* **88**: 30–40.

Körner C, Paulsen J. **2004**. A world-wide study of high altitude treeline temperatures. *Journal of Biogeography* **31**: 713–732.

Kronenberg L, Yates S, Boer MP, Kirchgessner N, Walter A, Hund A. **2019**. Temperature response of wheat affects final height and the timing of key developmental stages under field conditions. *bioRxiv:* 756700.

Kronenberg L, Yu K, Walter A, Hund A. **2017**. Monitoring the dynamics of wheat stem elongation: genotypes differ at critical stages. *Euphytica* **213**: 157.

Lancashire P, Bleiholder H, Vandenboom T, Langeluddeke P, Stauss R, Weber E, Witzenberger A. **1991**. A Uniform Decimal Code for Growth-Stages of Crops and Weeds. *Annals of Applied Biology* **119**: 561–601.

Langmead B, Salzberg SL. **2012**. Fast gapped-read alignment with Bowtie 2. *Nature Methods* **9**: 357–359.

Laurie DA, Pratchett N, Snape JW, Bezant JH. **1995**. RFLP mapping of five major genes and eight quantitative trait loci controlling flowering time in a winter x spring barley (Hordeum vulgare L.) cross. *Genome / National Research Council Canada = Génome / Conseil National De Recherches Canada* **38**: 575–585.

Lawit SJ, Wych HM, Xu D, Kundu S, Tomes DT. **2010**. Maize DELLA Proteins dwarf plant8 and dwarf plant9 as Modulators of Plant Development. *Plant and Cell Physiology* **51**: 1854–1868.

Lee JH, Yoo SJ, Park SH, Hwang I, Lee JS, Ahn JH. **2007**. Role of SVP in the control of flowering time by ambient temperature in Arabidopsis. *Genes & Development* **21**: 397–402.

Lehmann MM, Rinne KT, Blessing C, Siegwolf RTW, Buchmann N, Werner RA. **2015**. Malate as a key carbon source of leaf dark-respired CO_2 across different environmental conditions in potato plants. *Journal of Experimental Botany* **66**: 5769–5781.

Lenth RV. **2016**. Least-Squares Means: The R Package lsmeans. *Journal of Statistical Software* **69**.

Leonardos ED, Micallef BJ, Micallef MC, Grodzinski B. **2006**. Diel patterns of leaf C export and of main shoot growth for Flaveria linearis with altered leaf sucrose–starch partitioning. *Journal of Experimental Botany* **57**: 801–814.

Limin AE, Fowler DB. **2002**. Developmental Traits Affecting Low-temperature Tolerance Response in Near-isogenic Lines for the Vernalization Locus Vrn-A1 in Wheat (Triticum aestivum L. em Thell). *Annals of Botany* **89**: 579–585.

Liu X, Huang M, Fan B, Buckler ES, Zhang Z. **2016**. Iterative Usage of Fixed and Random Effect Models for Powerful and Efficient Genome-Wide Association Studies. *PLOS Genetics* **12**: e1005767.

Luo Q. **2011**. Temperature thresholds and crop production: a review. *Climatic Change* **109**: 583–598.

Mäkinen H, Kaseva J, Trnka M, Balek J, Kersebaum KC, Nendel C, Gobin A, Olesen JE, Bindi M, Ferrise R, *et al.* 2018. Sensitivity of European wheat to extreme weather. *Field Crops Research* **222**: 209–217.

Massonnet C, Vile D, Fabre J, Hannah MA, Caldana C, Lisec J, Beemster GTS, Meyer RC, Messerli G, Gronlund JT, *et al.* 2010. Probing the Reproducibility of Leaf Growth and Molecular Phenotypes: A Comparison of Three Arabidopsis Accessions Cultivated in Ten Laboratories. *Plant Physiology* **152**: 2142–2157.

Matos DA, Cole BJ, Whitney IP, MacKinnon KJ-M, Kay SA, Hazen SP. **2014**. Daily Changes in Temperature, Not the Circadian Clock, Regulate Growth Rate in Brachypodium distachyon. *PLOS ONE* **9**: e100072.

McClung CR. **2001**. Circadian Rhythms in Plants. *Annual Review of Plant Physiology and Plant Molecular Biology* **52**: 139–162.

McMaster GS, Wilhelm WW. **1997**. Growing degree-days: one equation, two interpretations. *Agricultural and Forest Meteorology* **87**: 291–300.

Mielewczik M, Friedli M, Kirchgessner N, Walter A. **2013**. Diel leaf growth of soybean: a novel method to analyze two-dimensional leaf expansion in high temporal resolution based on a marker tracking approach (Martrack Leaf). *Plant Methods* **9**: 1–14.

Miralles DJ, Richards RA, Slafer GA. **2000**. Duration of the stem elongation period influences the number of fertile florets in wheat and barley. *Functional Plant Biology* **27**: 931–940.

Miralles DJ, Slafer GA. **2007**. PAPER PRESENTED AT INTERNATIONAL WORKSHOP ON INCREASING WHEAT YIELD POTENTIAL, CIMMYT, OBREGON, MEXICO, 20–24 MARCH 2006 Sink limitations to yield in wheat: how could it be reduced? *The Journal of Agricultural Science* **145**: 139–149.

Miralles DJ, Slafer GA, Richards RA, Rawson HM. **2003**. Quantitative developmental response to the length of exposure to long photoperiod in wheat and barley. *The Journal of Agricultural Science* **141**: 159–167.

Mistele B, Schmidhalter U. **2008**. Estimating the nitrogen nutrition index using spectral canopy reflectance measurements. *European Journal of Agronomy* **29**: 184–190.

Mittag M. **2001**. Circadian rhythms in microalgae. *International Review of Cytology* **206**: 213–247.

Mo Y, Vanzetti LS, Hale I, Spagnolo EJ, Guidobaldi F, Al-Oboudi J, Odle N, Pearce S, Helguera M, Dubcovsky J. **2018**. Identification and characterization of Rht25, a locus on chromosome arm 6AS affecting wheat plant height, heading time, and spike development. *Theoretical and Applied Genetics* **131**: 2021–2035.

Mohler V, Lukman R, Ortiz-Islas S, William M, Worland AJ, van Beem J, Wenzel G. **2004**. Genetic and physical mapping of photoperiod insensitive gene Ppd-B1 in common wheat. *Euphytica* **138**: 33–40.

Monroy AF, Dryanova A, Malette B, Oren DH, Farajalla MR, Liu W, Danyluk J, Ubayasena LWC, Kane K, Scoles GJ, *et al.* 2007. Regulatory gene candidates and gene expression analysis of cold acclimation in winter and spring wheat. *Plant Molecular Biology* **64**: 409–423.

Monteith JL. **1984**. Consistency and Convenience in the Choice of Units for Agricultural Science. *Experimental Agriculture* **20**: 105–117.

Mori T, Johnson CH. **2001**. Circadian programming in cyanobacteria. *Seminars in Cell & Developmental Biology* **12**: 271–278.

Nagelmüller S, Kirchgessner N, Yates S, Hiltpold M, Walter A. **2016**. Leaf Length Tracker: a novel approach to analyse leaf elongation close to the thermal limit of growth in the field. *Journal of Experimental Botany* **67**: 1897–1906.

Nagelmüller S, Yates S, Walter A. **2018**. Diel leaf growth of rapeseed at critically low temperature under winter field conditions. *Functional Plant Biology* **45**: 1110–1118.

Nelissen H, Gonzalez Sanchez N, Inzé D. **2016**. Leaf growth in dicots and monocots : so different yet so alike. *CURRENT OPINION IN PLANT BIOLOGY* **33**: 72–76.

Nicholson P, Asachary S, Gosman N, Steed A, Chen X. **2008**. Role of phytohormone signalling in resistance of wheat to Fusarium head blight. *Cereal Research Communications* **36**: 213–216.

Nozue K, Covington MF, Duek PD, Lorrain S, Fankhauser C, Harmer SL, Maloof JN. **2007**. Rhythmic growth explained by coincidence between internal and external cues. *Nature* **448**: 358–361.

Nusinow DA, Helfer A, Hamilton EE, King JJ, Imaizumi T, Schultz TF, Farré EM, Kay SA. **2011**. The ELF4–ELF3–LUX complex links the circadian clock to diurnal control of hypocotyl growth. *Nature* **475**: 398–402.

Ochagavía H, Prieto P, Savin R, Griffiths S, Slafer GA. **2018**. Earliness per se effects on developmental traits in hexaploid wheat grown under field conditions. *European Journal of Agronomy* **99**: 214–223.

Ochagavia H, Prieto P, Zikhali M, Griffiths S, Slafer GA. **2019**. Earliness Per Se by Temperature Interaction on Wheat Development. *Scientific Reports* **9**: 2584.

Ohnishi S, Miyoshi T, Shirai S. **2010**. Low temperature stress at different flower developmental stages affects pollen development, pollination, and pod set in soybean. *Environmental and Experimental Botany* **69**: 56–62.

Ortiz R, Sayre KD, Govaerts B, Gupta R, Subbarao GV, Ban T, Hodson D, Dixon JM, Iván Ortiz-Monasterio J, Reynolds M. 2008. Climate change: Can wheat beat the heat? *Agriculture, Ecosystems & Environment* **126**: 46–58.

Pantin F, Simonneau T, Muller B. 2012. Coming of leaf age: control of growth by hydraulics and metabolics during leaf ontogeny. *New Phytologist* **196**: 349–366.

Pantin F, Simonneau T, Rolland G, Dauzat M, Muller B. 2011. Control of Leaf Expansion: A Developmental Switch from Metabolics to Hydraulics. *Plant Physiology* **156**: 803–815.

Parent B, Millet EJ, Tardieu F. 2018. The use of thermal time in plant studies has a sound theoretical basis provided that confounding effects are avoided. *Journal of Experimental Botany* **70**: 2359–2370.

Parent B, Shahinnia F, Maphosa L, Berger B, Rabie H, Chalmers K, Kovalchuk A, Langridge P, Fleury D. 2015. Combining field performance with controlled environment plant imaging to identify the genetic control of growth and transpiration underlying yield response to water-deficit stress in wheat. *Journal of Experimental Botany* **66**: 5481–5492.

Parent B, Tardieu F. 2012. Temperature responses of developmental processes have not been affected by breeding in different ecological areas for 17 crop species. *New Phytologist* **194**: 760–774.

Pask AJD, Pietragalla J, Mullan DM, Reynolds MP. 2012. *Physiological breeding II: a field guide to wheat phenotyping*. CIMMYT.

Passioura JB. 2006. The perils of pot experiments. *Functional Plant Biology* **33**: 1075–1079.

Paulsen J, Körner C. 2014. A climate-based model to predict potential treeline position around the globe. *Alpine Botany* **124**: 1–12.

Paulus S, Schumann H, Kuhlmann H, Léon J. 2014. High-precision laser scanning system for capturing 3D plant architecture and analysing growth of cereal plants. *Biosystems Engineering* **121**: 1–11.

Peacock JM. 1975. Temperature and Leaf Growth in Lolium perenne. II. The Site of Temperature Perception. *Journal of Applied Ecology* **12**: 115–123.

Penfield S. 2008. Temperature perception and signal transduction in plants. *New Phytologist* **179**: 615–628.

Peng FY, Hu Z, Yang R-C. 2015. Genome-Wide Comparative Analysis of Flowering-Related Genes in Arabidopsis, Wheat, and Barley. *International Journal of Plant Genomics* **2015**: 874361.

Peng J, Richards DE, Hartley NM, Murphy GP, Devos KM, Flintham JE, Beales J, Fish LJ, Worland AJ, Pelica F, *et al.* 1999. 'Green revolution' genes encode mutant gibberellin response modulators. *Nature* **400**: 256–261.

Pérez-Gianmarco TI, Slafer GA, González FG. **2018**. Wheat pre-anthesis development as affected by photoperiod sensitivity genes (Ppd-1) under contrasting photoperiods. *Functional Plant Biology*.

Pilkington SM, Encke B, Krohn N, Höhne M, Stitt M, Pyl E-T. **2015**. Relationship between starch degradation and carbon demand for maintenance and growth in Arabidopsis thaliana in different irradiance and temperature regimes. *Plant, Cell & Environment* **38**: 157–171.

Poethig RS, Sussex IM. **1985**. The developmental morphology and growth dynamics of the tobacco leaf. *Planta* **165**: 158–169.

Poiré R, Wiese-Klinkenberg A, Parent B, Mielewczik M, Schurr U, Tardieu F, Walter A. **2010**. Diel time-courses of leaf growth in monocot and dicot species: endogenous rhythms and temperature effects. *Journal of Experimental Botany*: erq049.

Poorter H, Fiorani F, Pieruschka R, Wojciechowski T, van der Putten WH, Kleyer M, Schurr U, Postma J. **2016**. Pampered inside, pestered outside? Differences and similarities between plants growing in controlled conditions and in the field. *New Phytologist* **212**: 838–855.

Poorter H, Fiorani F, Stitt M, Schurr U, Finck A, Gibon Y, Usadel B, Munns R, Atkin OK, Tardieu F, *et al.* 2012. The art of growing plants for experimental purposes: a practical guide for the plant biologist. *Functional Plant Biology* **39**: 821–838.

Porter AS, Evans-Fitz.Gerald C, McElwain JC, Yiotis C, Elliott-Kingston C. **2015**. How well do you know your growth chambers? Testing for chamber effect using plant traits. *Plant Methods* **11**: 44.

Porter JR, Gawith M. **1999**. Temperatures and the growth and development of wheat: a review. *European Journal of Agronomy* **10**: 23–36.

Porter JR, Kirby EJM, Day W, Adam JS, Appleyard M, Ayling S, Baker CK, Beale P, Belford RK, Biscoe PV, *et al.* 1987. An analysis of morphological development stages in avalon winter wheat crops with different sowing dates and at ten sites in England and Scotland. *The Journal of Agricultural Science* **109**: 107–121.

Porter JR, Semenov MA. **2005**. Crop responses to climatic variation. *Philosophical Transactions of the Royal Society B: Biological Sciences* **360**: 2021–2035.

Purcell LC. **2000**. Soybean canopy coverage and light interception measurements using digital imagery. *Crop Science* **40**: 834–837.

Purcell S, Neale B, Todd-Brown K, Thomas L, Ferreira MAR, Bender D, Maller J, Sklar P, de Bakker PIW, Daly MJ, *et al.* 2007. PLINK: a tool set for whole-genome association and population-based linkage analyses. *American Journal of Human Genetics* **81**: 559–575.

R Core Team. **2015**. *R: A language and environment for statistical computing*. Vienna, Austria: R Foundation for Statistical Computing.

Rajendran K, Tester M, Roy SJ. **2009**. Quantifying the three main components of salinity tolerance in cereals. *Plant, Cell & Environment* **32**: 237–249.

Rasse DP, Tocquin P. **2006**. Leaf carbohydrate controls over Arabidopsis growth and response to elevated CO2: an experimentally based model. *New Phytologist* **172**: 500–513.

Ray DK, Gerber JS, MacDonald GK, West PC. **2015**. Climate variation explains a third of global crop yield variability. *Nature Communications* **6**: 1–9.

Ray DK, Ramankutty N, Mueller ND, West PC, Foley JA. **2012**. Recent patterns of crop yield growth and stagnation. *Nature Communications* **3**: 1–7.

Reynolds M, Foulkes MJ, Slafer GA, Berry P, Parry MAJ, Snape JW, Angus WJ. **2009a**. Raising yield potential in wheat. *Journal of Experimental Botany* **60**: 1899–1918.

Reynolds M, Langridge P. **2016**. Physiological breeding. *Current Opinion in Plant Biology* **31**: 162–171.

Reynolds M, Manes Y, Izanloo A, Langridge P. **2009b**. Phenotyping approaches for physiological breeding and gene discovery in wheat. *Annals of Applied Biology* **155**: 309–320.

Reynolds MP, Rajaram S, Sayre KD. **1999**. Physiological and Genetic Changes of Irrigated Wheat in the Post–Green Revolution Period and Approaches for Meeting Projected Global Demand. *Crop Science* **39**: 1611.

Rezaei EE, Siebert S, Hüging H, Ewert F. **2018**. Climate change effect on wheat phenology depends on cultivar change. *Scientific Reports* **8**: 4891.

Richter A, Wanek W, Werner RA, Ghashghaie J, Jäggi M, Gessler A, Brugnoli E, Hettmann E, Göttlicher SG, Salmon Y, *et al.* 2009. Preparation of starch and soluble sugars of plant material for the analysis of carbon isotope composition: a comparison of methods. *Rapid Communications in Mass Spectrometry* **23**: 2476–2488.

Rodrigues FA, Fuganti-Pagliarini R, Marcolino-Gomes J, Nakayama TJ, Molinari HBC, Lobo FP, Harmon FG, Nepomuceno AL. **2015**. Daytime soybean transcriptome fluctuations during water deficit stress. *BMC Genomics* **16**: 505.

Rodríguez-Álvarez MX, Boer MP, van Eeuwijk FA, Eilers PHC. **2018**. Correcting for spatial heterogeneity in plant breeding experiments with P-splines. *Spatial Statistics* **23**: 52–71.

Roth L, Aasen H, Walter A, Liebisch F. **2018a**. Extracting leaf area index using viewing geometry effects—A new perspective on high-resolution unmanned aerial system photography. *ISPRS Journal of Photogrammetry and Remote Sensing* **141**: 161–175.

Roth L, Hund A, Aasen H. **2018b**. PhenoFly Planning Tool: flight planning for high-resolution optical remote sensing with unmanned areal systems. *Plant Methods* **14**: 116.

RStudio Team. **2015**. *RStudio: Integrated Development for R*. Boston, MA: RStudio, Inc.

Ruckle ME, Bernasconi L, Kölliker R, Zeeman SC, Studer B. **2018**. Genetic Diversity of Diurnal Carbohydrate Accumulation in White Clover (Trifolium repens L.). *Agronomy* **8**: 47.

Ruckle ME, Meier MA, Frey L, Eicke S, Kölliker R, Zeeman SC, Studer B. **2017**. Diurnal Leaf Starch Content: An Orphan Trait in Forage Legumes. *Agronomy* **7**: 16.

Ruts T, Matsubara S, Wiese-Klinkenberg A, Walter A. **2012**. Diel patterns of leaf and root growth: endogenous rhythmicity or environmental response? *Journal of Experimental Botany*: err334.

Sadok W, Naudin P, Boussuge B, Muller B, Welcker C, Tardieu F. **2007**. Leaf growth rate per unit thermal time follows QTL-dependent daily patterns in hundreds of maize lines under naturally fluctuating conditions. *Plant, Cell & Environment* **30**: 135–146.

Salomé PA, Weigel D, McClung CR. **2010**. The Role of the Arabidopsis Morning Loop Components CCA1, LHY, PRR7, and PRR9 in Temperature Compensation. *The Plant Cell* **22**: 3650–3661.

Sanchez-Bermejo E, Balasubramanian S. **2016**. Natural variation involving deletion alleles of FRIGIDA modulate temperature-sensitive flowering responses in Arabidopsis thaliana. *Plant, Cell & Environment* **39**: 1353–1365.

Sankaran S, Khot LR, Espinoza CZ, Jarolmasjed S, Sathuvalli VR, Vandemark GJ, Miklas PN, Carter AH, Pumphrey MO, Knowles NR, *et al.* 2015. Low-altitude, high-resolution aerial imaging systems for row and field crop phenotyping: A review. *European Journal of Agronomy* **70**: 112–123.

Schauberger B, Ben-Ari T, Makowski D, Kato T, Kato H, Ciais P. **2018**. Yield trends, variability and stagnation analysis of major crops in France over more than a century. *Scientific Reports* **8**: 1–12.

Schmutz J, Cannon SB, Schlueter J, Ma J, Mitros T, Nelson W, Hyten DL, Song Q, Thelen JJ, Cheng J, *et al.* 2010. Genome sequence of the palaeopolyploid soybean. *Nature* **463**: 178–183.

Schmutz J, McClean PE, Mamidi S, Wu GA, Cannon SB, Grimwood J, Jenkins J, Shu S, Song Q, Chavarro C, *et al.* 2014. A reference genome for common bean and genome-wide analysis of dual domestications. *Nature Genetics* **46**: 707–713.

Schnable PS, Ware D, Fulton RS, Stein JC, Wei F, Pasternak S, Liang C, Zhang J, Fulton L, Graves TA, *et al.* 2009. The B73 maize genome: complexity, diversity, and dynamics. *Science (New York, N.Y.)* **326**: 1112–1115.

Schori A, Fossati A, Soldati A, Stamp P. **1993**. Cold tolerance in soybean (Glycine max L. Merr.) in relation to flowering habit, pod set and compensation for lost reproductive organs. *European Journal of Agronomy* **2**: 173–178.

Sharifi MR, Rundel PW. **1993**. The Effect of Vapour Pressure Deficit on Carbon Isotope Discrimination in the Desert Shrub Larrea tridentata(Creosote Bush). *Journal of Experimental Botany* **44**: 481–487.

Sharma N, Ruelens P, D'hauw M, Maggen T, Dochy N, Torfs S, Kaufmann K, Rohde A, Geuten K. **2017**. A Flowering Locus C Homolog Is a Vernalization-Regulated Repressor in Brachypodium and Is Cold Regulated in Wheat. *Plant Physiology* **173**: 1301–1315.

Siddique KHM, Kirby EJM, Perry MW. **1989**. Ear: Stem ratio in old and modern wheat varieties; relationship with improvement in number of grains per ear and yield. *Field Crops Research* **21**: 59–78.

Slafer GA. **2003**. Genetic basis of yield as viewed from a crop physiologist's perspective. *Annals of Applied Biology* **142**: 117–128.

Slafer GA, Abeledo LG, Miralles DJ, Gonzalez FG, Whitechurch EM. **2001**. Photoperiod Sensitivity during Stem Elongation as an Avenue to Raise Potential Yield in Wheat. In: Bedö Z, Láng L, eds. Developments in Plant Breeding. Wheat in a Global Environment. Springer Netherlands, 487–496.

Slafer GA, Araus JL. **2007**. Physiological traits for improving wheat yield under a wide range of conditions. *Frontis*: 145–154.

Slafer GA, Calderini DF, Miralles DJ. **1996**. Yield components and compensations in wheat: opportunities for further increasing yield potential. In: Reynolds MP, Rajaram S, McNab A, eds. Increasing Yield Potential in Wheat: Breaking the Barriers : Proceedings of a Workshop Held in Ciudad Obregón, Sonora, Mexico. Mexico: CIMMYT, 101–133.

Slafer GA, Halloran GM, Connor DJ. **1995**. Influence of photoperiod on culm length in wheat. *Field Crops Research* **40**: 95–99.

Slafer GA, Kantolic AG, Appendino ML, Miralles DJ, Savin R. **2009**. Chapter 12 - Crop Development: Genetic Control, Environmental Modulation and Relevance for Genetic Improvement of Crop Yield. In: Sadras V, Calderini D, eds. Crop Physiology. San Diego: Academic Press, 277–308.

Slafer GA, Kantolic AG, Appendino ML, Tranquilli G, Miralles DJ, Savin R. **2015**. Chapter 12 - Genetic and environmental effects on crop development determining adaptation and yield. In: Calderini VOSF, ed. Crop Physiology (Second Edition). San Diego: Academic Press, 285–319.

Slafer GA, Rawson HM. **1994**. Sensitivity of Wheat Phasic Development to Major Environmental Factors: a Re-Examination of Some Assumptions Made by Physiologists and Modellers. *Functional Plant Biology* **21**: 393–426.

Slafer GA, Rawson HM. **1995a**. Rates and Cardinal Temperatures for Processes of Development in Wheat: Effects of Temperature and Thermal Amplitude. *Functional Plant Biology* **22**: 913–926.

Slafer GA, Rawson HM. **1995b**. Intrinsic earliness and basic development rate assessed for their response to temperature in wheat. *Euphytica* **83**: 175–183.

Slafer GA, Rawson HM. **1995c**. Base and optimum temperatures vary with genotype and stage of development in wheat. *Plant, Cell & Environment* **18**: 671–679.

Slafer GA, Rawson HM. **1995d**. Photoperiod × temperature interactions in contrasting wheat genotypes: Time to heading and final leaf number. *Field Crops Research* **44**: 73–83.

Slafer GA, Rawson HM. **1996**. Responses to photoperiod change with phenophase and temperature during wheat development. *Field Crops Research* **46**: 1–13.

Snape JW, Butterworth K, Whitechurch E, Worland AJ. **2001**. Waiting for fine times: genetics of flowering time in wheat. *Euphytica* **119**: 185–190.

Spannagl M, Mayer K, Durner J, Haberer G, Fröhlich A. **2011**. Exploring the genomes: From Arabidopsis to crops. *Journal of Plant Physiology* **168**: 3–8.

Srinivasachary, Gosman N, Steed A, Simmonds J, Leverington-Waite M, Wang Y, Snape J, Nicholson P. **2008**. Susceptibility to Fusarium head blight is associated with the Rht-D1b semi-dwarfing allele in wheat. *Theoretical and Applied Genetics* **116**: 1145–1153.

Stitt M, Zeeman SC. **2012**. Starch turnover: pathways, regulation and role in growth. *Current Opinion in Plant Biology* **15**: 282–292.

Sulpice R, Pyl E-T, Ishihara H, Trenkamp S, Steinfath M, Witucka-Wall H, Gibon Y, Usadel B, Poree F, Piques MC, *et al.* 2009. Starch as a major integrator in the regulation of plant growth. *Proceedings of the National Academy of Sciences* **106**: 10348–10353.

Svensgaard J, Roitsch T, Christensen S. **2014**. Development of a Mobile Multispectral Imaging Platform for Precise Field Phenotyping. *Agronomy* **4**: 322–336.

Tang Y, Liu X, Wang J, Li M, Wang Q, Tian F, Su Z, Pan Y, Liu D, Lipka AE, *et al.* 2016. GAPIT Version 2: An Enhanced Integrated Tool for Genomic Association and Prediction. *The Plant Genome* **9**.

Tcherkez G, Nogués S, Bleton J, Cornic G, Badeck F, Ghashghaie J. **2003**. Metabolic Origin of Carbon Isotope Composition of Leaf Dark-Respired CO2 in French Bean. *Plant Physiology* **131**: 237–244.

The International Barley Genome Sequencing Consortium. **2012**. A physical, genetic and functional sequence assembly of the barley genome. *Nature* **491**: 711–716.

Thines B, Harmon FG. **2010**. Ambient temperature response establishes ELF3 as a required component of the core Arabidopsis circadian clock. *Proceedings of the National Academy of Sciences* **107**: 3257–3262.

Thomashow MF. **2010**. Molecular Basis of Plant Cold Acclimation: Insights Gained from Studying the CBF Cold Response Pathway. *Plant Physiology* **154**: 571–577.

Tilman D, Balzer C, Hill J, Befort BL. **2011**. Global food demand and the sustainable intensification of agriculture. *Proceedings of the National Academy of Sciences* **108**: 20260–20264.

To JPC, Haberer G, Ferreira FJ, Deruère J, Mason MG, Schaller GE, Alonso JM, Ecker JR, Kieber JJ. **2004**. Type-A Arabidopsis Response Regulators Are Partially Redundant Negative Regulators of Cytokinin Signaling. *The Plant Cell* **16**: 658–671.

Trapnell C, Pachter L, Salzberg SL. **2009**. TopHat: discovering splice junctions with RNA-Seq. *Bioinformatics* **25**: 1105–1111.

Trapnell C, Roberts A, Goff L, Pertea G, Kim D, Kelley DR, Pimentel H, Salzberg SL, Rinn JL, Pachter L. **2012**. Differential gene and transcript expression analysis of RNA-seq experiments with TopHat and Cufflinks. *Nature Protocols* **7**: 562–578.

Trevaskis B. **2015**. Wheat gene for all seasons. *Proceedings of the National Academy of Sciences* **112**: 11991–11992.

Trevaskis B, Hemming MN, Dennis ES, Peacock WJ. **2007a**. The molecular basis of vernalization-induced flowering in cereals. *Trends in Plant Science* **12**: 352–357.

Trevaskis B, Tadege M, Hemming MN, Peacock WJ, Dennis ES, Sheldon C. **2007b**. Short Vegetative Phase-Like MADS-Box Genes Inhibit Floral Meristem Identity in Barley. *Plant Physiology* **143**: 225–235.

Troughton JH, Card KA. **1975**. Temperature effects on the carbon-isotope ratio of C3, C4 and crassulacean-acid-metabolism (CAM) plants. *Planta* **123**: 185–190.

Turner A, Beales J, Faure S, Dunford RP, Laurie DA. **2005**. The Pseudo-Response Regulator Ppd-H1 Provides Adaptation to Photoperiod in Barley. *Science* **310**: 1031–1034.

VanRaden PM. **2008**. Efficient Methods to Compute Genomic Predictions. *Journal of Dairy Science* **91**: 4414–4423.

Varshney RK, Chen W, Li Y, Bharti AK, Saxena RK, Schlueter JA, Donoghue MTA, Azam S, Fan G, Whaley AM, *et al.* 2012. Draft genome sequence of pigeonpea (Cajanus cajan), an orphan legume crop of resource-poor farmers. *Nature Biotechnology* **30**: 83–89.

Varshney RK, Song C, Saxena RK, Azam S, Yu S, Sharpe AG, Cannon S, Baek J, Rosen BD, Tar'an B, *et al.* 2013. Draft genome sequence of chickpea (*Cicer arietinum*) provides a resource for trait improvement. *Nature Biotechnology* **31**: 240–246.

Virlet N, Sabermanesh K, Sadeghi-Tehran P, Hawkesford MJ. **2016**. Field Scanalyzer: An automated robotic field phenotyping platform for detailed crop monitoring. *Functional Plant Biology*.

Voorend W, Lootens P, Nelissen H, Roldán-Ruiz I, Inzé D, Muylle H. **2014**. LEAF-E: a tool to analyze grass leaf growth using function fitting. *Plant Methods* **10**: 37.

Walter A, Liebisch F, Hund A. **2015**. Plant phenotyping: from bean weighing to image analysis. *Plant Methods* **11**: 1–11.

Walter A, Scharr H, Gilmer F, Zierer R, Nagel KA, Ernst M, Wiese A, Virnich O, Christ MM, Uhlig B, *et al.* 2007. Dynamics of seedling growth acclimation towards altered light conditions can be quantified via GROWSCREEN: a setup and procedure designed for rapid optical phenotyping of different plant species. *New Phytologist* **174**: 447–455.

Walter A, Silk WK, Schurr U. **2009**. Environmental Effects on Spatial and Temporal Patterns of Leaf and Root Growth. *Annual Review of Plant Biology* **60**: 279–304.

Wanek W, Heintel S, Richter A. **2001**. Preparation of starch and other carbon fractions from higher plant leaves for stable carbon isotope analysis. *Rapid Communications in Mass Spectrometry* **15**: 1136–1140.

Wang S, Wong D, Forrest K, Allen A, Chao S, Huang BE, Maccaferri M, Salvi S, Milner SG, Cattivelli L, *et al.* 2014. Characterization of polyploid wheat genomic

diversity using a high-density 90 000 single nucleotide polymorphism array. *Plant Biotechnology Journal* **12**: 787–796.

Wehrens R, Kruisselbrink J. **2018**. Flexible Self-Organizing Maps in kohonen 3.0. *Journal of Statistical Software* **87**: 1–18.

Werner RA, Bruch BA, Brand WA. **1999**. ConFlo III – an interface for high precision δ13C and δ15N analysis with an extended dynamic range. *Rapid Communications in Mass Spectrometry* **13**: 1237–1241.

Werner T, Motyka V, Strnad M, Schmülling T. **2001**. Regulation of plant growth by cytokinin. *Proceedings of the National Academy of Sciences* **98**: 10487–10492.

White JW, Andrade-Sanchez P, Gore MA, Bronson KF, Coffelt TA, Conley MM, Feldmann KA, French AN, Heun JT, Hunsaker DJ, *et al.* 2012. Field-based phenomics for plant genetics research. *Field Crops Research* **133**: 101–112.

White JW, Conley MM. **2013**. A Flexible, Low-Cost Cart for Proximal Sensing. *Crop Science* **53**: 1646–1649.

Whitechurch EM, Slafer GA. **2002**. Contrasting Ppd alleles in wheat: effects on sensitivity to photoperiod in different phases. *Field Crops Research* **73**: 95–105.

Whitechurch EM, Slafer GA, Miralles DJ. **2007**. Variability in the Duration of Stem Elongation in Wheat and Barley Genotypes. *Journal of Agronomy and Crop Science* **193**: 138–145.

Wiese A, Christ MM, Virnich O, Schurr U, Walter A. **2007**. Spatio-temporal leaf growth patterns of Arabidopsis thaliana and evidence for sugar control of the diel leaf growth cycle. *New Phytologist* **174**: 752–761.

Wigge PA. **2013**. Ambient temperature signalling in plants. *Current Opinion in Plant Biology* **16**: 661–666.

Winfield MO, Lu C, Wilson ID, Coghill JA, Edwards KJ. **2009**. Cold- and light-induced changes in the transcriptome of wheat leading to phase transition from vegetative to reproductive growth. *BMC Plant Biology* **9**: 55.

Winfield MO, Lu C, Wilson ID, Coghill JA, Edwards KJ. **2010**. Plant responses to cold: transcriptome analysis of wheat. *Plant Biotechnology Journal* **8**: 749–771.

de Winter L, Klok AJ, Cuaresma Franco M, Barbosa MJ, Wijffels RH. **2013**. The synchronized cell cycle of Neochloris oleoabundans and its influence on biomass composition under constant light conditions. *Algal Research* **2**: 313–320.

Worland AJ. **1996**. The influence of flowering time genes on environmental adaptability in European wheats. *Euphytica* **89**: 49–57.

Wu J, Kong X, Wan J, Liu X, Zhang X, Guo X, Zhou R, Zhao G, Jing R, Fu X, *et al.* 2011. Dominant and Pleiotropic Effects of a GAI Gene in Wheat Results from a Lack of Interaction between DELLA and GID1. *Plant Physiology* **157**: 2120–2130.

Würschum T, Langer SM, Longin CFH, Tucker MR, Leiser WL. **2017**. A modern Green Revolution gene for reduced height in wheat. *The Plant Journal* **92**: 892–903.

Xue W, Xing Y, Weng X, Zhao Y, Tang W, Wang L, Zhou H, Yu S, Xu C, Li X, *et al.* 2008. Natural variation inGhd7 is an important regulator of heading date and yield potential in rice. *Nature Genetics* **40**: 761–767.

Yan L, Fu D, Li C, Blechl A, Tranquilli G, Bonafede M, Sanchez A, Valarik M, Yasuda S, Dubcovsky J. **2006**. The wheat and barley vernalization gene VRN3 is an orthologue of FT. *Proceedings of the National Academy of Sciences* **103**: 19581–19586.

Yang W, Guo Z, Huang C, Duan L, Chen G, Jiang N, Fang W, Feng H, Xie W, Lian X, *et al.* 2014. Combining high-throughput phenotyping and genome-wide association studies to reveal natural genetic variation in rice. *Nature Communications* **5**: 5087.

Yang Q, Pando BF, Dong G, Golden SS, Oudenaarden A van. **2010**. Circadian Gating of the Cell Cycle Revealed in Single Cyanobacterial Cells. *Science* **327**: 1522–1526.

Yates S, Jaškūnė K, Liebisch F, Nagelmüller S, Kirchgessner N, Kölliker R, Walter A, Brazauskas G, Studer B. **2019**. Phenotyping a Dynamic Trait: Leaf Growth of Perennial Ryegrass Under Water Limiting Conditions. *Frontiers in Plant Science* **10**.

Yates S, Mikaberidze A, Krattinger S, Abrouk M, Hund A, Yu K, Studer B, Fouche S, Meile L, Pereira D, *et al.* 2018. Precision phenotyping reveals novel loci for quantitative resistance to septoria tritici blotch in European winter wheat. *bioRxiv*: 502260.

Yoshida R, Fekih R, Fujiwara S, Oda A, Miyata K, Tomozoe Y, Nakagawa M, Niinuma K, Hayashi K, Ezura H, *et al.* 2009. Possible role of early flowering 3 (ELF3) in clock-dependent floral regulation by short vegetative phase (SVP) in Arabidopsis thaliana. *The New Phytologist* **182**: 838–850.

Youssefian S, Kirby EJM, Gale MD. **1992a**. Pleiotropic effects of the GA-insensitive Rht dwarfing genes in wheat. 1. Effects on development of the ear, stem and leaves. *Field Crops Research* **28**: 179–190.

Youssefian S, Kirby EJM, Gale MD. **1992b**. Pleiotropic effects of the GA-insensitive Rht dwarfing genes in wheat. 2. Effects on leaf, stem, ear and floret growth. *Field Crops Research* **28**: 191–210.

Zagotta MT, Hicks KA, Jacobs CI, Young JC, Hangarter RP, Meeks-Wagner DR. **1996**. The Arabidopsis ELF3 gene regulates vegetative photomorphogenesis and the photoperiodic induction of flowering. *The Plant Journal: For Cell and Molecular Biology* **10**: 691–702.

Zanke CD, Ling J, Plieske J, Kollers S, Ebmeyer E, Korzun V, Argillier O, Stiewe G, Hinze M, Beier S, *et al.* 2014a. Genetic architecture of main effect QTL for heading date in European winter wheat. *Frontiers in Plant Science* **5**.

Zanke C, Ling J, Plieske J, Kollers S, Ebmeyer E, Korzun V, Argillier O, Stiewe G, Hinze M, Neumann K, *et al.* 2014b. Whole Genome Association Mapping of Plant Height in Winter Wheat (Triticum aestivum L.). *PLoS ONE* **9**.

Zanten M van, Bours R, Pons TL, Proveniers MCG. **2013**. Plant acclimation and adaptation to warm environments. In: Temperature and Plant Development. John Wiley & Sons, Ltd, 49–78.

Zeeman MJ, Werner RA, Eugster W, Siegwolf RTW, Wehrle G, Mohn J, Buchmann N. **2008**. Optimization of automated gas sample collection and isotope ratio mass spectrometric analysis of δ13C of CO2 in air. *Rapid Communications in Mass Spectrometry* **22**: 3883–3892.

Zhang Z, Ersoz E, Lai C-Q, Todhunter RJ, Tiwari HK, Gore MA, Bradbury PJ, Yu J, Arnett DK, Ordovas JM, *et al.* 2010. Mixed linear model approach adapted for genome-wide association studies. *Nature Genetics* **42**: 355–360.

Zhao XY, Liu MS, Li JR, Guan CM, Zhang XS. **2005**. The wheat TaGI1, involved in photoperiodic flowering, encodesan Arabidopsis GI ortholog. *Plant Molecular Biology* **58**: 53–64.

Zheng X, Levine D, Shen J, Gogarten SM, Laurie C, Weir BS. **2012**. A high-performance computing toolset for relatedness and principal component analysis of SNP data. *Bioinformatics* **28**: 3326–3328.

Zhou M, Xu M, Wu L, Shen C, Ma H, Lin J. **2014**. CbCBF from Capsella bursa-pastoris enhances cold tolerance and restrains growth in Nicotiana tabacum by antagonizing with gibberellin and affecting cell cycle signaling. *Plant Molecular Biology* **85**: 259–275.

Zikhali M, Griffiths S. **2015**. The Effect of Earliness per se (Eps) Genes on Flowering Time in Bread Wheat. In: Advances in Wheat Genetics: From Genome to Field. Springer, Tokyo, 339–345.

Zikhali M, Leverington-Waite M, Fish L, Simmonds J, Orford S, Wingen LU, Goram R, Gosman N, Bentley A, Griffiths S. **2014**. Validation of a 1DL earliness per se (eps) flowering QTL in bread wheat (Triticum aestivum). *Molecular Breeding* **34**: 1023–1033.

Zikhali M, Wingen LU, Griffiths S. **2016**. Delimitation of the Earliness per se D1 (Eps-D1) flowering gene to a subtelomeric chromosomal deletion in bread wheat (Triticum aestivum). *Journal of Experimental Botany* **67**: 287–299.

Supplementary material chapter 2

Figures

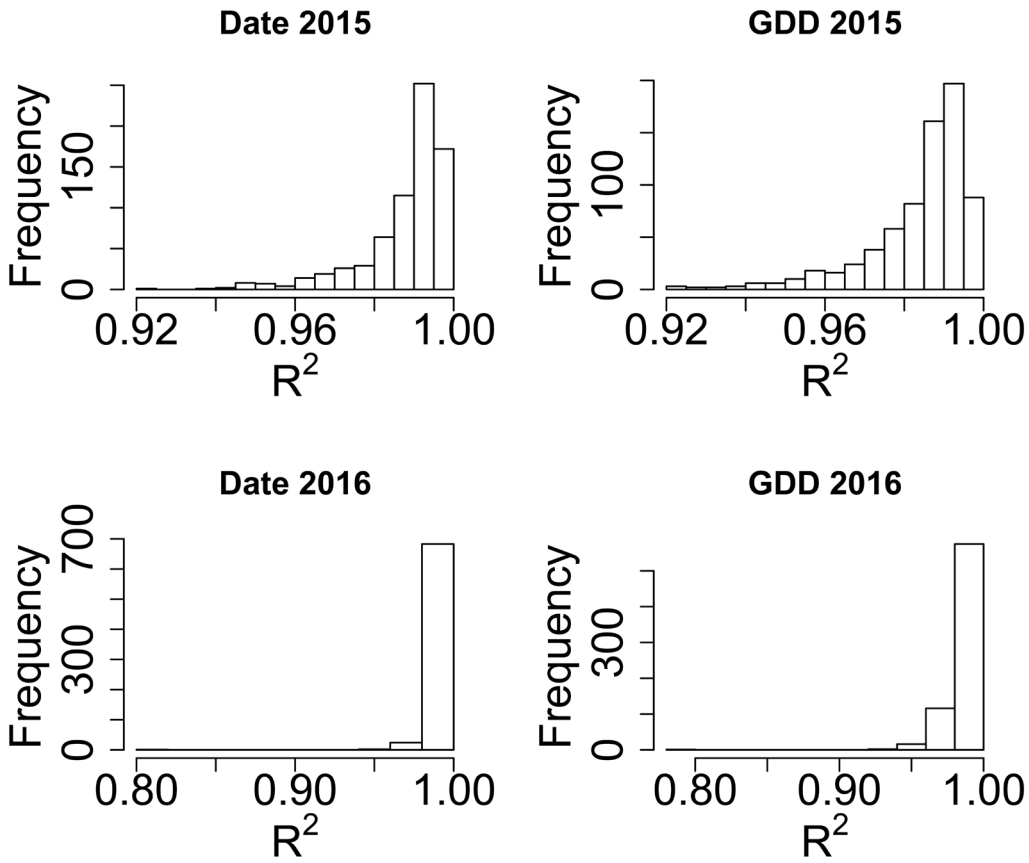

Fig. S1: R^2 distribution of the plot wise linear regression of canopy height versus time and growing degree days, respectively for the years 2015 and 2016.

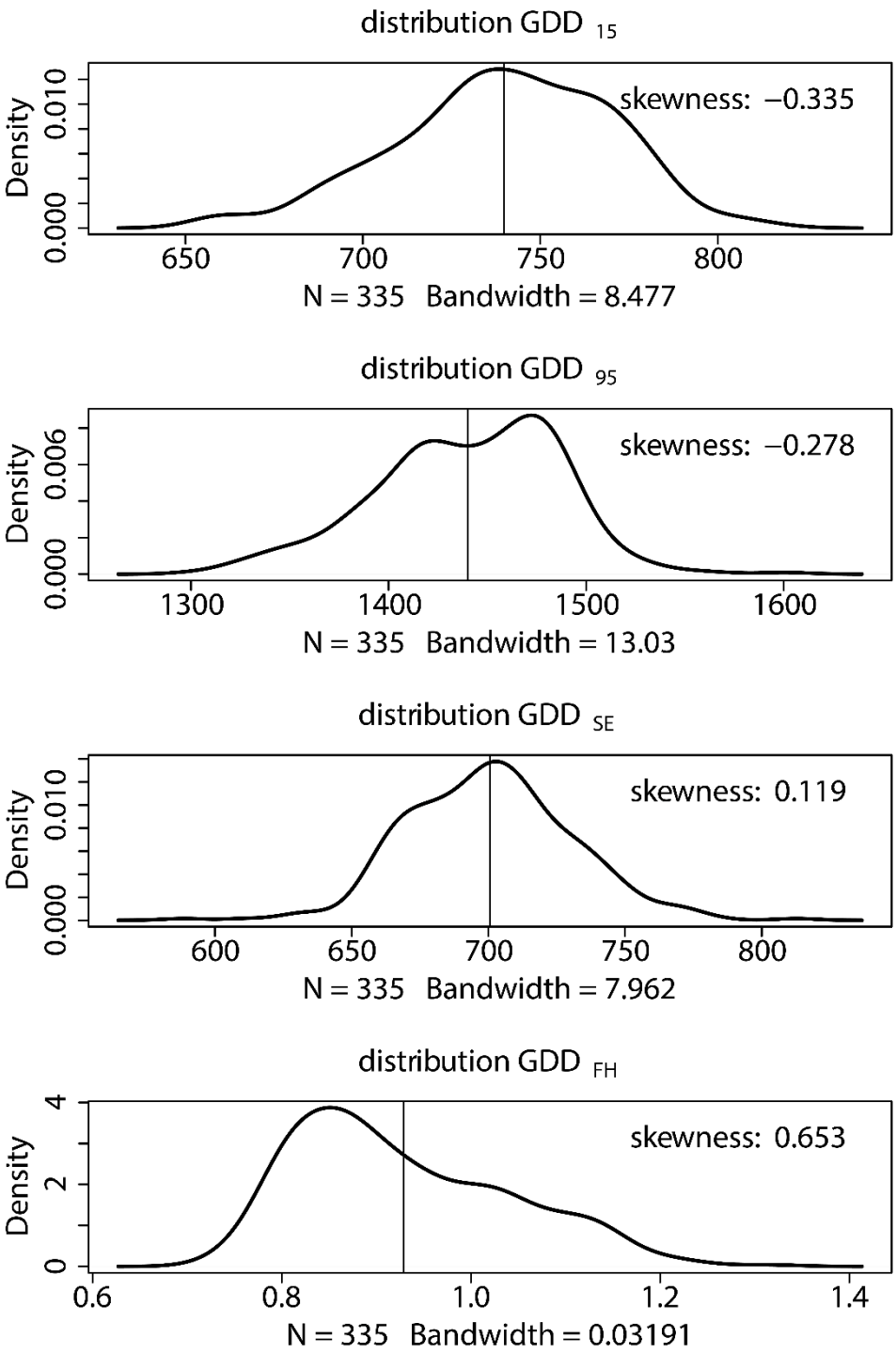

Fig. S2: Distribution of best linear unbiased predictors across two years of all 335 genotypes for the traits growing degree days (GDD) until 15% final height (GDD_{15}), GDD until 95% final height (GDD_{95}), duration of stem elongation phase (GDD_{SE}) and final canopy height (FH). Vertical black lines depict the respective mean value.

Supplementary material chapter 3

Figures

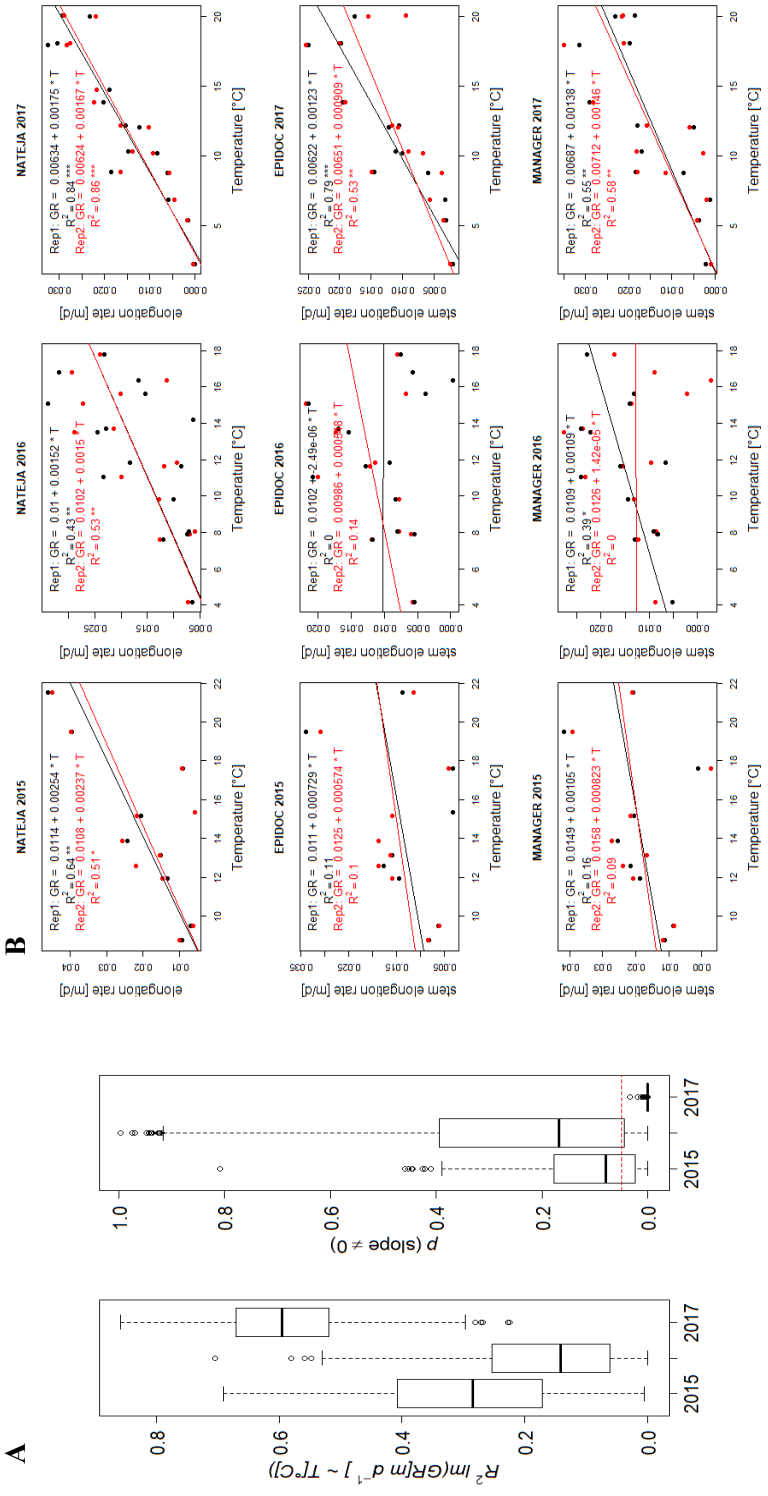

Fig. S1: Summary of plot based linear model fits of stem elongation rate vs. temperature. A Distribution of linear model R^2 and p-values of plot based linear model fits grouped by year. B. Genotype showing the best (NATEJA 2017 Rep1) and the two genotypes showing worst (EPIDOC 2016 Rep1; MANAGER 2016 Rep2) plot based linear model fit out of all plot based linear models fitted.

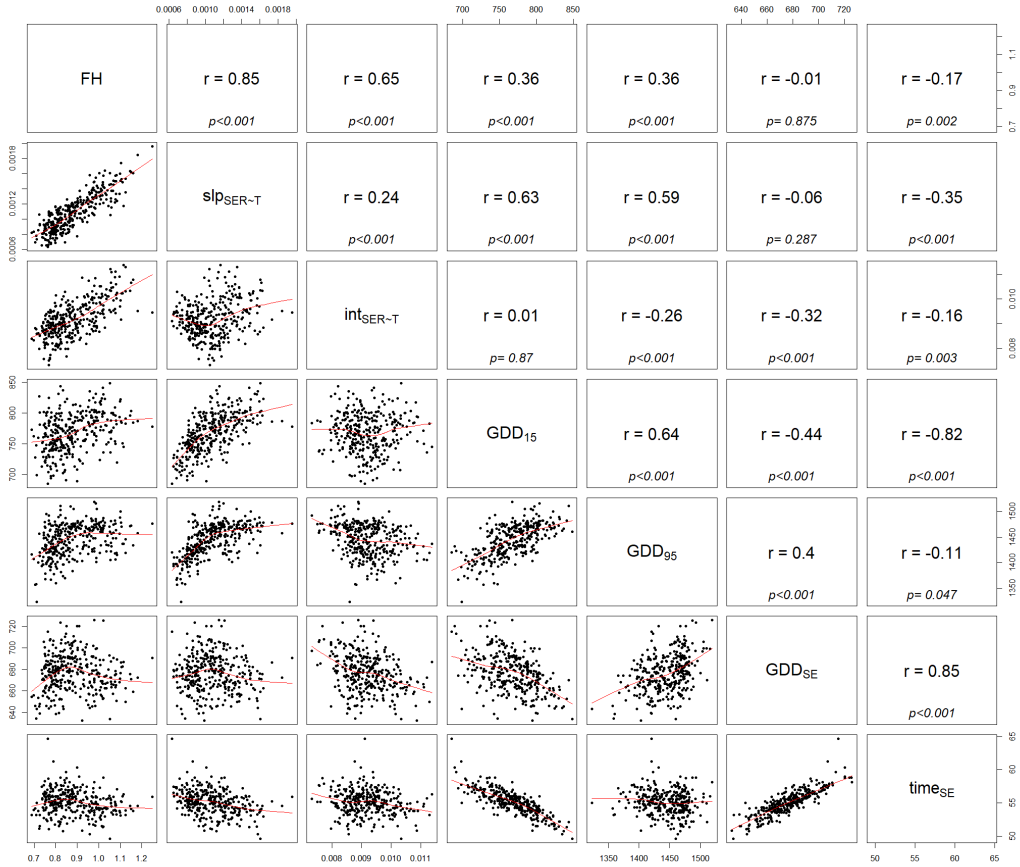

Fig. S2: Pearson correlation coefficients among 3-year BLUPS of all investigated traits.

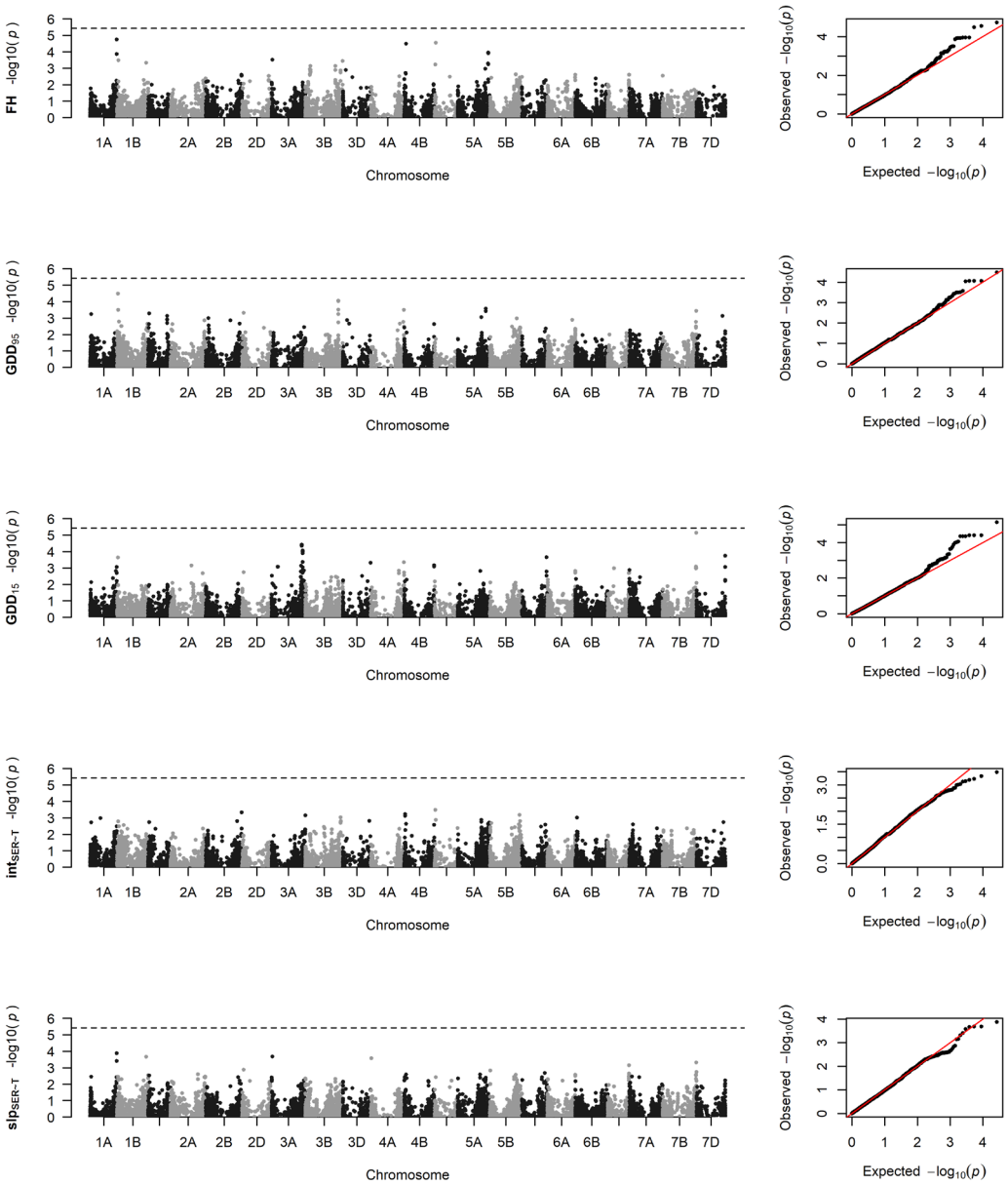

Fig. S3: Manhattan plots and quantile-quantile plots depicting the GWAS results using the MLM approach for final height (FH), growing degree days until start (GDD_{15}) and end (GDD_{95}) of stem elongation; vigour-related intercept ($int_{GR\sim T}$) and temperature-related slope ($slp_{GR\sim T}$) of stem elongation in response to temperature. Horizontal lines mark the Bonferroni corrected significance threshold for $p < 0.05$ (dashed line) and $p < 0.001$ (solid line).

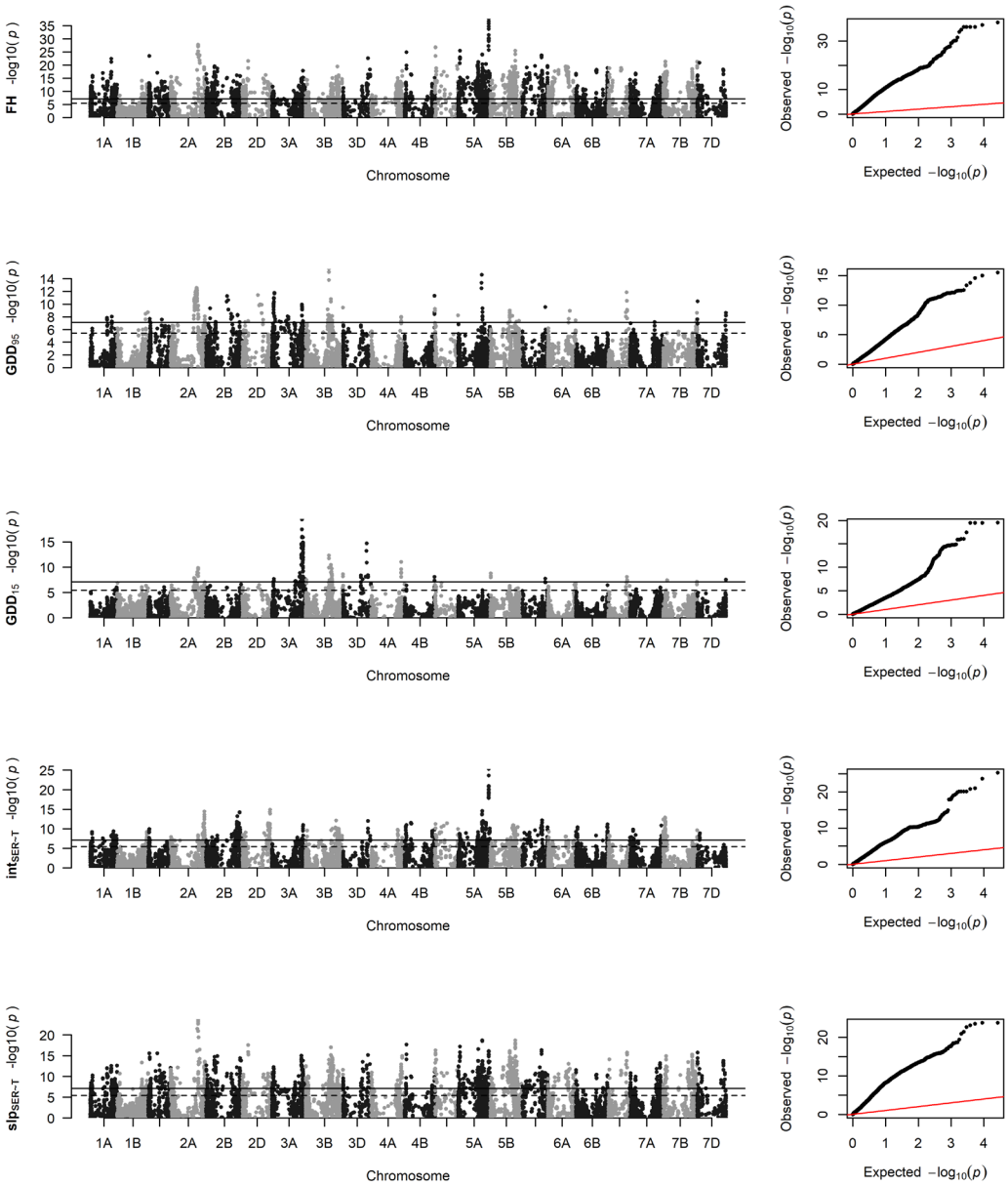

Fig. S4: Manhattan plots and quantile-quantile plots depicting the GWAS results using the GLM approach for final height (FH), growing degree days until start (GDD_{15}) and end (GDD_{95}) of stem elongation; vigour-related intercept ($int_{GR\sim T}$) and temperature-related slope ($slp_{GR\sim T}$) of stem elongation in response to temperature. Horizontal lines mark the Bonferroni corrected significance threshold for $p < 0.05$ (dashed line) and $p < 0.001$ (solid line).

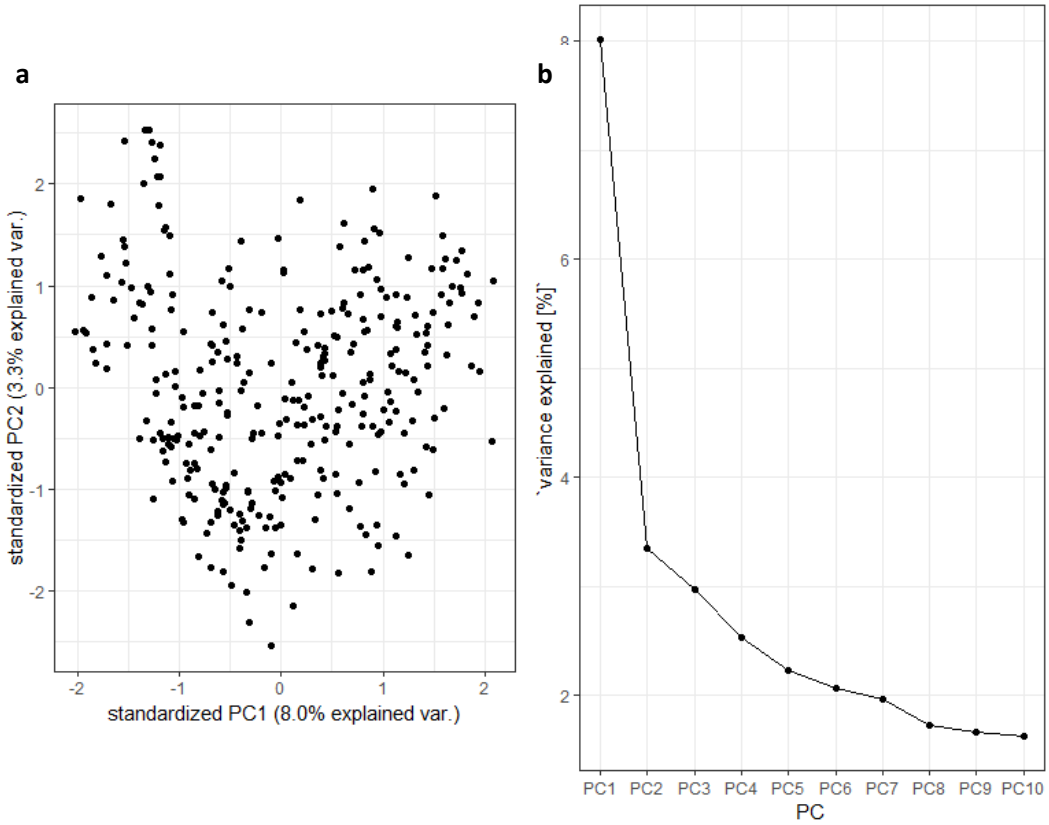

Fig. S5: Principal component analysis among marker genotypes. a: Biplot of the first two principal components. **b:** Screeplot showing the explained proportion of the variance for individual components.

Tables

Table S1: Genes of interest related to floral transition and flowering. Genome positions (r.start-r.end) were derived by blasting the respective published sequence (GenBank ID; https://www.ncbi.nlm.nih.gov/genbank/) against the IWGSC reference genome.

Gene	Chr	r.start	r.end	GenBank ID
PPD_A1	chr2A	36'934'562	36'933'892	DQ885753.1
PPD_D1	chr2D	33'953'359	33'952'698	DQ885766.1
RHT_A1	chr4A	582'479'578	582'477'716	JF930277.1
RHT_B1	chr4B	30'861'382	30'863'247	JX993610.1
RHT_D1	chr4D	18'781'062	18'782'933	AJ242531.1
TaELF3	chr1D	493'485'605	493'484'553	KR055809.1
TaFT3_A1	chr1A	528'066'476	528'066'282	KX161737.1
TaFT3_B1	chr1B	581'414'952	581'414'758	KX161739.1
TaFT3_D1	chr1D	430'469'335	430'469'144	KX161740.1
VRN_A1	chr5A	587'423'240	587'423'056	AY616452.1
VRN_B1	chr5B	573'815'903	573'815'719	AY747603.1
VRN_B3	chr7B	9'703'464	9'703'735	DQ890162.1
VRN_D1	chr5D	467'184'278	467'184'094	AY747597.1
VRN_D4	chr5D	467'184'278	467'184'094	KR422424.1

Table S2: Chromosome wise distance thresholds for LD-decay < r^2 = 0.2.

Chromosome	r^2 threshold [bp]
1A	6'161'631
1B	17'286'788
1D	12'822'505
2A	10'381'104
2B	11'361'169
2D	10'416'001
3A	9'887'297
3B	5'969'718
3D	4'233'196
4A	4'298'677
4B	11'488'268
4D	4'220'358
5A	10'344'140
5B	17'533'559
5D	4'862'712
6A	4'692'731
6B	19'679'489
6D	1'416'632
7A	7'133'812
7B	6'604'947
7D	NA

Table S3: Corresponding marker-trait associations for final canopy height with respect to Zanke et al. 2014*b*. MTA Zanke et al 2014*b* denotes marker trait associations reported by Zanke et al. 2014*b*, Closest MTA denotes the closest respective associated marker found in this study. Distance gives the distance in base pairs and r^2 the pairwise linkage disequilibrium between the two respective SNP.

Chr	MTA Zanke et al. 2014*b*	Closest_MTA	distance	r^2
1B	Ra_c2110_494	BS00089734_51	-3'464'516	0.22
5A	Kukri_c75091_220	wsnp_Ku_rep_c71232_70948744	-5'660	0.99
5A	wsnp_Ex_c23795_33033959	wsnp_Ku_rep_c71232_70948744	1'457	0.99
5B	RAC875_c94973_396	BS00109560_51	-2'919'770	0.62
5B	wsnp_Ex_c5155_9140608	BS00109560_51	2'442'796	0.82
6A	BS00062823_51	BS00022120_51	51'119'779	0.60

For supplementary Table S4:
3-year BLUPs of the investigated traits FH, GDD_{15}, GDD_{95}, GDD_{SE}, $time_{SE}$, $slp_{SER\sim T}$, $int_{SER\sim T}$ please refer to: https://www.biorxiv.org/content/10.1101/756700v1.supplementary-material.

Supplementary material chapter 5

Figures

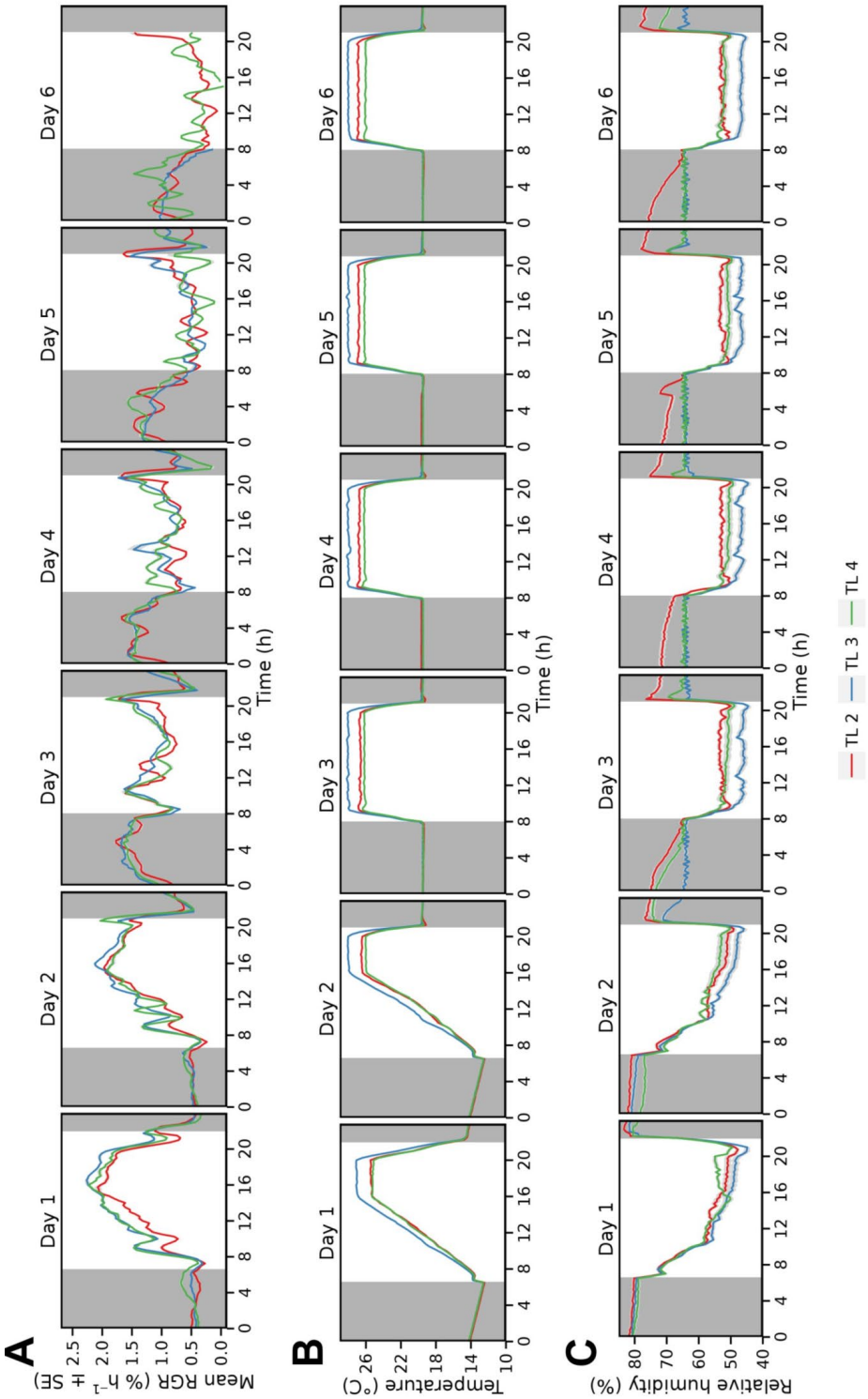

Fig. S1: Diel growth pattern of soybean in the preliminary experiment 2015. (a) Mean relative growth rate (% h^{-1} ± SE) of the second trifoliate leaf (TL 2, red line) TL 3 (blue line) and TL 4 (green line); n = 6 per TL; (b) Temperature (°C) and (c) relative humidity (%) conditions during the experiment. Shaded areas indicate the dark period.

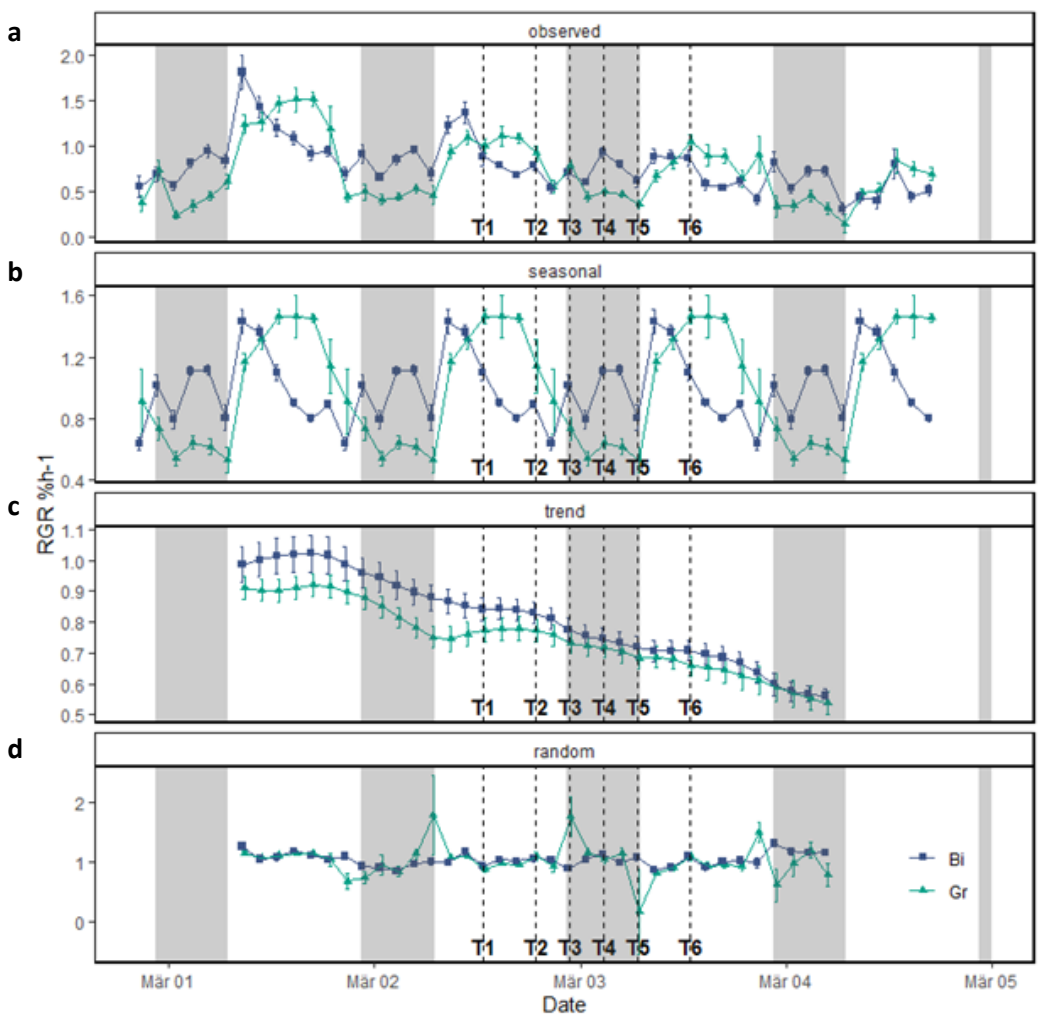

Fig. S2: Time series decomposition of the observed growth pattern for both treatments (a), into diel component (b), overall trend (c) and random remainder (d). Blue squares indicate the binary (Bi) and green triangles the gradually fluctuating (Gr) temperature-conditions. The shaded grey area indicates the dark period and vertical black dashed lines indicate the sampling time points for RNA-seq and carbohydrate analysis.

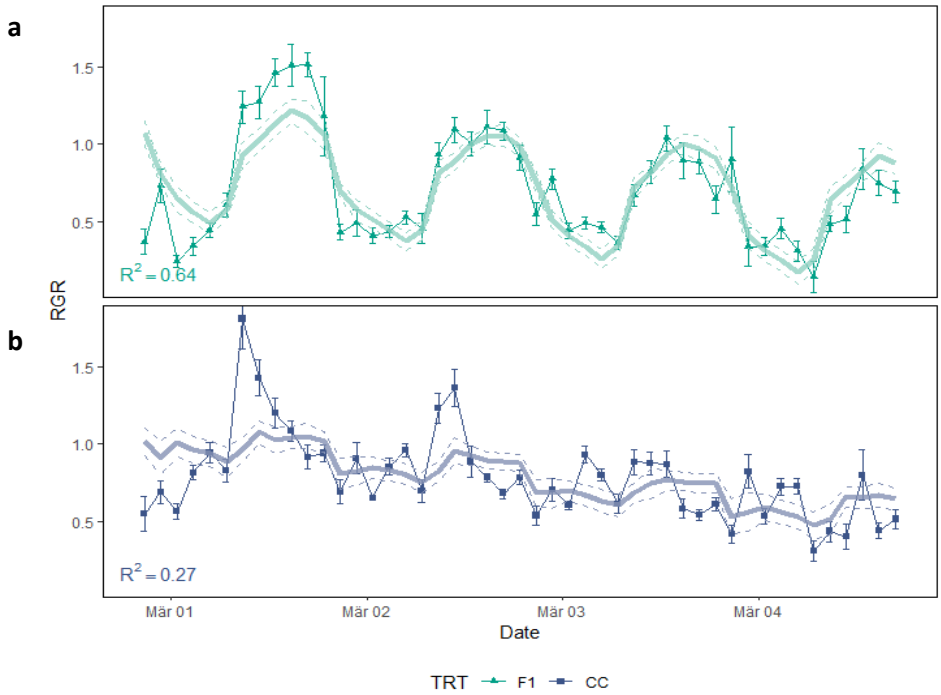

Fig. S3: Prediction of RGR using temperature, vapour pressure deficit, light and the square root of the leaf area as predictors in a growth model and applying it on each treatment (Bi, Gr) individually. Green triangles and blue circles show the observed mean values (n = 9) for the Gr and Bi treatment respectively and error bars show respective SE. The solid green and blue lines show the predicted values of the model for the Gr and Bi treatment respectively. Dashed lines show the SE of the predictions. For the model equation and anova results see eq. 1 and table 2, respectively.

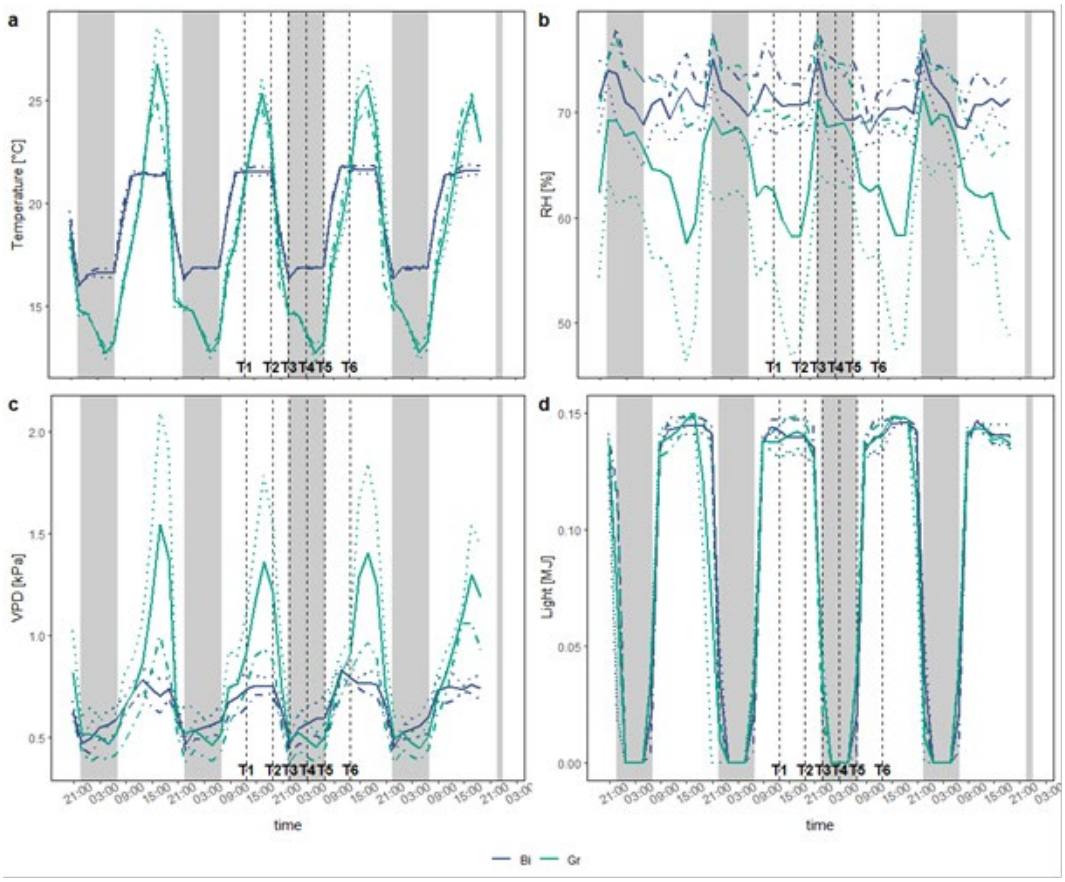

Fig. S4:| Diurnal course of temperature (a), relative humidity (RH; b), vapour pressure deficit (VPD; c) and light (d) between the two temperature treatments. Blue lines indicate the binary temperature treatment (Bi) and green lines indicate the gradient temperature regime (Gr). Solid lines indicate the mean values between the two iterations whereas dotted lines and dot-dashed lines indicate the first and second iteration respectively. The vertical dashed lines indicate the six sampling time points (T1-T6) and shaded areas indicate the dark period.

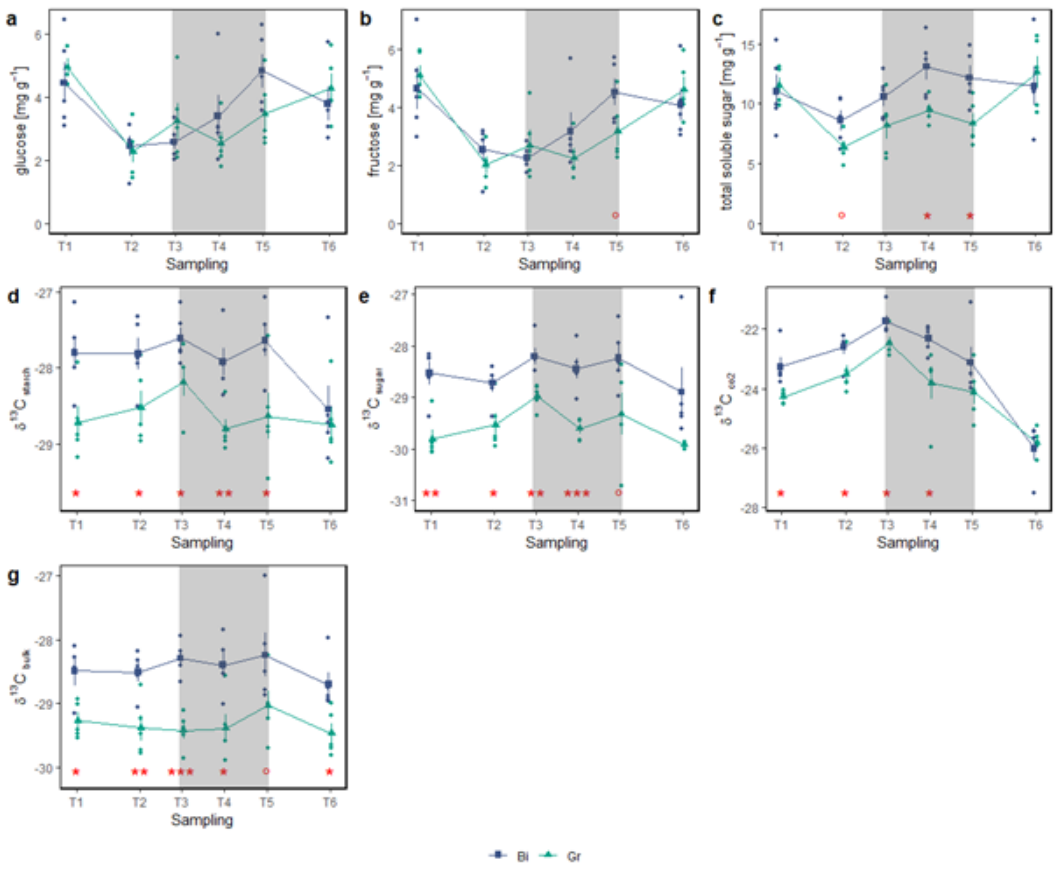

Fig. S5: Leaf concentration of glucose (a), fructose (b)and total soluble sugar (c) as well as δ13C values of starch (d), sugars (e), dark respired CO2 (f) and plant bulk matter (g). Blue squares and green triangles show the mean of n = 5 samples for the respective treatment and time point (Bi = binary temperature regime, blue squares; Gr = gradient temperature regime, green triangles; time points = T1-T6). Blue and green dots show individual measurement points of the respective treatment and error bars indicate the standard error. Red stars and dots indicate significant differences between the treatments (*** = $P < 0.001$, ** = P 0.01, * = $P < 0.05$, ° = $P < 0.1$) and shaded areas indicate the dark period.

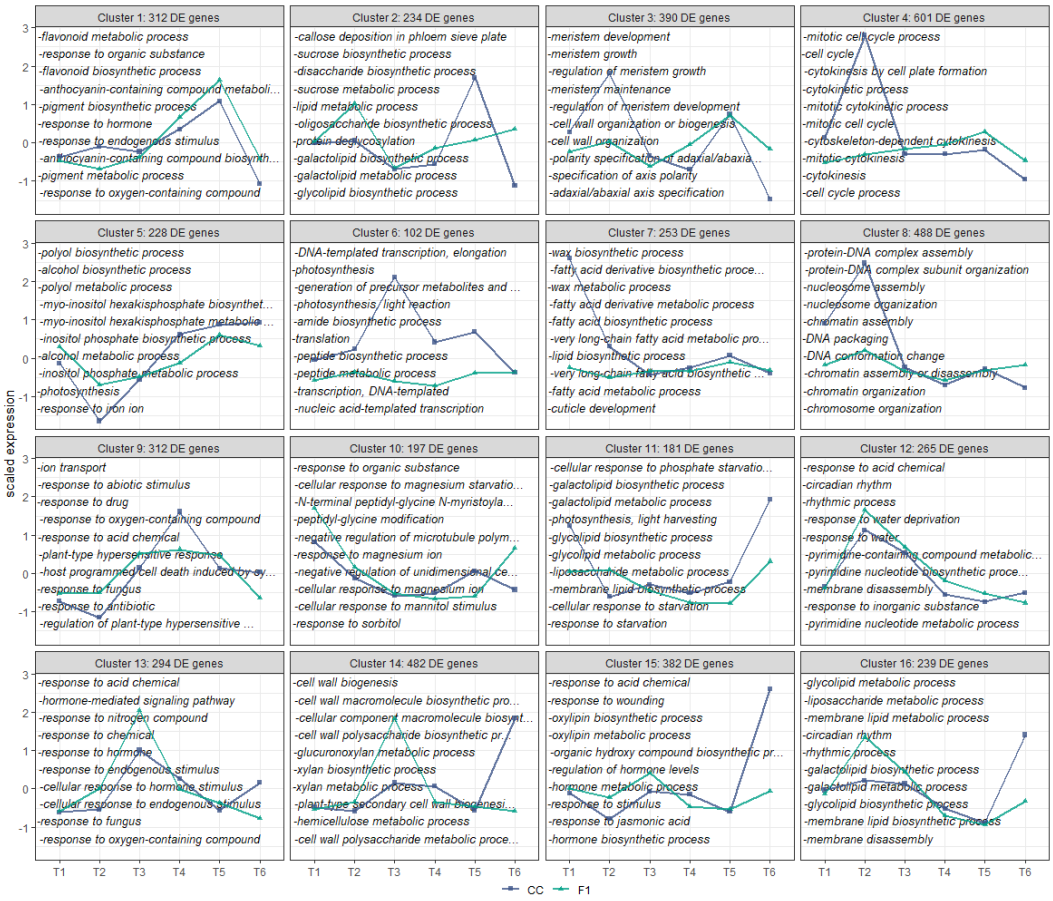

Fig. S6: Self organizing maps of normalized expression patterns of DE genes per treatment across all time points. Model expression pattern (i.e "codebook vectors") of each SOM cluster are shown for both treatments (CC = blue squares, F1 = green triangles) The top 10 significantly enriched GO-terms are listed in each cluster.

Tables

Table S1: Time points of samplings and day/night change.

Time	Event
12:45	sampling T1
18:45	sampling T2
22:30	Lights out
22:45	sampling T3
02:45	sampling T4
06:45	sampling T5
07:00	Lights on
12:45	sampling T6

Acknowledgements

First of all, I would like to thank Prof. Dr. Achim Walter for his encouragement and advice, and for giving me the opportunity to write my doctoral thesis in his group. I also owe sincere thanks to PD Dr. Andreas Hund, whose input and constant advice was essential for this project. The discussions we had together with Achim were very helpful. I am also grateful to Steven Yates for introducing me to the colourful world of genes and the pitfalls of bioinformatics. Without Norbert Kirchgessner and Hansueli Zellweger's untiring efforts, I would not have had a field and the technical equipment to obtain the data for this thesis in the first place. Moreover, we had a great time measuring in the FIP. Thank you for that, Norbert and Hansueli. I would also like to express my gratitude to Dr. Simon Griffiths for agreeing to co-examine this thesis and for providing valuable input. To my fellow PhD-students Jonas Anderegg and Lukas Roth I am also thankful. Collaborating on field measurements and discussing ways of data analysis and interpretation was not only instructive but also fun. Furthermore, I thank the members of the ETH crop science and the ETH molecular plant breeding groups for providing such an inspiring and friendly environment. Lastly, I thank my friends and family, especially Caterina, for their love and support.

Curriculum vitae

Personal Data

Name	Lukas Kronenberg
Born	20 December 1989 in Sursee, Switzerland
Citizen of	Dagmersellen, Switzerland

Education

03. 2016 – 12. 2019:	PhD student, Crop Science Group, ETH Zurich, Switzerland
10. 2014 – 03. 2016:	MSc in Agricultural Sciences, ETH Zurich, Switzerland
09. 2009 – 10. 2014:	BSc in Agricultural Sciences, ETH Zurich, Switzerland
08. 2002 – 06. 2008:	Matura Kantonsschule Sursee, Switzerland

Teaching Experience

Thesis supervision:	Two bachelor thesis supervised and graded One master thesis supervised
Regular courses:	Teaching assistant (introduction to 3D-laser scanning) in MSc course "crop phenotyping", main lecturer PD Dr. Andreas Hund

Work Experience

11. 2013 – 12. 2013	Internship Syngenta Crop Protection AG, Stein
03. 2013 – 07. 2019	Course instructor, Stiftung Arkadis Olten, Bildungsklub für Menschen mit geistiger Behinderung
02. 2009 – 07. 2009	Builder, Josef Arnet AG Dagmersellen

Service
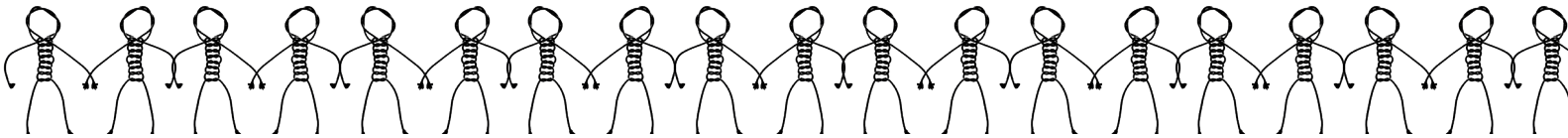
Since 05. 2019:	Civil Protection Service; platoon leader (Lt)
05. 2011 – 05. 2019:	Civil Protection Service; group leader (Kpl)
10. 2009 – 05. 2011:	Civil Protection Service; private (Sdt)